



TAMPEREEN TEKNILLINEN YLIOPISTO
TAMPERE UNIVERSITY OF TECHNOLOGY

AMANDA ATTOBRAH

PREPARATION AND AEROSOLIZATION STUDIES OF FINE POWDERS COMPOSED OF POORLY SOLUBLE DRUGS FOR PULMONARY DRUG DELIVERY

Master of Science Thesis

EXAMINERS: Professor Mika Valden, Dr. Janne Raula

EXAMINER AND TOPIC APPROVED BY FACULTY COUNCIL OF THE FACULTY OF NATURAL SCIENCES ON 8TH JUNE, 2016

ABSTRACT

AMANDA ATTOBRAH: Preparation and Aerosolization Studies of Fine Powders Composed of Poorly Soluble Drugs for Pulmonary Drug Delivery

TAMPERE UNIVERSITY OF TECHNOLOGY

Master of Science Thesis, 58 pages, 24 Appendix pages

May, 2016

Master's Degree Programme in Science and Bioengineering

Major subject: Nanotechnology

Examiners: Professor Mika Valden, Dr. Janne Raula

Keywords: Physical vapour deposition (PVD), Aerosol flow reactor, pulmonary therapy, leucine nanocrystals, Scanning electron microscopy (SEM)

Drug delivery via the pulmonary route has increasingly received much attention in recent years. Inhalable particles that are capable of reaching the deep lungs for the intended application can be achieved by particle engineering methods and use of appropriate inhalation device.

This study seeks to develop a carrier-free formulation for poorly water soluble drugs with desirable aerosol properties for pulmonary therapy. The Active Pharmaceutical Ingredients (APIs) used in this work, Pirfenidone and Budesonide are treatment drugs for some pulmonary diseases hence their delivery via the pulmonary route will be better suited for fast local action.

Carrier-free drug powders were formulated using particle engineering methods to achieve the desirable aerosol properties for inhalation therapy. The aerosol flow reactor method was utilized in this study and the leucine coating on the powder particles were formed by physical vapour deposition of leucine. Prior to the aerosol flow reactor step, precursor solutions were prepared with varying concentrations of leucine and also an exogenous surfactant, Dipalmitoylphosphatidylcholine (DPPC). The precursor solutions were prepared by wet milling of leucine and DPPC in ethanol. The drug was then added to the milled suspension to get the precursor solution ready for the aerosol process. In the aerosol flow reactor, the leucine formed nanocrystals which were deposited onto the dried drug particles by physical vapour deposition (PVD). Two poorly-water soluble drugs were formulated using varying leucine concentrations and the resulting powders were investigated with different inhalers for their aerosolization behaviours. The morphologies of the coated fine powders were also studied by scanning electron microscopy.

Pirfenidone powders showed agglomerated particles with the degree of agglomeration increasing with decreasing leucine concentration. This made the powders less flowable and dispersible, but the deagglomeration principle of the inhalation device improved the aerosolization properties. The powder with less leucine content had agglomerates which were rather difficult to separate even with the inhalation device's deagglomeration principle. The particle size distribution was much higher and most likely to be too large for inhalation. The Budesonide particles, having sustained the heat in the aerosol flow reactor showed much spherical particles with minimal surface contact. The powders showed good aerosolization properties for deep lung deposition. The particle size distributions of all Budesonide powders with leucine coating were also well within the appropriate inhalable range.

PREFACE

This project was carried out at the Department of Applied Physics, Aalto University, Otaniemi campus. I would like to express my profound gratitude to Professor Esko Kauppinen and Doctor Janne Juhani Raula of the Nanomaterials group at Aalto University for giving me this opportunity.

I am particularly indebted to Dr. Janne Raula and Ville Vartanen (MSc) for their immense support and guidance during my thesis work. As my supervisors, they have painstakingly reviewed my thesis, advised and motivated me. They were kind and gave me practical experience on the use of several scientific instruments at the applied physics lab and the nanomicroscopy centre. I am also thankful to Professor Mika Valden for his expertise advice, guidance and help on my thesis and throughout my studies.

Additionally, I would like to thank all the staff and students of Nanomaterials group at Aalto University, especially Nurcin and Mariko for their kindness towards me during the time I worked on my thesis.

I am also grateful to my friends and family who have supported my decision to study abroad and continually encouraged me. Above all, my sincerest gratitude goes to Almighty God for his fervent love and favour.

Tampere, August 2016

Amanda Attobrah

TABLE OF CONTENTS

LIST OF ABBREVIATIONS AND SYMBOLS	vi
1.INTRODUCTION	1
2.PULMONARY DRUG DELIVERY	3
2.1.1.Anatomy, physiology and histology of pulmonary system	3
2.1.2.Factors affecting pulmonary drug delivery	5
2.2.Solubility And Bioavailability Of Drugs	8
2.2.1.Poorly water-soluble drugs for pulmonary delivery	9
2.2.2.Methods to improve solubility and bioavailability	10
2.3.Formulation Design Of Poorly-Water Soluble Drugs.....	12
2.3.1.Excipients as carrier mechanisms.....	12
2.3.2.Particle engineering	14
2.3.3.Aerosol flow reactor method for DPIs	15
2.4.Inhalation Aerosol Devices	17
3.PARTICLE CHARACTERIZATION AND SIZE DISTRIBUTION.....	22
3.1. Scanning Electron Microscopy (SEM)	22
3.2. Particle Size Distribution: Berner Low Pressure Impactor (BLPI).....	26
4.MATERIALS AND METHODS.....	28
4.1.Particle Preparation	28
4.1.1.Wet milling	29
4.1.2.Preparing precursor solution.....	29
4.1.3.Aerosol particle preparation	30
4.2.Dispersion Experiments	32
4.3.Particle Morphology.....	34
5.RESULTS	35
5.1.Particle Composition And Morphology	35
5.1.1.Particle composition	35
5.1.2.Particle morphology	37
5.2.Powder Dispersibility And Particle Size Distribution.....	39
6.DISCUSSION	47
6.1.Particle Composition and Morphology	47
6.1.1.Particle composition	47

6.1.2. Particle morphology	48
6.2. Powder Dispersibility and Particle Size Distribution.....	48
6.2.1. Powder dispersibility	48
6.2.2. Particle size distribution	50
7. CONCLUSIONS.....	52
REFERENCES	54
APPENDICES	59

LIST OF ABBREVIATIONS AND SYMBOLS

API	Active Pharmaceutical Ingredient
BCS	Biopharmaceutics Classification System
BSE	Back Scattered Electrons
Bu	Budesonide
CFC	Chlorofluorocarbon
CV _{ED}	Variation coefficient of ED
DPI	Dry Powder Inhaler
DPPC	Dipalmitoylphosphatidylcholine
ED	Emitted dose
EH	Easyhaler®
FCA	Force Control Agent
FPD	Fine Particle Dose
FPF	Fine Particle Fraction
GSD	Geometric Standard Deviation
HFA	Hydrofluoroalkane
IFR	Inspiratory Flow Rate
IPF	Idiopathic Pulmonary Fibrosis
IR	Immediate Release
L	Leucine
MMAD	Mass Mean Aerodynamic Diameter
NMR	Nuclear Magnetic Resonance
Ph	Phospholipid (DPPC)
Pi	Pirfenidone
PK	Pharmacokinetics

pMDI	Pressurized Metered Dose Inhaler
PVD	Physical Vapour Deposition
SE	Secondary Electrons
SEM	Scanning Electron Microscopy
SP	Surfactant Protein
Tw	Twister™
Z	Atomic number

1. INTRODUCTION

Recently, pulmonary drug delivery has gained an immense interest as a quick and effective way for treatment. Many reasons that account for this discovery include patient acceptance of this technique due to great advancement in the devices used in pulmonary drug delivery [1]. Not only has this technology been attractive for patients and health professionals, but also the fact that lungs provide high surface area with moist and highly vascularised tissues for fast absorption even with low doses of the drug.[2] These features of the lung tissues make the pulmonary route of drug delivery a promising alternative than other routes such as intravenous and traditional oral route of drug delivery, especially for treatment of pulmonary diseases and also to administer insulin in diabetics.[3], [1] In the treatment of pulmonary infections, drug delivery via the pulmonary route is most attractive as the treatment targets the disease site directly. [4]

For drugs with a narrow therapeutic window, the pulmonary route helps to moderate the systemic side effects as there is reduced systemic exposure because the drug is targeted to the infected site. [5] There is also the benefit of eliminating side effects of drug excipients especially for patients who are unable to respond well to the presence of the excipients, example is lactose intolerance and the use of lactose carriers. It has also been reported that some systemic diseases can be well treated by pulmonary drug delivery. Such treatments include systemic use of insulin [6], growth factors and oxytocin, all of which are injected intravenously. This discovery makes pulmonary drug delivery attractive to patients as a non-invasive method of drug administration. [4] Pulmonary delivery of drugs, unlike oral drug administration is without hepatic first-pass metabolism [5], [7], [8], independent of dietary complications and also differences in patient metabolisms that influence gastrointestinal absorption. [8]

The aerodynamic features of drug particles used in Dry Powder Inhalation (DPI) therapy play a very important role in the delivery of the drug to the lungs. For drug particles to successfully reach the lungs for deposition, the particle size should be approximately 0.5-5 μ m. [9], [10] Size reduction and particle engineering techniques such as jet milling, wet polishing or spray drying are available to achieve the desired particle size [11]. However, there is the tendency of such fine particles to have much stronger co- and adhesive forces and form agglomerates caused by Van der Waals forces [12] due to the light weight of the particles. These agglomerates are unable to reach the lungs when the drug is inhaled, but rather stick to the upper airways. Fine particles are often formulated with coarser excipient particles such as lactose for accurate reproduction of drug dosing upon patient's inhalation [10] [2] On inhalation, the fine drug particles need to be separated from the carriers for deep lung deposition. This deagglomeration, however, is not often successful due to the above mentioned interactions leading to poor drug

delivery. Therefore, coated carrier-free powders are preferred where the fine drug particles are coated with crystals to achieve a rough nano-sized surface which reduce agglomeration and improve aerosolization of the particles. Particle engineering techniques to obtain spherical particles also tend to reduce agglomeration. [13] Particle agglomeration can also be reduced by co-formulation with force control agents (FCAs) or lactose particles and low density additives such as L-leucine. Alternatively, other forms of mannitol and indigenous lung materials like dipalmitolphosphatidylcholine (DPPC) can be replaced with the lactose. [14]

In this project, DPPC a naturally occurring phospholipid in the lungs is used as an exogenous surfactant to carry poorly water soluble drug particles coated with water soluble L-leucine nanocrystals for proper deposition and greater bioavailability in the lungs. Coating can be performed on any solid particles. A precursor solution is preformulated to combine the carrier, DPPC, L-leucine and poorly water soluble drug which do not have similar solubilities. The resulting precursor solution with required particle concentration is then ready for the aerosol processing to produce a well flowable and dispersible powder of drug particles coated with leucine nanocrystals. DPPC is the most abundant pulmonary surfactant and has been used clinically as a non-toxic exogenous surfactant [15].

There has recently been an increase in the number of candidates described as poorly water soluble drugs in drug discovery. The poor dissolution property of the drugs makes them less bioavailable. Formulation development methods which improve the solubility of these drugs in turn enhance their bioavailability. [16] Growing interest in pulmonary drug delivery also coincides with new active pharmaceutical ingredients (APIs) with low and/or inconsistent bioavailability. Once an inhaled API has by-passed pulmonary barriers and reached the alveolar region of the lungs, it needs to be absorbed. Gastrointestinal (GI) mechanisms of drug absorption form the basis of explaining pulmonary drug absorption. [17] Main differences in these two routes remain the lungs' different physiologic and cellular structures with higher surface area and thin alveolar-blood barrier [5], [17] for faster absorption than the GI tract. However, there is very little physiological significance of drug solubility when administered via the pulmonary route because of the presence of low masses of inhaled drug doses, and a small but well distributed fluid volume in the lungs. [17] This study employs excipient combination using leucine and DPPC for improved aerodynamic performance and stabilise physical/chemical properties of the poorly-soluble drugs.

AIMS: This work seeks to develop a carrier-free formulation technology for poorly soluble drugs with desirable aerosolization properties to be used in inhalation therapy. The study aims to produce drug powders using particle engineering technologies to enable the powder formulation to be properly inhaled into the deep lungs with the proper dosing and dispersibility without any carrier particles.

2. PULMONARY DRUG DELIVERY

2.1.1. Anatomy, physiology and histology of pulmonary system

The prominence of pulmonary drug delivery is expected to remain increasing exponentially for the treatment of pulmonary and systemic diseases. The lungs have a large surface area which provides them the prospect to be an effective systematic delivery system. [18] [19] In humans, the lungs are known to have about 2300 km of airways and 500 million alveoli. There is approximately 70-140 m² of surface area in the adult human lungs. [20] The lungs, as part of the lower respiratory tract contain bronchial tubes and millions of air sacs called alveoli. The functional unit of the lungs is a respiratory lobule (pulmonary acinus), which contains the respiratory bronchioles as well as any associated alveoli. The alveoli are responsible for gas exchange during respiration. About 87% of the total lung volume is estimated to be alveolar, 6% composed of tissue and the remaining 1% is gas. [21] [22] Figure 1 illustrates the anatomical features of the human pulmonary system.

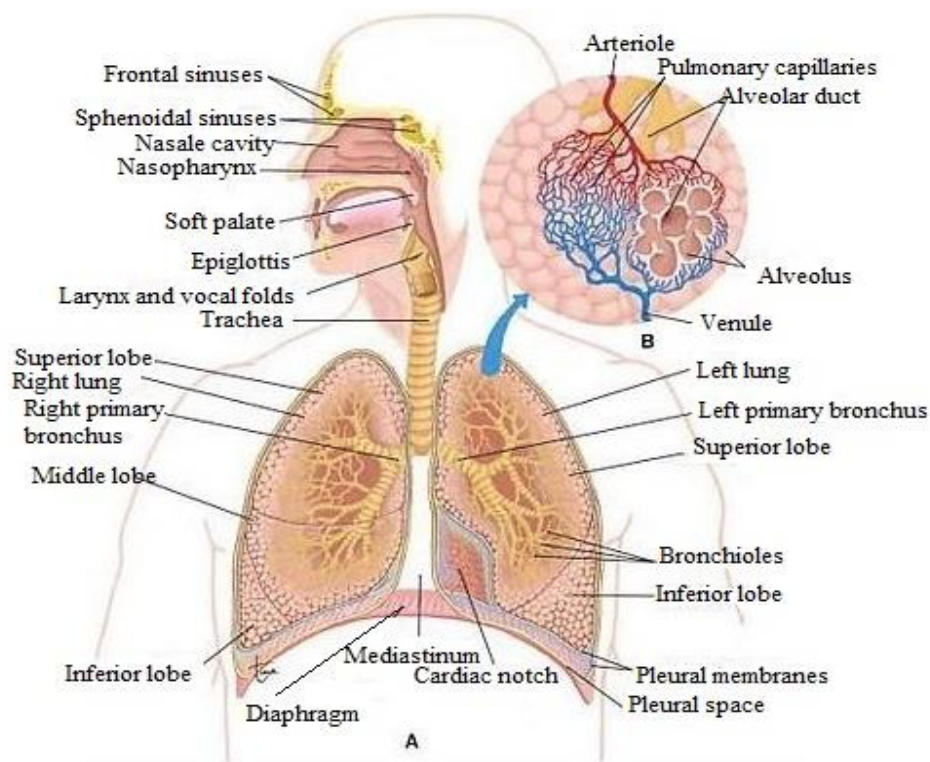


Figure 1. Anatomy of respiratory system [23]

In the alveoli, there are the simple squamous epithelial type I and also the cuboidal surfactant septal cells (type II) of the alveoli. [23] Ciliated epithelial cells of larger and smaller airways and types I and II cells play a major role in pulmonary drug delivery. Of the two main components of the alveolar epithelium, the type I pneumocytes consist of about 95% of the entire alveolar surface and only 5% being type II cells. [20] A thin layer of tissue fluid lines within each alveolus, which is important for gas exchange because a gas needs to dissolve in a liquid to be able to enter or exit a cell. Surface tension of the tissue fluid makes inflation impossible for the alveolar sacs but this problem is resolved by pulmonary surfactant, produced by the type II pneumocytes. The surfactant mixes with tissue fluid in the alveoli to reduce the surface tension and keep the alveolar sac open. [23]

Pulmonary surfactant layer comprises about 90% phospholipid and 10% surfactant proteins [3], [24]. The surfactant proteins (SP) consist of 4 specific proteins (SP)- A, B C and D [3]. The phospholipids work together with the lipophilic surfactant proteins, (SP) -B and -C, to lessen surface tension and avoid alveolar collapse. Hydrophilic surfactant proteins (SP) -A and -D a major role in immune response as they are capable of binding to particulates such as bacteria, viruses or allergens and modulate their interactions with lung cells and also immune response leading to enhanced clearance of pathogens. [3] With a transmission electron microscope, surfactant can be observed as an extremely thin (4nm) layer that covers the alveolar epithelial surface [21]. Figure 2 shows an electron micrograph of type II pneumocytes with secretory granules and figure 3 illustrates the entire lung surfactant system.

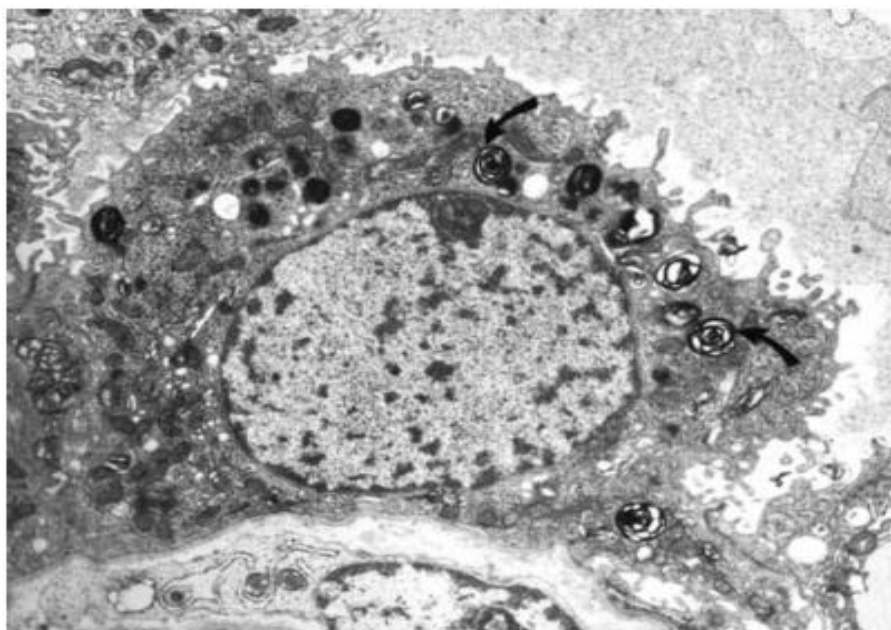


Figure 2. Electron micrograph of type II epithelial cells with secretory granules (arrows) [21]

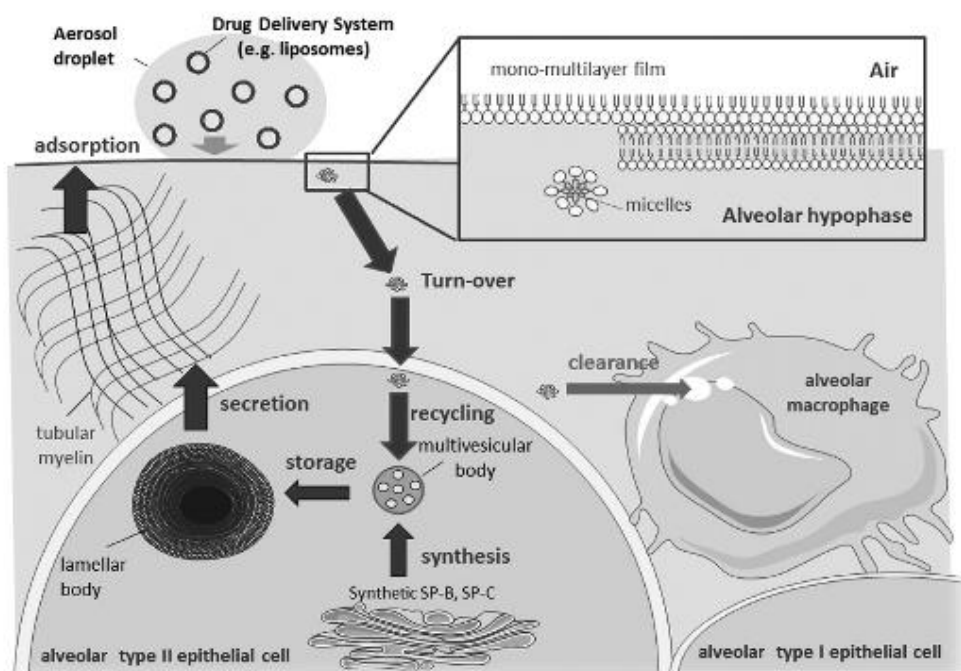


Figure 3. Lung surfactant system [25]

In the alveolar airspaces there are large migratory phagocytes moving easily throughout the alveolar airspaces and interstitium, known as the alveolar macrophages. They function primarily as a clearance mechanism to engulf and digest microorganisms and foreign materials present in the lungs. [26] Once in the airspace, particularly after engulfing materials, alveolar macrophages do not travel through the intact alveolar or bronchial epithelial layer back into the interstitium [27].

2.1.2. Factors affecting pulmonary drug delivery

As a rapidly increasing drug delivery route of interest, pulmonary drug delivery still faces some challenges despite the numerous advantages it provides [7]. The general effectiveness of an inhalation system is known by the mathematical model of the product of fraction of the emitted dose (ED), the dose delivered to the lungs and the bioavailability in the lungs [14]. For efficient development of inhalation treatments for both local and systemic therapeutics, it is important that the entire system of drug, drug formulation and delivery device is optimized and well-designed [2]. Not only do drug formulations and delivery devices affect aerosol therapies, but physiological factors also influence the effectiveness of aerosolized medications [2], [7], [8].

The physiology of the lungs is designed to keep foreign particles out of the body. Drug delivery

by inhalation needs to overcome this physiological barrier. [10] Improvement and assessment of innovative aerosol formulations involve understanding the deposition and passage of drug molecules across the lung epithelial layer. Before drug molecules administered via the pulmonary route get to the epithelial cells for absorption, they need to overcome certain non-epithelial barriers which include surfactant, alveolar macrophages and mucus. [7], [8].

In the upper airways, there is mucociliary clearance where inhaled particles of larger sizes are removed via the mucociliary escalator. The particles are usually conveyed to the glottis where they are either swallowed or expectorated. [24] In diseases such as cystic fibrosis, asthma, cilia syndrome and bronchiectasis, mucociliary clearance is impaired. [8] With the correct particle size, shape and density, inhaled particles overcome this mucociliary barrier and are deposited deeper in the lungs [3], [24]. Several particle engineering techniques are available to achieve the appropriate particle size, shape and other characteristics.

However, these smaller inhaled drug particles are also subject to alveolar clearance by the alveolar macrophages after they are deposited deeper in the lungs or absorbed into the pulmonary circulation.[8], [28] Alveolar macrophage is a major lung clearance mechanism can affect drug delivery to the lungs because they serve as the first line host defence against any inhaled particles.[7][24] Small soluble particles tend to be phagocytosed by alveolar macrophages more than larger insoluble particles[5]. Soluble particles are easily dissolved and absorbed into the lungs epithelium while poorly soluble particles need to be dissolved before absorption [8]. For drugs intended for local action, the immediate clearance is a problem because when the particles are phagocytosed, they may be transported into the systemic circulation and cleared from the lung tissue [5].

Pulmonary surfactant, a lipid-protein constituent of fluid layer that covers the respiratory surface aids in cell signalling and has an effect on the absorption of inhaled drug particles [3], [8], [24]. In some respiratory diseases (for instance Infant Respiratory Distress Syndrome, IRDS), the normal functionality of a surfactant system is impaired and this causes a rise in the air-liquid interface of the lungs. The deficiency of active surfactant system will gradually result in the progressive weakening of lung function. In cases such as IRDS, exogenous surfactant therapy can be applied with minimal side effects. [24], [29] Surfactants, with both lipophilic and hydrophilic components can enhance emulsification as the interfacial tension between water and organic solvents is reduced. This feature of surfactants helps to stabilize and solubilize poorly water soluble drug particles, reducing their aggregation. [29] Drug delivery with pulmonary surfactants is often desired since the presence of the surfactant could act as a substitutive material when endogenous surfactant is damaged or as an additional therapeutic agent when surfactant replacement therapy (SRT) is needed [24], [29].

Inhalation powder formulations need to contain an active pharmaceutical ingredient (API) in the required aerodynamic size distribution for successful deposition in the required target area at the flow rate of inhalation [30]. In *in-vitro* studies, the emitted dose from an inhaler (ED) and fine particle fraction (FPF) which describes the alveolar deposition of fine particles are

measured using a multistage cascade impactor [14]. The FPF is the measured mass of particles with reference to the ED. The mass median aerodynamic diameter (MMAD) of the inhaled particles are essential for effective delivery of drugs to the lungs. MMAD, derived from the mass, diameter and density of the particles is usually the form in which the aerodynamic diameter of particles is expressed. [31] [14] Aerodynamic diameter is the diameter of a spherical particle of a unit density which achieves the same velocity in upstream air as a non-spherical particle of ununiformed density. Smaller aerodynamic diameter of drug particles can be achieved by micronization methods such as jet-milling. Reduction of both aerodynamic diameter and density of particles are recently achieved by spray drying and spray-freeze drying.

Surface energies of powder drug particles affect the drug's effectiveness as increased surface energy enhances interparticulate interactions. This is why FCAs such as magnesium stearate and low density additives like L-leucine are formulated with inhalation drugs. [14] When drug particles are in the preferred size range of 1-5 μ m, their surface electric forces and Van der Waal's forces surpass the gravitational force acting on them. This results in the particles cohesiveness and poor flowability [2][5]. To resolve this problem, coarser lactose particles are blended with the drug particles for proper deep lung deposition. Fine particles with a mean diameter of 1-5 μ m can be surface engineered to achieve a rough surface to reduce agglomeration of the particles when inhaled. This technique is a carrier-free alternative to mixing fine drug particles with coarser lactose particles for the same result of improved powder fluidization. [32]

Inhalation device and inspiratory flow of the patient also affect the effectiveness of inhaled drug [33]. In most DPIs, successful deposition of inhaled drugs is improved by fast inhalation. Large powder agglomerates from DPIs and sometimes the presence of coarser lactose molecules make penetration into lung tissues difficult. The distribution of the powder into separate fine particles is often dependant on the turbulent air flow within the inhalation device. The turbulent airstream cause agglomerates to break apart and also separate the coarse carrier from the drug particles. [2] Each DPI has an airflow resistance that runs the necessary respiratory effort. In high resistance DPIs, it is more challenging to create an inspiration flow rate that is sufficient enough to attain maximum dose from the DPI. High-resistance DPIs affect particle dispersion even at lower inspiratory rates. [33]

2.2. Solubility and Bioavailability of Drugs

From the biopharmaceutical point of view, there are four different categories of drug substances and this grouping system is in direct relation to the formulation designs of the various groups [16]. The drugs are classified based on their solubility and bioavailability properties. This is known as the biopharmaceutics classification system (BCS). The solubility of a drug in water plays an important role in its absorption especially after oral administration. [34] A drug is classified as highly permeable when the degree of absorption in the intestines is found to be at least 90% of the administered dose.

A highly soluble drug is one whose highest dose strength is soluble in 250ml or less aqueous media within the pH range of 1.0 – 7.5 at 37°C. This is because the amount of fluid available in the upper gastrointestinal tract is 250ml in a fasted state. Outside of these conditions, the drug substance is considered poorly soluble. [16] [34] These reasons also account for the expanded interest even in systemic drug delivery via the lungs as these conditions seen in oral administration of drugs are eliminated in pulmonary drug delivery [9]. Table 1 below shows the various classes of drugs based on bioavailability according to the BCS.

Table 1. *Biopharmaceutics Classification System (BCS) of drugs* [16] [34]

	High Solubility	Low Solubility
High Permeability	Class I	Class II
	<p>Immediate release (IR) Solid Dosage forms such as conventional tablet or capsule formulations.</p> <p>For oral absorption, there is no rate-limiting step.</p>	<p>Dissolution is a rate-limiting step in bioavailability so even a small increase will result in dissolution rate becomes a great bioavailability enhancement. Factors such as effectiveness of the surface area, thickness of the diffusion layer, diffusion coefficient, saturation solubility, amount of dissolved drug and amount of dissolution media control the drug dissolution rate. Formulation design with techniques such as micronization, crystal modification and self-emulsification are very</p>

		helpful in overcoming solubility issues.
Low Permeability	Class III	Class IV
	<p>The bioavailability of these drugs is rate-limited by membrane permeability in the GI tract. Lipophilic drugs often have higher membrane permeability than hydrophilic drugs. Surfactants, lipids and bile salts are some permeation enhancers that can be preformulated with such drugs to improve their permeabilities. Drugs in these category can be administered in IR solid dosage forms with permeation enhancers.</p>	<p>This category is the most challenging as both solubility and absorption need to be improved for proper bioavailability of the drug. Here, combination of approaches used for Class II drugs together with permeation enhancers as in Class III drugs will help to improve bioavailability.</p>

2.2.1. Poorly water-soluble drugs for pulmonary delivery

Solubility is a major challenge as an estimated 40% of drugs are lipophilic and difficult to formulate due to their poor solubility in water [35], [36]. In the lungs, however, the meaning of low solubility has very little physiological effect on absorption due to small masses in the inhaled drug dose and also small, dispersed fluid on the lung surface. Among inhaled poorly water-soluble APIs, inhaled corticosteroids are the most common category. [9]Corticosteroids are mainly used to treat lung inflammatory diseases, especially asthma. They have been found to be lipophilic and also with small molecular weights which make them good candidates for passive membrane permeability. An ideal inhaled corticosteroid is sustained in the lung tissue for extended time of anti-inflammatory action, but with a low absorption to reduce systemic action of the API. [9] Many formulation techniques that target an improved solubility and bioavailability of these drugs exist. Most of these techniques are well suited for oral administration of the drugs.

The BCS for oral drug delivery could be partially comparable to drugs delivered via the pulmonary route for systemic action. There could then be a possibility of associating absorption with a rise in solubility/dissolution behaviour for poorly soluble and highly permeable drugs. However, for pulmonary drug delivery planned towards localized effects, this comparison is not applicable. The reason is due to the fact that stability is necessary between dissolution of an adequate amount of drug to perform its pharmacological action and limiting the clearance mechanisms to retain a constant concentration of dissolved drug in the lung.

Hence, for poorly-soluble drugs, an enhancement in their solubility properties and their controlled release may be necessary in order to augment localized therapy. Considering all these parameters, the modification of the aqueous solubility and dissolution profile of a drug through the exploitation of formulation technologies might directly influence the lung and systemic pharmacokinetics (PK) of the drug, and hence on its pharmacological action. [37]

2.2.2. Methods to improve solubility and bioavailability

The solubility–dissolution performance of a drug is a crucial factor to its bioavailability. One of the most challenges of drug development is an enhancement in the solubility of poorly soluble drugs. Methods that normally alleviate solubility issues include micronization, salt formation, use of a surfactant and use of prodrugs. According to the IUPAC definition, a prodrug is a compound that undergoes biotransformation before exhibiting pharmacological effects. It is an inactive compound, when metabolized in the body, produces the intended drug. Figure 4 below shows pharmaceutical particle technologies that improve drug solubility and bioavailability.

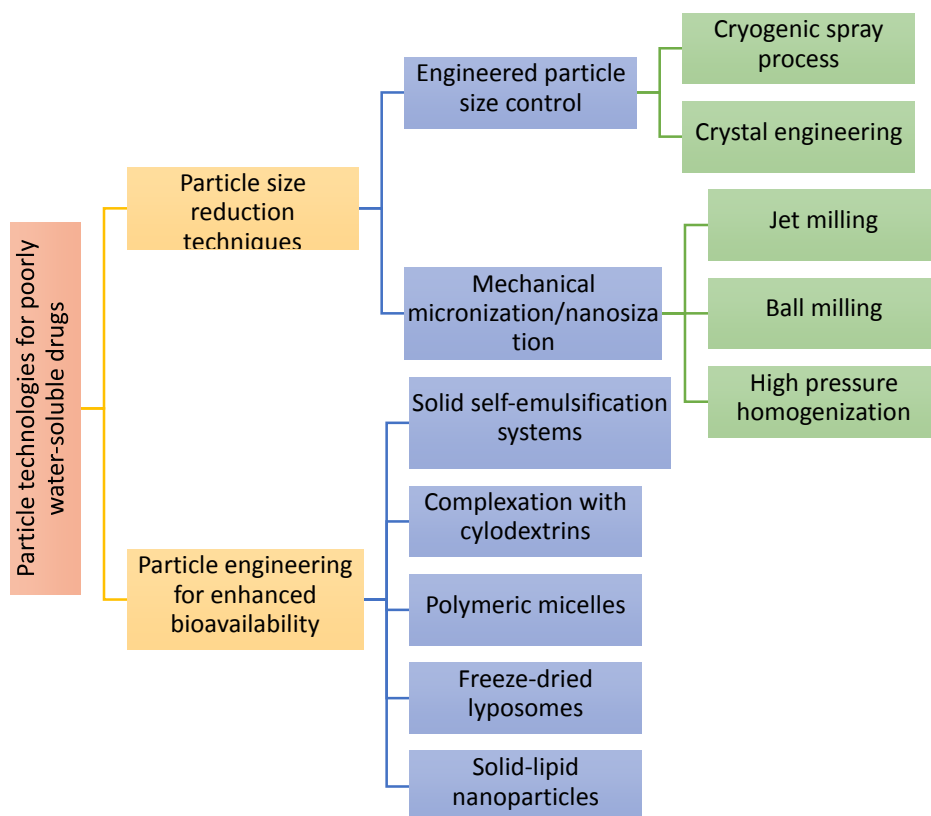


Figure 4. *Pharmaceutical particle technologies for improved solubility and bioavailability of drugs* [34]

Other techniques use liposomes, emulsion, micro-emulsion, solid dispersion. Inclusion complexation with cyclodextrins (a family of compounds made up of sugar molecules bound together in a ring) is practical technique but not generally applicable to all drugs. These techniques cannot be applied to drugs which are insoluble in aqueous or organic solvents. Nanosuspension technology favour drugs which are hydrophobic but soluble in lipids, and also drugs which are insoluble both in water and organic solvents. Nanosuspension is submicron colloidal dispersion of pure drug particles, and stabilised by surfactants. In nanosuspensions, the particle size distribution of the drug particles is typically less than one micron and the mean particle size ranges between 200 and 600nm. The purpose of a nanosuspension is not only limited to resolving poor solubility issues, but also modification of the pharmacokinetics of the drug enhancing drug effectiveness and safety. Nonetheless, these techniques have certain limitations and thus cannot be applied to various molecules. [38], [39], [40]

In the last ten years, nanoparticle engineering methodologies for pharmaceutical applications have been developed. Particle technology methods such as particle size reduction and particle engineering greatly enhance drug solubility and bioavailability, and is applicable to pulmonary drug delivery. The use of nanosuspension technology is also a good approach towards pulmonary administration of drugs with poor solubility. Nanosuspensions are made of nano-sized particles of the poorly soluble drug, without any matrix material, and is suspended in

submicron dispersions, and stabilized by surfactants. This is mostly beneficial in pulmonary drug delivery for local action. [38], [40]

2.3. Formulation Design of Poorly-Water Soluble Drugs

2.3.1. Excipients as carrier mechanisms

Excipients are inactive constituents which are deliberately included in drug formulations but do not apply therapeutic effects at the anticipated usage, though they can enhance product delivery and efficacy. They also may stabilise the physical and chemical properties of the API, and improve its mechanical and pharmaceutical properties such as dissolution permeation through the cells. There is a limited number of approved excipients for inhalation drugs. Table 2 gives a list of such approved excipients and others of major interest.

Table 2. List of approved and interesting excipients for DPI formulations [41]

Excipient	Description	Status
Sugars <ul style="list-style-type: none"> • Lactose • Glucose • Mannitol • Trehalose 	Used as coarse/fine carrier	Lactose is approved and commonly used carrier Glucose is approved Mannitol is approved Trehalose is an emerging alternative
Hydrophobic additives <ul style="list-style-type: none"> • Magnesium stearate 	Protect drugs from moisture	Approved
Lipids <ul style="list-style-type: none"> • DPPC • Distearoyl-sn-glycero-3-phosphatidylcholine (DSPC) • Dimyristoylphosphatidylcholine (DMPC) • Cholesterol 	Used in liposomes, matrix, coating	Biocompatible and biodegradable, very interesting excipients

Amino acids <ul style="list-style-type: none"> • Leucine • Trileucine 	Enhanced efficiency	aerosol	Endogenous substance, no data on lung toxicity
Surfactants <ul style="list-style-type: none"> • Poloxamer • Bile salts 	Producing porous particles	light,	Poloxamer may not be pro-inflammatory at low doses. Bile salts are endogenous substances which may be accepted at low doses.
Absorption enhancers <ul style="list-style-type: none"> • Hydroxypropylated-β-CD, natural γ-CD • Bile salts • Chitosan, trimethylchitosan 	Absorption proteins peptides	for and	Hydroxypropylated- β -CD, natural γ -CD yielded promising result. Bile salts also yielded promising results but may be toxic in chronic use. Pro-inflammatory results have been observed with chitosan and trimethylchitosan
Biodegradable polymers <ul style="list-style-type: none"> • Poly(lactic-co-glycolic) acid (PLGA) 	Used in sustained drug formulations		Immunogenicity effect observed

Excipient combinations can be employed to further improve the performance of inhalation powder formulations. With a greater flexibility in particle engineering techniques to explore excipient combinations, it is more likely to find a more suitable and acceptable formulation for further product development. [42]

2.3.2. Particle engineering

Conventional inhalation powder formulation technologies such as jet milling often have limitations due to their difficulty in formulating therapeutics. Recent innovations in particle engineering aim to overcome such limitations with limited or no carrier excipients. In addition, the use of carrier-free formulations allows for an improved delivery of inhaled drugs that are required in high doses, such as with antibiotics delivery. [42], [43] Most commonly used particle engineering methods include emulsion, supercritical fluid and spray/freeze-spray drying. Emulsion based systems have been shown to produce spherical particles from non-miscible solvent emulsions generation by sonication or homogenization. The solid composite particles produced are often dense and have a narrow particle size distribution.

Emulsion-based methods have the disadvantage of being difficult to scale up to commercial or industrial scale, as large quantities of the solvents will be required and there is a need for effective removal of solvent residues from the products.[10], [42] Based on an anti-solvent principle, supercritical fluid processing often uses supercritical carbon dioxide as the anti-solvent to produce inhalable particles by introducing the drug solution in the direction of the carbon dioxide, under supercritical conditions.

Spray drying is able to produce both low and high density particles. In spray drying, a feed solution or slurry is atomised using hot compressed air or gas to produce dry inhalable particles. The concentration of the solid particles is determined by the droplet concentration in the atomization. When the feed solution is a milled suspension, crystalline particles are produced whereas when drug and excipients are molecularly dissolved the resulting particles are amorphous. Spray drying can also be applied for heat sensitive materials. [10], [42] Spray drying is a good example of particle engineering technique with the capability of scaling up. However, one concern about the spray drying process is the physical and chemical stability of the particles. Re-crystallisation often occurs in many amorphous or partly amorphous particles, when there is a higher relative humidity (about 70%) causing a moisture-related instability. Co-spray drying with excipients would help to improve the hygroscopicity of amorphous particles, and prevent recrystallization. [44] Spray-freeze drying, a variation of spray drying is a more expensive batch process which avoids producing an air-liquid interface by atomizing particles into a cryogenic liquid, followed by lyophilisation. Scaling-up to industrial scale could be problematic with spray-freeze drying technique, as large volumes of cryogenic liquid may pose a safety hazard. [42]

2.3.3. Aerosol flow reactor method for DPIs

An ideal process should be continuous, single-step (that is, from solution to respirable product), and tuneable to produce particles with preferred physicochemical and aerodynamic features for pulmonary delivery. It should be a process that is able to yield products with a perfect batch-to-batch consistency, high yield, financially competitive, easily scaled up and appropriate for regulatory approval. [10]

The aerosol flow reactor method is a novel one-step continuous process for micro-particle production from drug, excipient and L-leucine liquid solutions. This method produces spherical drug micro-particles, and uses physical vapour deposition to coat the particles with L-leucine nano-sized crystals. [45], [46] The aerosol flow technique often avoids the use of harsh chemicals/solvents. The prepared drug solution (precursor solution) is atomised by an ultrasonic atomiser into droplets. The droplets are then suspended in a carrier gas, fed into a heated stainless steel reactor and the particles are collected after being dried inside the reactor. The reactor is tubular, with a completely laminar flow in the heated part. The temperature of the reactor is adjusted to allow a complete solvent evaporation and particle formation inside the reactor. The resulting particles also show spherical and smooth surfaces. [46]. Inside the heated part of reactor, the droplets are dried and leucine is evaporated. According to a study by Raula et al. in 2008 which investigated the production of leucine nanoparticles at varying conditions by the aerosol flow reactor method, growth and particle formation mechanisms of leucine nanoparticles depends on the L-leucine saturation conditions present in the reactor. The reactor temperature also affects the vaporisation rate of L-leucine. The study suggested that higher reactor temperatures of over 150°C to 200°C allows for complete evaporation of leucine, regardless of its concentration in the precursor solution. [47]

At the reactor downstream, the aerosol with dry particles is rapidly cooled and diluted in turbulent flow. This section of the reactor is composed of a porous stainless steel tube to avoid particle deposition on the walls of the tube and also to initiate the nucleation and deposition of L-leucine vapour onto the drug particle surface.[48] Due to the rapid cooling, L-leucine vapour begins to nucleate and subsequently crystallize on the surface of drug particles by physical vapour deposition (PVD).[49] The size of crystals which varies from a few to hundreds of nanometres is controlled by the saturation conditions of L-leucine. Figure 5 below shows the formation of leucine coating on spherical particles at varying conditions according to the study by Raula et al. in 2008[45].

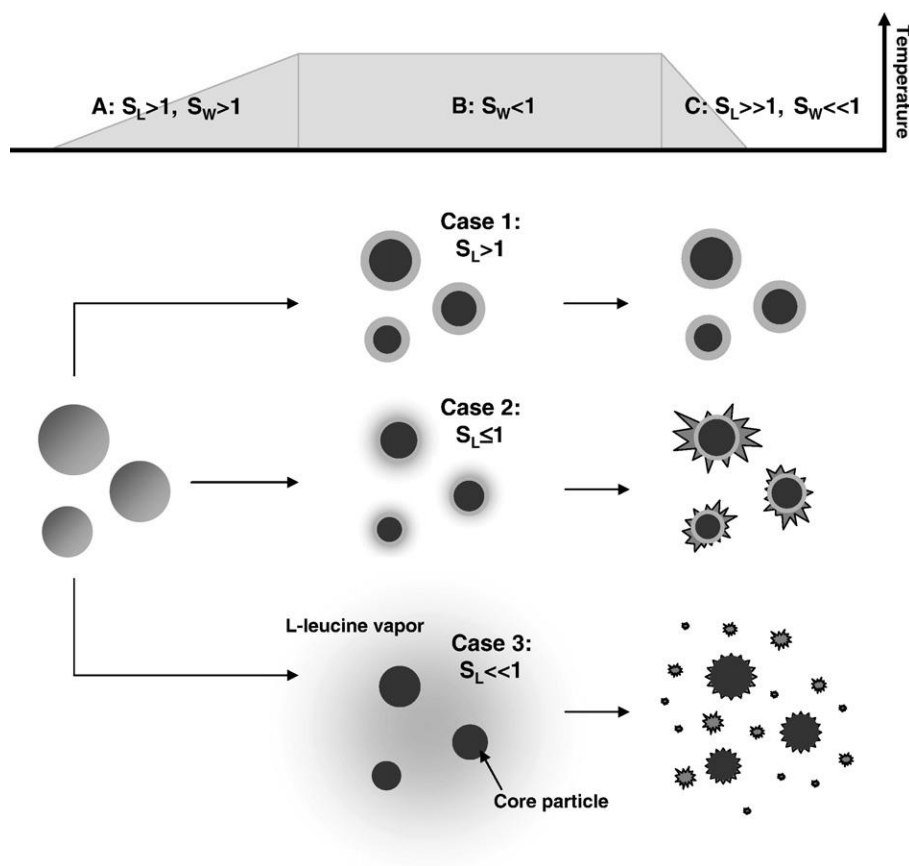


Figure 5. Formation of L-leucine particles in an aerosol flow reactor at varying vapour pressures [49]

In case I of figure 5, the saturation ratio of leucine (S_L) is above unity and no sublimation occurs. Upon further increase of the reactor temperature, the droplets were dried and leucine was subsequently sublimed. In case 2, S_L was close to unity and the sublimation of leucine occurred. When the sublimation occurs, it is assumed that the leucine vapour is in close proximity to the core surfaces. In case 3, S_L is far below unity and that is when all of the leucine sublimed. In the cooling segment of the reactor, different leucine particles were produced based on cases 1-3. When sublimation begins as in case 2, there is partial sublimation resulting in homogeneous nucleation of leucine. Two leucine coating layers are formed due to diffusion (in case 1) and the partial sublimation to form large leucine crystals. In case 3, pure leucine coating formed is due to homogeneous nucleation as well as heterogeneous nucleation onto the core particle.

2.4. Inhalation Aerosol Devices

An effective inhalation therapy not only depends on a pharmacologically active material and its well-designed formulation, but also on the delivery system. Before modern inhalation devices were developed, asthma patients used to smoke asthma cigarettes containing stramonium powder and tobacco as a form of treatment back in the 19th and early 20th centuries. Pressurized metered-dose inhalers (pMDIs), nebulizers and DPIs are the three major delivery systems for modern inhalation therapy. Among them, DPIs have several advantages such as good portability, low costs and no use of propellants and also improved stability of the formulation due to its dry state. Moreover, DPIs are much easier to handle than pMDIs due to breath-actuated passive aerosolization (in DPIs). [50], [51], [2] Figure 6 below illustrates the evolution of inhalation devices.

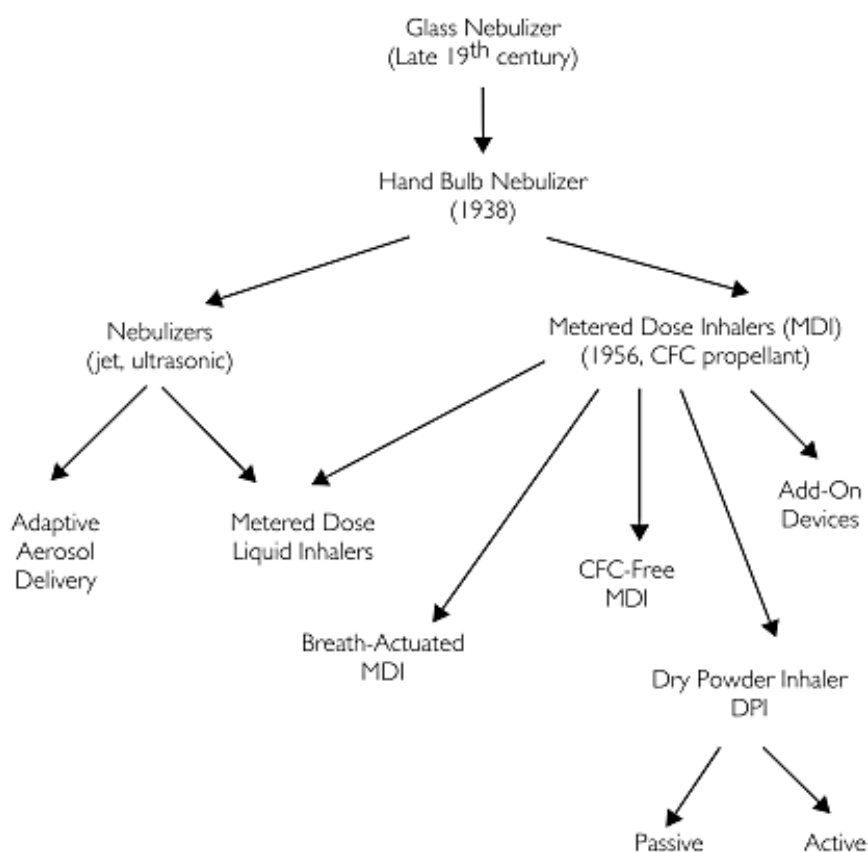


Figure 6. Evolution of inhalation devices [2]

Nebulizers produce an inhalable drug aerosol from a solution or suspension. The two main kinds of nebulizers are the jet nebulizer and the ultrasonic nebulizer, with jet nebulizer being the most commonly used. The jet nebulizer functions by generating aerosols from the liquid drug using a source of compressed gas. Based on the Bernoulli principle, a compressed gas goes through a constricted opening forming an area of low pressure at the outlet of the

neighbouring liquid feed tube. The drug solution is then drawn up from the fluid reservoir and dispersed into droplets in the gas stream. Ultrasonic nebulizers on the other hand, use piezoelectric crystal vibrating at high frequency to create a fountain of drug solution droplets in the nebulizer chamber. The higher the frequency, the smaller the droplets. Despite being relatively inexpensive, the gas compressors in jet nebulizers are often bulky and noisy. There is also the tendency of residual drugs being wasted, making it an expensive delivery system if the drug involved is expensive. [2], [52]

The pMDI was developed to overcome the problem of bulkiness in nebulizers. MDIs emit drug aerosol driven by propellants. There has been great improvement in the design of MDI propellants from chlorofluorocarbons (CFCs) to more environmentally friendly propellants like hydrofluoroalkanes (HFAs). The delivery efficacy of MDIs is dependent upon the breathing pattern, inspiratory flow rate (IFR) and hand-to-mouth coordination of the patients. Breath-actuated pMDIs have been developed to help patients with poor MDI technique. For particle sized within the respirable range of 1-5 μ m, proper deposition is more dependent on IFR than any other parameter. MDIs require slower inhalations to improve the deposition of inhaled drug particles in the peripheral regions of the lung. [2]

DPIs were developed to improve the coordination difficulties faced by using MDIs and also eliminate the use of propellants. Unlike MDIs which require inhaling slowly and holding of breath to improve lung deposition, proper deposition of drug into lungs is improved by fast inhalation with DPIs. [2] The dry powder strategy is characterised by giving the drug to the patient in the form of dry powder, administered using a specifically designed device for such formulation. Generally, inhalation devices depend on the inspiration flow of the patient for the dispersal of the aerosol and deposition into the deep lungs (breath-actuated devices). Table 3 summarises the main inhalation devices with pros and cons of each device.

Table 3. Pros and cons of different inhalation devices [2]

Inhalation device	Pros	Cons
Nebulizers (jet and ultrasonic)	<ul style="list-style-type: none"> No specific inhalation technique or coordination needed Able to aerosolize most drug solutions Delivers large doses Well suited for infants, sick people and physically 	<ul style="list-style-type: none"> Time consuming and noisy Bulky Contents easily contaminated Relatively expensive (gas compressors) Poor delivery

	impaired people who are too weak to handle other inhalation devices	<p>efficiency</p> <ul style="list-style-type: none"> • Drug wastage • Wide variations in performances due to difference in models and operating conditions
Pressurized metered dose inhalers (pMDIs)	<ul style="list-style-type: none"> • Compact and portable • Affordable • Repeatable dosing <p>Environment is sealed therefore there is no degradation of the drug</p> <ul style="list-style-type: none"> • Multidose (approximately 200 doses) 	<ul style="list-style-type: none"> • Inhalation technique and patient coordination necessary • There is a high oral deposition of the drug • Maximum dose of 5mg • Restricted range of drugs available
Dry powder Inhalers (DPIs)	<ul style="list-style-type: none"> • Compact • Portable • Easy to use • Breath actuated • No hand-mouth coordination is required 	<ul style="list-style-type: none"> • Respirable dose depends on patient's inspiratory flow rate • Humidity may cause powders to agglomerate and capsules to soften • Dose lost if patient unintentionally exhales into inhaler • Most DPIs contain lactose

Aerosolisation behaviours of DPIs depend on the powder formulation as well as the design of inhaler devices. [43], [52] Increased humidity and quick temperature changes are known to affect the performance of a DPI. The DPI performance can also be affected by the turbulence produced inside the device. The device's turbulence affects the deagglomeration of the powdered drug dose and consistency of the inhaled dose. All DPIs present a resistance to air-flow, and DPIs have been classified on the basis of their resistance and pressure drop across the device. [33] It is more difficult for higher resistance DPIs to produce an inspiratory flow that is sufficiently high to attain a maximum dose from the inhaler. Nonetheless, higher-resistance devices improve lung deposition of the powder. [2] Table 4 below summarises the various categories of DPIs based on their resistance to inspiratory flow and pressure drop across device.

Table 4. Major categories of DPIs on the basis of their intrinsic resistance and pressure drop across the device. [33], [53]

DPI Type	Pressure drop across device
Low-resistance DPIs	$< 5\text{Mbar}^{(1/2)} (\text{L/min})^{-1}$
Medium-resistance DPIs	$5\text{-}10 \text{ Mbar}^{(1/2)} (\text{L/min})^{-1}$
High resistance DPIs	$>10 \text{ Mbar}^{(1/2)} (\text{L/min})^{-1}$

A DPI is classified as low-resistance when the inspiratory flow of $> 90 \text{ L/min}$ by the patient is required. Medium-resistance DPIs require inspiratory flow of about $50\text{-}60 \text{ L/min}$ and high resistance devices require an inspiratory flow of $< 50 \text{ L/min}$ for proper lung deposition. An ideal DPI should include at least most of the following features: portable and easy to use, able to generate a consistent emitted dose across a wide range of inspiratory flows rates, fine particle fraction of high reproducibility, high physical and chemical stability of powder, low extra-pulmonary loss of powder (that is low oropharyngeal deposition, low device retention and low exhaled loss). [33], [43]

There is a demand for DPIs to be consistent in the dosing. The dose measuring mechanism of the device is responsible for the dose consistency. In bulk or reservoir type DPIs, a good dose counter indicates how many doses are left in the device. It is widely believed that all DPIs function best at a pressure drop of 4KPa or flow rate of 60L/min , but studies have shown that similar levels of FPFs are observed at relatively low pressure drops of $2\text{-}3\text{KPa}$. A study by Hoppentocht et al. in 2014 has categorised DPIs into two classes; those that produce approximately the same FPF at different flow rates and those producing higher FPFs with increasing flow rates. [30] The perfect inhaler should also provide constant de-agglomeration regardless of air flow rate [54] Figure 7 illustrates the main functional features of a typical DPI, Turbohaler®.

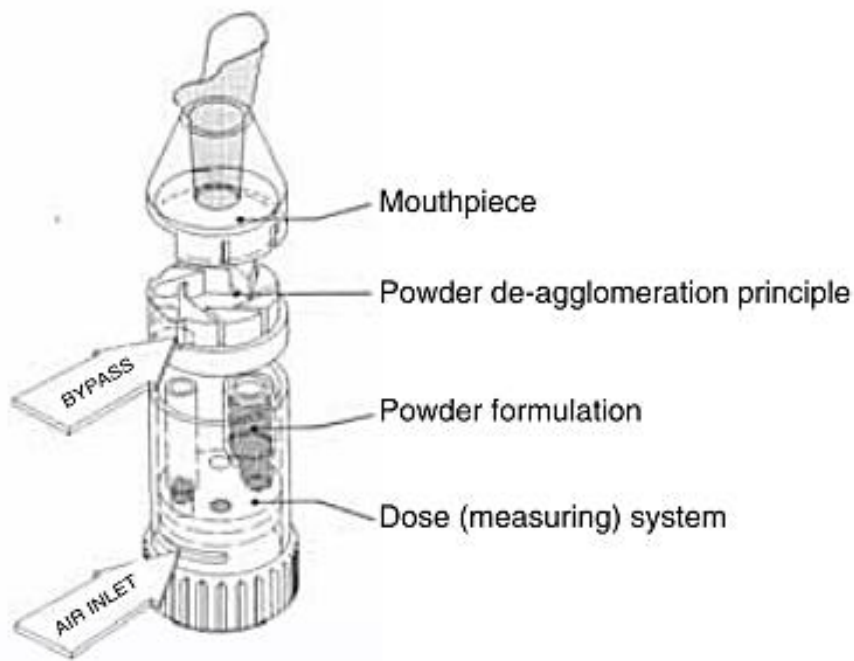


Figure 7. Primary functional design elements of a DPI [12]

A wide range of DPIs exist on today's market. Based on their dosing system, there are single-dose system which are loaded by the patient, multiple-unit dose systems that are in the form of separately packed doses as capsules, and reservoir type (bulk-powder) systems from which specific doses are measured or metered. The single-dose system has the disadvantage of patient alertness to load the drug. [2], [12], [43]

3. PARTICLE CHARACTERIZATION AND SIZE DISTRIBUTION

3.1. Scanning Electron Microscopy (SEM)

In electron microscopy, a much higher magnification for better image resolution than the conventional optical microscopes (which is only about 1000x maximum) is used. The magnification power of SEM can be as high as hundreds of thousand times and uses electrons to form an image which tells about the surface structure, crystalline conformation or electrical performance of samples. Accelerated high energy electrons with about 2 to 1000keV kinetic energies are focussed onto the sample to produce signals which form the image. Electron-sample interactions lead to image formation in SEM. [55] Figure 8 shows the interactions between high energy electrons and atoms of the specimen.

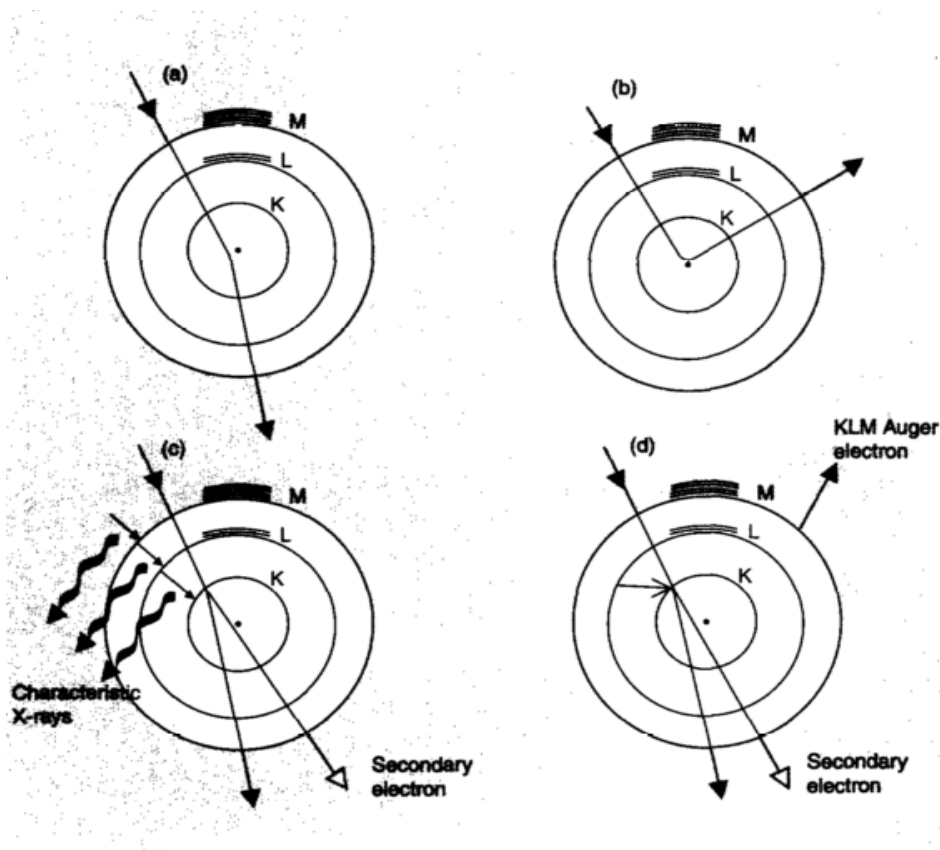


Figure 8. Interactions between high energy electrons and atoms of specimen [55] a) Low-angle scattering, b) High-angle or back scattering, c) Emission of secondary electrons and characteristic x-rays, d) secondary electron and auger electron emission

Interactions between electron beam and the specimen can be grouped into two main types which are elastic and inelastic interactions. In elastic scattering, the incident electrons are often deflected either by the atomic nucleus or electrons of the outer shell with comparable energy to the energy of incident electrons of the sample. When this happens, there is usually an insignificant energy loss from the collision and there is a direction change at a wide angle of the scattered electron. At angles more than 90° , the elastically scattered electrons are known as back scattered electrons (BSE) as seen in *Figure 8b*. [55]– [57]

Inelastic scattering happens as a result of a number of electron-specimen interactions. The quantity of energy loss depends from the collision on how the sample atoms get excited, whether singly or collectively and also on the binding energy of the atom. Secondary electrons (SE) are electrons that escape from the sample with energy less than 50eV. They originate from loosely bound conduction band in metallic sample or the outer shell of semiconductors and insulating samples. SEM images are formed from signals of secondary electrons (SE) emission. Other signals produced include characteristic x-ray, auger electrons and cathodoluminescence. [55], [56] Figure 9 below shows the regions where various signals emerge from.

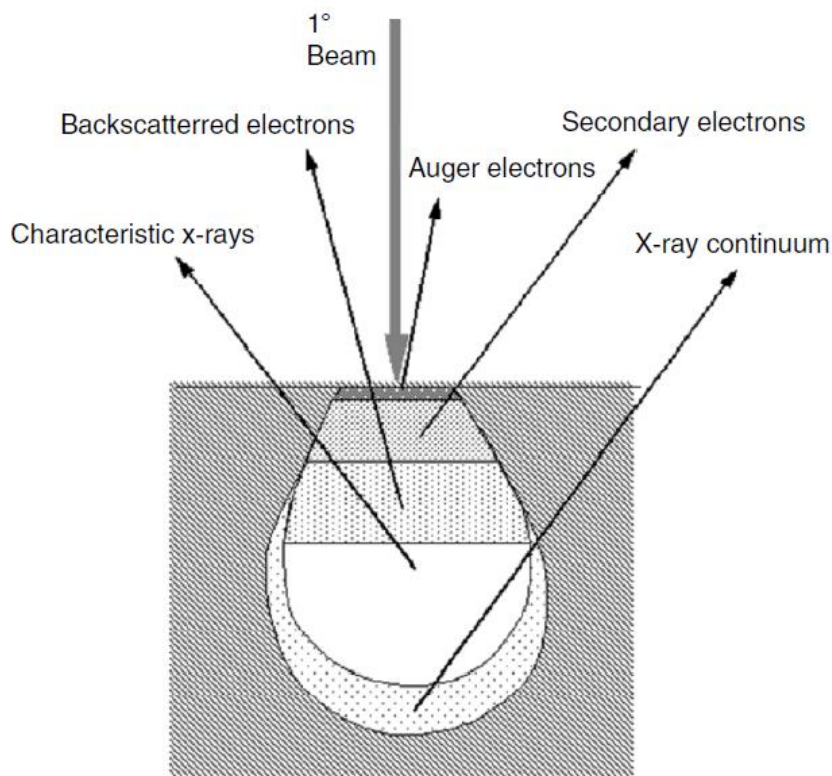


Figure 9. Beam-specimen interaction and regions where detected signals may be emitted [57]

With increasing atomic number (of sample), the rate of energy loss of incident beam also increases. As a result, electrons are unable to penetrate deeply into the sample causing an increase in the likelihood of elastic scattering with increasing atomic numbers. [55]

In SE signal, secondary electron coefficient (δ) is a ratio of the number of SE to the number of incident beam electrons. Due to their low energy levels, SEs usually escape from a shallow depth. [55], [56] About 90% of SEs have their energies less than 10eV with majority within the 2-5eV range. Since SEs are mainly used for topographical contrast in SEM, the amount of SEs reaching the detector plays a major role in the image produced. SEs that are unable to reach the detector will form darker shades in contrast than those that easily reach the detector. When the surface of the sample is perpendicular to the incident electron beam, the region of the sample surface from which SEs emerge from is smaller than when the sample is tilted. In tilting the sample surface, electron beam travel greater distances in the surface regions of the sample. This will result in more SEs being emitted within the escape depth. [56], [57] BSEs usually have higher energies than SEs, hence their (BSEs) inability to be absorbed by the sample. This makes the region from which BSEs emit from larger than where SEs are emitted from. As a result, the lateral resolution of a BSE image significantly poorer (1.0 μm) than it is for a SE image (10 nm). [56]

SEM images are typically greyscale and interpreting greyscale images requires understanding the origin of contrast mechanisms. In the absence of contrast, a high resolution and strong signal scan cannot reveal any information. Many microscopes have brightness and contrast controls. To manually adjust the controls, contrast should be turned down then brightness adjusted until there is a visible image on the screen. After this then contrast is also adjusted to obtain a visually appealing image. The surface of the sample may have uneven compositional atomic numbers. Some regions will have higher atomic numbers than other areas. Those regions with higher atomic number (Z) will emit more BSEs and appear brighter in the final image. The number of SEs emitted also increases with increasing atomic number. Hence contrast of SE signal and BSE signal can provide information on sample composition. This is why Z contrast is also called composition contrast. However, BSE signal gives better contrast than SE signal. Z contrast is relatively stronger at lower atomic numbers.

The microscope consists of seven main operational systems. These are the beam generation, vacuum, beam interaction, beam manipulation, detection, signal processing, and display and recording system. Figure 10 illustrates the major components of the SEM.

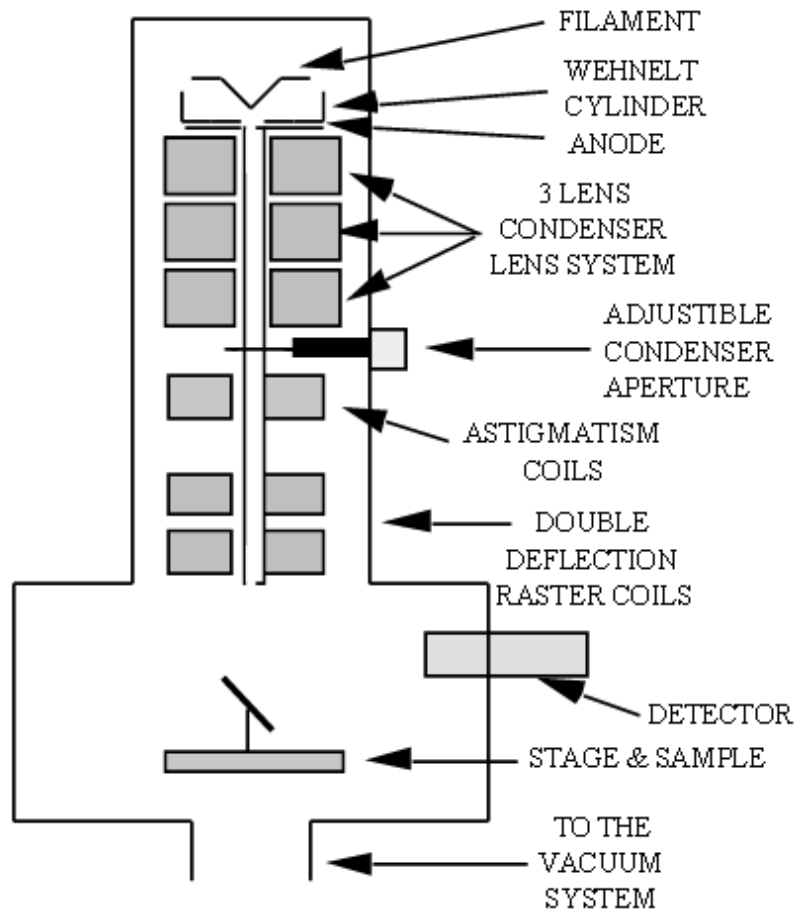


Figure 10. Major components of SEM column and specimen chamber [58]

A vacuum is often required when using SEM, due to the presence of electrons. Electrons easily disperse and collide with other molecules in the absence of a vacuum system. Hence the need for a vacuum to focus electron beam onto the specimen. From figure 10, the electron generating system can be located above the microscope column. This system produces the primary electron beam. The beam manipulation system is made of electromagnetic lenses and coils situated in the microscope column. The system controls the size, form and location of the electron beam on the sample surface. The beam interaction system encompasses the contact of electron beam with the sample and the types of resultant signals from the beam-specimen interactions.

The detection system comprises of various detectors, with varying sensitivity to different energies or particle emissions from the sample. The signal processing system processes any signal generated by the detection system, and also permits any further electronic manipulation of the image. Finally, the display and record systems are for visualizing electronic signals by means of a cathode ray tube. The system records the results with photographic or magnetic media. [58]

3.2. Particle Size Distribution: Berner Low Pressure Impactor (BLPI)

Measurement of aerodynamic size is mandatory for in all orally inhaled and nasal drug particles. Cascade impaction is a well-known technique for such measurement. The operation of cascade impactors is based on inertia impaction. On each stage of the impactor, there is a single or a series of nozzles. Particles saturated air is drawn through these nozzles on the impactor stages. The particles with suitable size in the airstream are directed to the surface of the collection plate for that specific stage. The impaction of a particle on a particular stage is determined by the particle aerodynamic diameter. Particles with sufficient inertia for a particular stage will impact on the collection plate of that stage while smaller particles with inadequate inertia stay in the airstream and move on to the next lower stage through the stage orifice. [51], [59]

The stages are put together in a stack by order of decreasing particle size. The largest particles are trapped on the highest stage collection plate while the finer particles are passed on to subsequent lower stages. [60] Figure 11 shows the flow of particle laden airstream through the impactor stages.

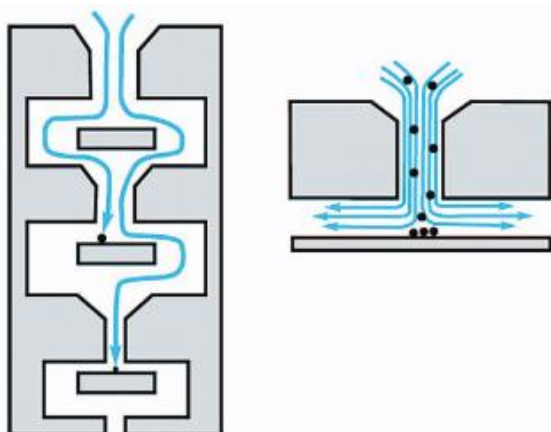


Figure 11. Flow through a cascade impactor [59]

Most experimental and theoretical studies with low pressure impactor are only concerned with single orifice impactor stagers. The BLPI comes with a multi orifice stage geometry and used extensively in size distribution studies for aerosols. [61]

According to the American and European pharmacopoeias, inertial impaction based methods have been explained to evaluate the in vitro inhalation performance of dry powder formulations by determining fine particles. [51], [62] Inertial impaction, is an aerodynamic process governed by aerodynamic diameter and allows for determining fine-particle dose (FPD). FPD is

equivalent to the mass of drug particles with the capability of deep lung deposition after being inhaled (that is, they have an aerodynamic diameter or MMAD of less than 5 μ m). FPF is a percentage of the FPD, and is usually associated with the total mass of drug in the inhalation device or drug particles recovered from the different stages of the impactor. FPD and FPF have similar functions of determining the ability of the drug formulation to be fluidised and disaggregated in time to be deposited at the various stages of the impactor. The dispersion performance of a powder formulation is often represented by the FPF. The higher the FPF, the better the powder dispersibility. Sometimes, the FPF can be calculated based on the emitted dose (ED). ED is the drug powder mass leaving the device after inhalation. The emitted dose reveals the capability of the powder to be aerosolized by the airflow in the inhalation device. [51], [63]

4. MATERIALS AND METHODS

4.1. Particle Preparation

The drugs studied were Pirfenidone (99%, from Wuhan Benjamin Pharmaceutical Chemical Co., China) and Budesonide (98.5%, from Henan Tianfu Chemicals Co., China) powders, both of which are used in pulmonary medicine and soluble in ethanol. Pirfenidone is an anti-fibrotic medication used for treating idiopathic pulmonary fibrosis (IPF), a severe chronic lung disease. According to the European Medicines Agency, it is commercially available under the trade name Esbriet® and is administered orally in capsule form for treatment of IPF in adults. Since these drugs are used in treating diseases related to the lungs, their administration via the pulmonary route could be more beneficial. Figure 12 presents the main stages involved in producing coated drug particles with enhanced solubility.

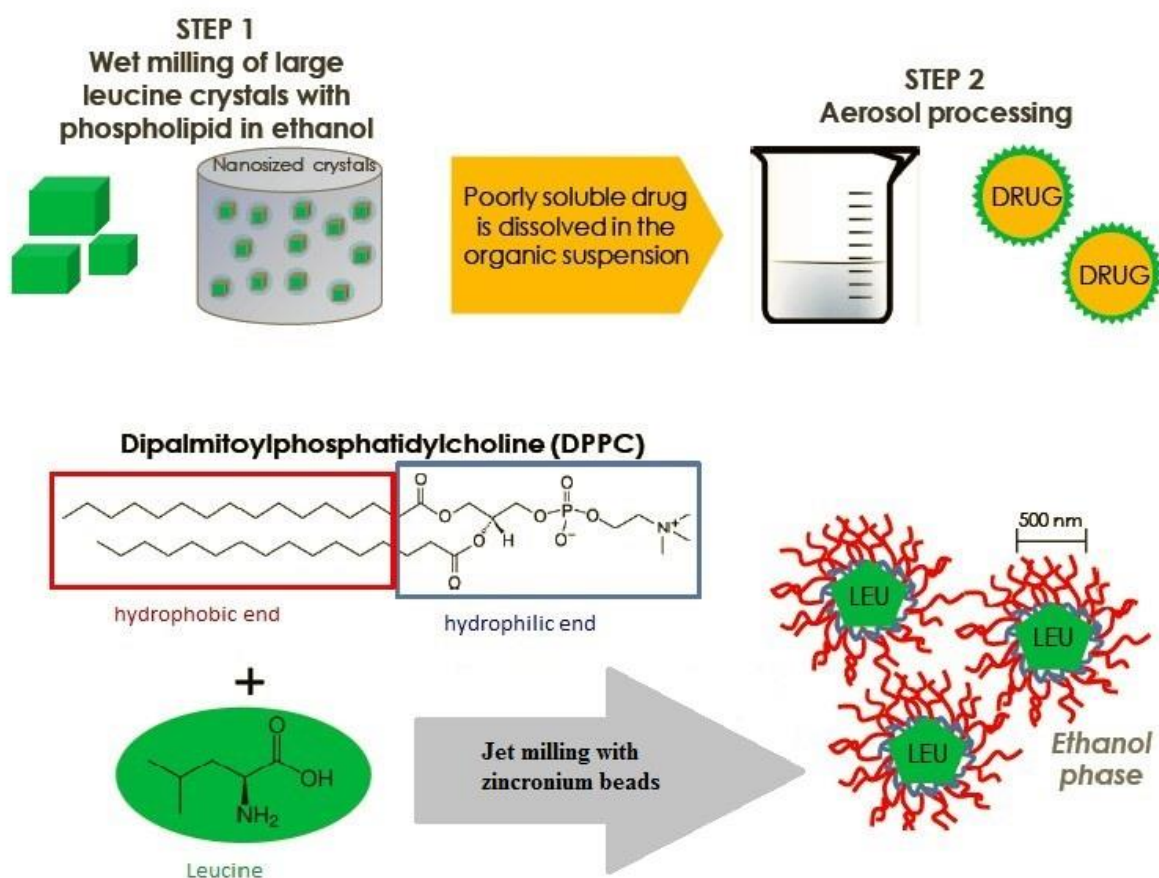


Figure 12. Various steps involved in preparation of leucine-coated drug particles (the lower part of the figure is what goes on in step 1) [64]

Mixing the poorly water soluble drug and coating material L-leucine directly to form a precursor solution for aerosol process is impossible as they have different solubilities. Hence

preformulation is required prior to the aerosol process. This project employs the technique of wet milling large leucine crystals with a phospholipid (DPPC) in ethanol, then dissolving the poorly water soluble drug in the organic suspension.

4.1.1.Wet milling

For the wet milling process, 100g of 3mm diameter zirconium (Zr) beads was weighed into a milling chamber of a planetary milling machine (Pulverisette 7 Premium, Fritsch Co., Germany), then 6g of powdered leucine was added to the Zr beads in the chamber. 1g of the phospholipid, which had been stored in a freezer was brought to room temperature and then dissolved in 20ml of pure ethanol. The dissolution process was hastened by heating the beaker containing the ethanol and DPPC over a warm water bath. The DPPC solution was then added to the leucine and Zr beads in the milling chamber. The counter chamber of the pulveriser was weighed and ensured that it was of similar weight to the other chamber containing the milling ingredients. Both chambers having similar weights provided a balance on both sides of the milling chambers. The chambers were locked in place and the pulveriser was run at 1100rpm for 3x3 minutes with 15minutes pause between the runs. The selected ball size was <5mm balls.

The 3x3min cycles were repeated 4 times, allowing the chamber cool for about an hour after each 3x3min cycle. After cooling the chamber after the 4th round, the milled slurry was washed with ethanol to further prepare the precursor solution.

4.1.2.Preparing precursor solution

The milled slurry was washed with 180ml pure ethanol and sieved to remove the Zr beads. To achieve concentrations of 20g/L drug, 15g/L leucine and 2.5g/L DPPC, 8g of drug and 200ml of ethanol were added to the milled suspension. The precursor solution prepared was 400ml in volume. This was the first precursor solution ready for the aerosol processing, with a leucine/DPPC concentration ratio of 6:1.

After the aerosol production, remaining precursor solution was subsequently diluted to get lower concentrations of leucine and DPPC while maintaining a constant concentration of the actual drug by adding more of the drug according to required concentrations. Table 5 below shows the various concentrations of precursor solutions prepared for the aerosol process.

Table 5. Concentrations of drug, leucine and phospholipid for various precursor solutions

Drug conc. (g/L)	Leucine conc. (g/L)	DPPC conc. (g/L)
20	15	2.5
20	5	0.83
20	0.875	0.146

4.1.3. Aerosol particle preparation

The coated drug particles were prepared by the aerosol flow reactor and PVD methods as explained in Chapter 2. The aerosol flow reactor of length 150cm and diameter 10cm was preheated to 180°C in all three zones (illustrated in figure 13). The precursor solution was put into a burette and fed into the ultrasonic atomiser. The atomiser produced solute droplets from the precursor solution, and the droplets were carried by nitrogen gas at a flow rate of 20L/min into the heated aerosol flow reactor. In the heated section of the reactor, where the flow was laminar, the droplets were dried, while leucine completely evaporated and carried to the cooling section. By PVD method, the leucine vapour was deposited onto the drug particles forming a layer of coating around the spherical particles.

In the cooling section, the flow was turbulent and dry air at a flow rate of 78L/min was used to rapidly cool the dry particles. The large volume of air flushed in prevented water re-condensation and also prevented the powder particles from sticking onto the walls of the reactor tubes at the cooling and collection section. The dried and cooled micro particles were collected with a cyclone for small scale purposes. An electric low-pressure impactor (ELPI) was connected to the tube linking the reactor cooling section to the cyclone. During the running of the reactor, the ELPI valve was opened to monitor the size distributions of the particles being produced. All coated powders produced were stored over silica prior to the dispersion experiments.

The aerosol process was performed for each concentration of precursor solution produced. Hence, for each drug studied, three particle samples were produced according to the concentrations in table 5. Figure 13 illustrates a schematic representation of the aerosol flow reactor used in particle preparation.

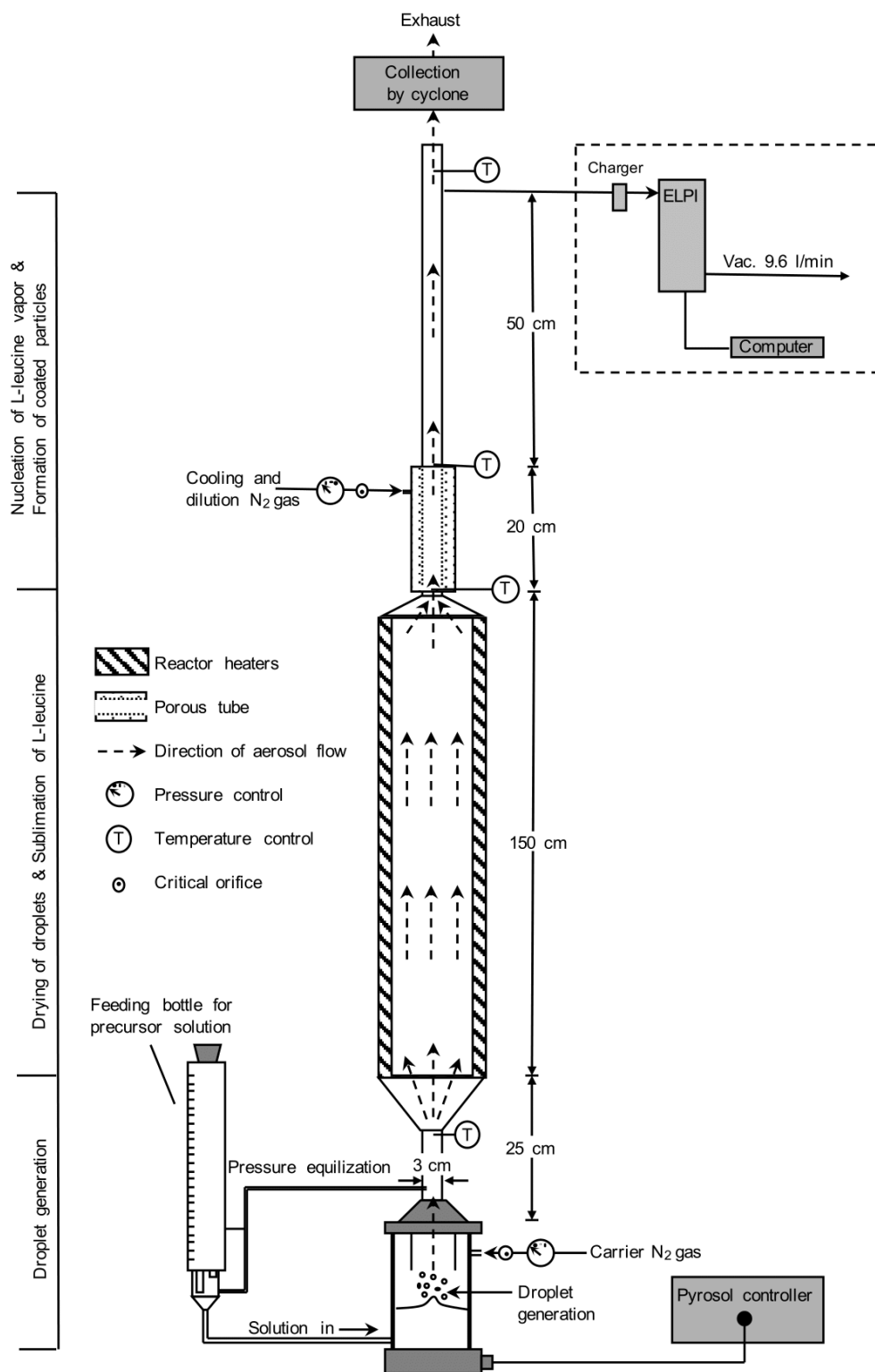


Figure 13. Experimental set-up of the aerosol flow reactor

4.2. Dispersion Experiments

A non-commercial computer assisted inhalation simulator was used to investigate the dispersibility of the produced powders. This in-house inhalation simulator [65] which functions by an interaction between pressurized air and vacuum, and uses a BLPI attachment as the measuring device.

All the dispersibility experiments were performed with the prepared carrier-free fine powders i.e. no coarse carrier particles were added. Two medium-resistance DPIs, a multidose reservoir or bulk-type Easyhaler® made by Orion Pharma and single-dose capsule type Twister™ inhaler made by Aptar Pharma, were used. Both inhalers are shown in Figure 14 below. The Easyhaler reservoir was filled with approximately 0.5g of powder, and Twister with capsules filled with 5.0 (± 0.1) mg/capsule. The loaded inhaler was attached to the mouthpiece of the inhalation simulator. Each inhaler was attached to a specific mouthpiece which was changed upon switching the inhaler. Upon inhalation, air flowing through the inhaler carried the powder and transferred it to the tubing of the device.



Figure 14. Left: Easyhaler® by Orion Pharma Oy, multidose inhaler. Right: Twister™ by Aptar Pharma, capsule inhaler.

Emission of the powder was sensed on-line by a light attenuation between two contrasting IR probes lined at the exit of the inhaler and also by gravimetric means. The inhalation run was performed 10 times and for the Easyhaler, the inhaler being held at an upright position was shaken vertically 3 times prior to the dose loading and powder inhalation in between the runs the inhaler. The shaking process removed possible remnants from the previous loading. For the Twister, the inhaler was emptied after each single dose inhalation.

Before each ten-emission experiment, five emissions were first run to stabilise air flows and pressure drops across the device to improve accurate results for the actual experiments. Pressure across the inhalers were manipulated to 2kPa and 4kPa, and ten emissions were performed on all fine powders at both pressure drops. Fast inhalation profiles were used in all dispersion experiments. In a fast inhalation profile, the maximum pressure drops and flow rates were attained in two seconds retaining these levels for 9 seconds then quickly dropped down and stopped within a second after the 9 seconds. The inhalation profiles were created for both

inhalers at different pressure drops were by an interplay between vacuum and pressurized air. Figure 15 shows the typical inhalation profiles.

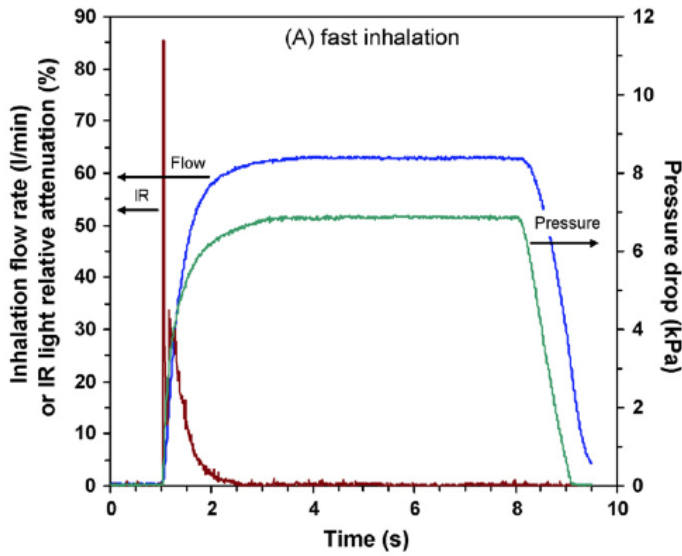


Figure 15. Typical inhalation profile run by the inhalation simulator where blue is flow rate, green is pressure drop over the inhaler and red is light detection for the powder emission.

The measured fine particle fractions were expressed in reference to the emitted doses. The EDs were evaluated by measuring the weight change of the inhaler after each inhalation run. MMADs and their related geometric standard deviations (GSD) were determined through gravimetric analysis of aluminium foil rings placed on the collection stages of a ten-stage BLPI. The MMAD and GSD were determined by the following expressions:

$$\text{MMAD} = \exp \left(\frac{\sum(m_i \ln D_i)}{M} \right)$$

$$\text{GSD} = \exp \left(\left(\frac{\sum(m_i D_i^3 (\ln D_i - \ln \text{MMAD})^2)}{\sum(m_i D_i^3) - 1} \right)^{1/2} \right)$$

Where m_i is the mass fraction of fine powder particles on the collection stages of the BLPI, M is the sum of mass fractions which is unity by definition. D_i is the aerodynamic diameter of the i th size stage of the BLPI.

4.3. Particle Morphology

Morphologies of the fine powder particles were studied using a field emission scanning electron microscope (Zeiss Sigma VP). In preparing the samples for the SEM imaging, a piece of carbon tape was fixed onto a clean SEM pin specimen stub and the thin top layer of the carbon tape was carefully removed. Using a spatula, a pinch of the powder sample was then sprinkled onto the carbon tape and the stub was carefully tapped to get rid of loose powder particles. Compressed air was then used to further blow off excess powder particles, leaving a thin layer of powder particles well fixed onto the carbon tape.

After fixing the sample particles onto the carbon tape, the stubs were placed onto the SEM sample stage, metal (gold was used) sputtering was performed to coat the non-conductive samples. The gold sputtering was done to reduce charging effects, make the non-conductive sample more stable under the electron beam and improve the quality of the image formed. The sample stage with the samples was then placed into the SEM specimen chamber for the actual imaging.

4.4. Particle Composition

Particle composition were analyzed by ^1H -NMR spectroscopy (Bruker 400 MHz UltraShield NMR) in deuterated ethanol (Sigma Aldrich).

5. RESULTS

5.1. Particle Composition and Morphology

5.1.1. Particle composition

Using nuclear magnetic resonance (NMR) spectroscopy, the compositions of the precursor solutions and fine powders were obtained. Due to insolubility of leucine in deuterated ethanol, its content in the final powder was determined by back calculating from the precursor solution assuming that the leucine/DPPC ratio remains the same in the final powders as it was in the precursor solution. Table 6 shows the various compositions in the precursor solutions and powders produced from them.

Table 6. Composition of precursor solutions and produced powders assuming L/Ph ratio remains the same in produced powders. Abbreviation: C_{total} , total concentration of precursor solution; Pi, Pirfenidone; Bu, Budesonide; L, Leucine; Ph, Phospholipid

Sample	Precursor solution				Produced powder		
	C_{total} (g/L)	Drug (w-%)	L (w-%)	Ph (w-%)	Drug (w-%)	L (w-%)	Ph (w-%)
Pi20L0.875Ph0.146	37.50	95.1	4.2	0.7	87.8	10.4	1.7
Pi20L5Ph0.83	25.83	77.4	19.4	3.2	64.2	30.7	5.1
Pi20L15Ph2.5	21.02	53.3	40.0	6.7	35.6	55.2	9.2
Bu20L0.875Ph0.146	37.50	95.1	4.2	0.7	82.4	15.1	2.5
Bu20L5Ph0.83	25.83	77.4	19.4	3.2	75.1	21.4	3.6
Bu20L15Ph2.5	21.02	53.3	40.0	6.7	56.0	37.7	6.3

However, NMR spectroscopy on the produced powders revealed a lot less leucine content than the amount obtained from the back-calculation of the precursor solution composition. Table 7 below shows the actual leucine content in the produced powders.

Table 7. Actual compositions of precursor solutions and their corresponding produced powder determined by NMR spectroscopy. Abbreviation: C_{total} , total concentration of precursor solution; Pi, Pirfenidone; Bu, Budesonide; L, Leucine; Ph, Phospholipid

Sample	Precursor solution				Produced powder		
	C_{total} (g/L)	Drug (w-%)	L (w-%)	Ph (w-%)	Drug (w-%)	L (w-%)	Ph (w-%)
Pi20L0.875Ph0.146	37.50	95.1	4.2	0.7	97.4	0.7	1.9
Pi20L5Ph0.83	25.83	77.4	19.4	3.2	91.8	0.9	7.3
Pi20L15Ph2.5	21.02	53.3	40.0	6.7	78.8	0.9	20.3
Bu20L0.875Ph0.146	37.50	95.1	4.2	0.7	98.6	0.4	1.0
Bu20L5Ph0.83	25.83	77.4	19.4	3.2	95.6	0.5	3.9
Bu20L15Ph2.5	21.02	53.3	40.0	6.7	87.8	0.5	11.6

5.1.2. Particle morphology

Figures 16 and 17 below are SEM images showing the surface morphology and structure of the drug powders produced with various concentrations of leucine and DPPC.

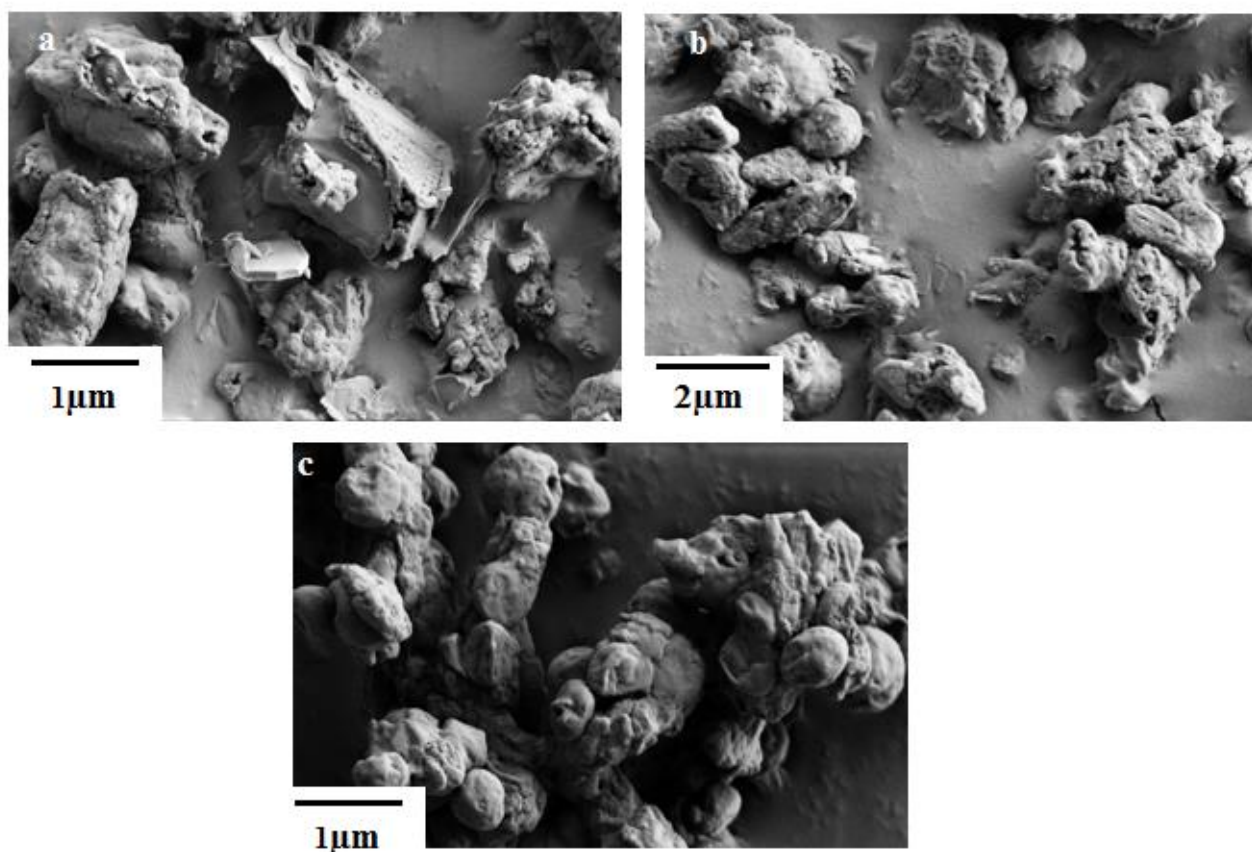


Figure 16. SEM images of Pirfenidone powders produced at different Leucine concentrations:
a) Pi20L0.875Ph0.146 b) Pi20L5Ph0.83 c) Pi20L15Ph2.5

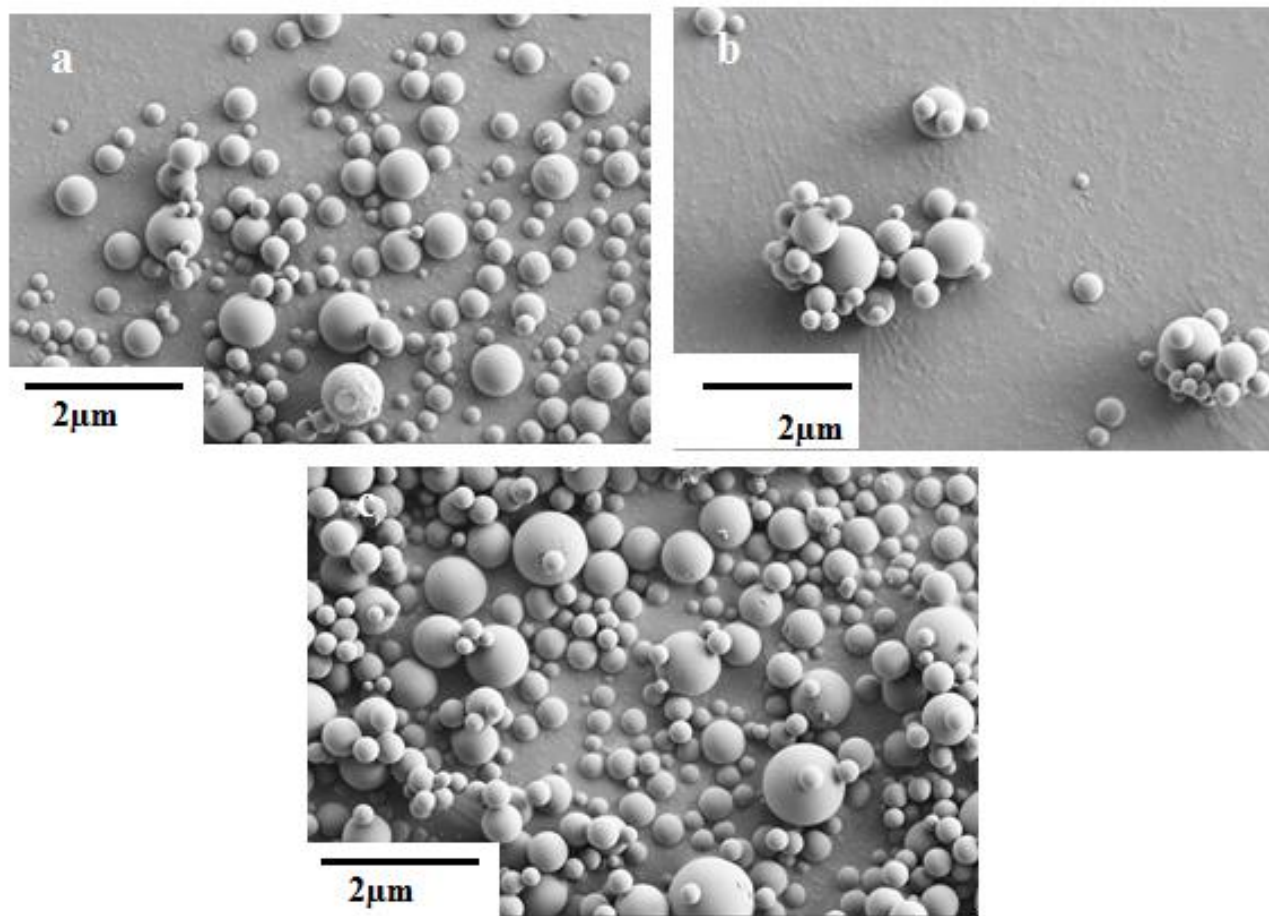


Figure 17. SEM images of Budesonide powders produced at different Leucine concentrations:
a) Bu20L0.875Ph0.146 b) Bu20L5Ph0.83 c) Bu20L15Ph2.5

5.2. Powder Dispersibility and Particle Size Distribution

Dispersion experiments performed on the coated drug powders yielded EDs, FPFs and coefficient variation of the emitted dose CVs represented in **figures 18 to 23** below. All experiments were performed at two pressure drops (2kPa and 4kPa) across the inhalers (Easyhaler and Twister). The pressure drops 2kPa and 4kPa correspond to inspiratory flow rates of 40 l/min and 55 l/min for Easyhaler and 43 l/min and 55 l/min for Twister.

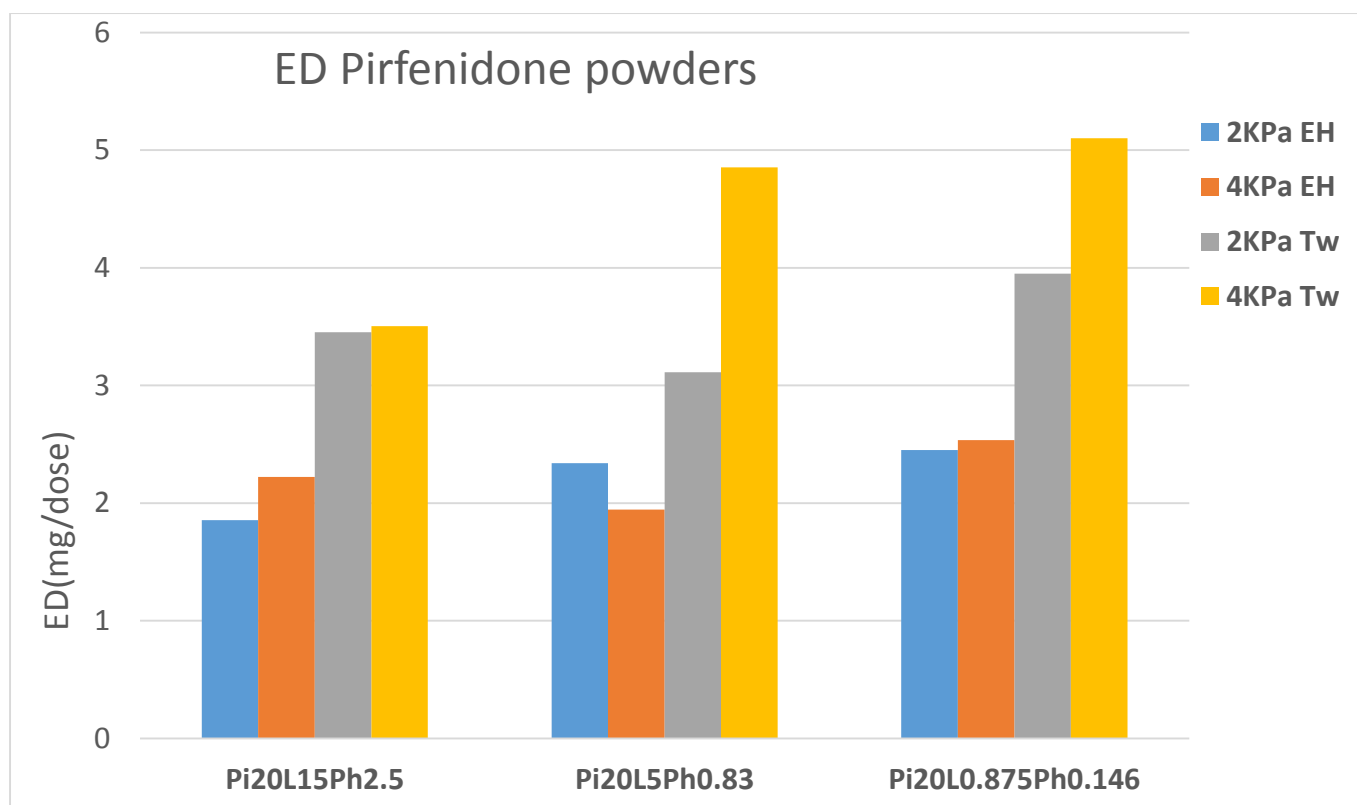


Figure 18. EDs of Pirfenidone powders at different pressure drops using different inhalers. Abbreviation used: EH, Easyhaler; Tw, Twister

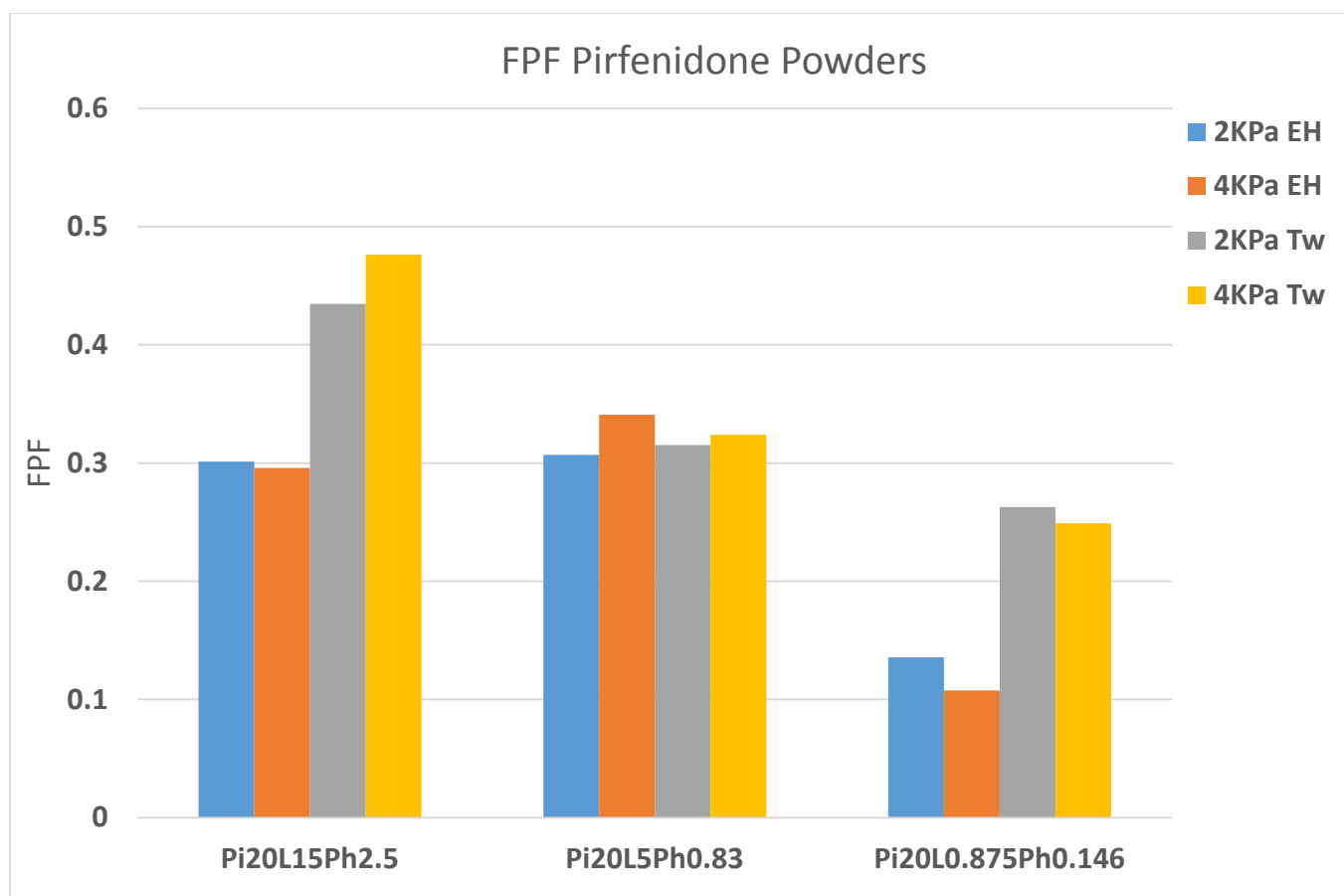


Figure 19. FPFs of Pirfenidone powders at different pressure drops using different inhalers

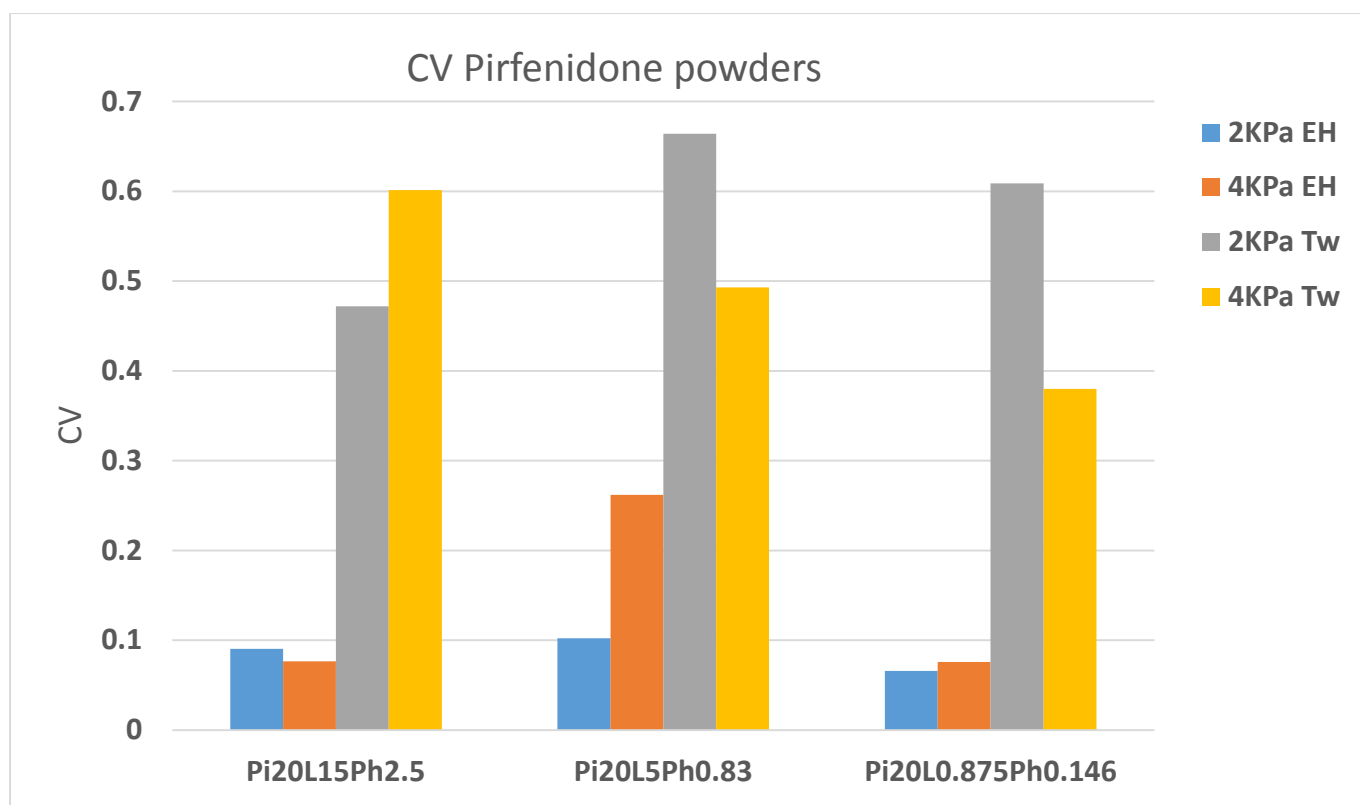


Figure 20. Variation coefficients of EDs (CVs) of Pirfenidone powders at different pressure drops using different inhalers

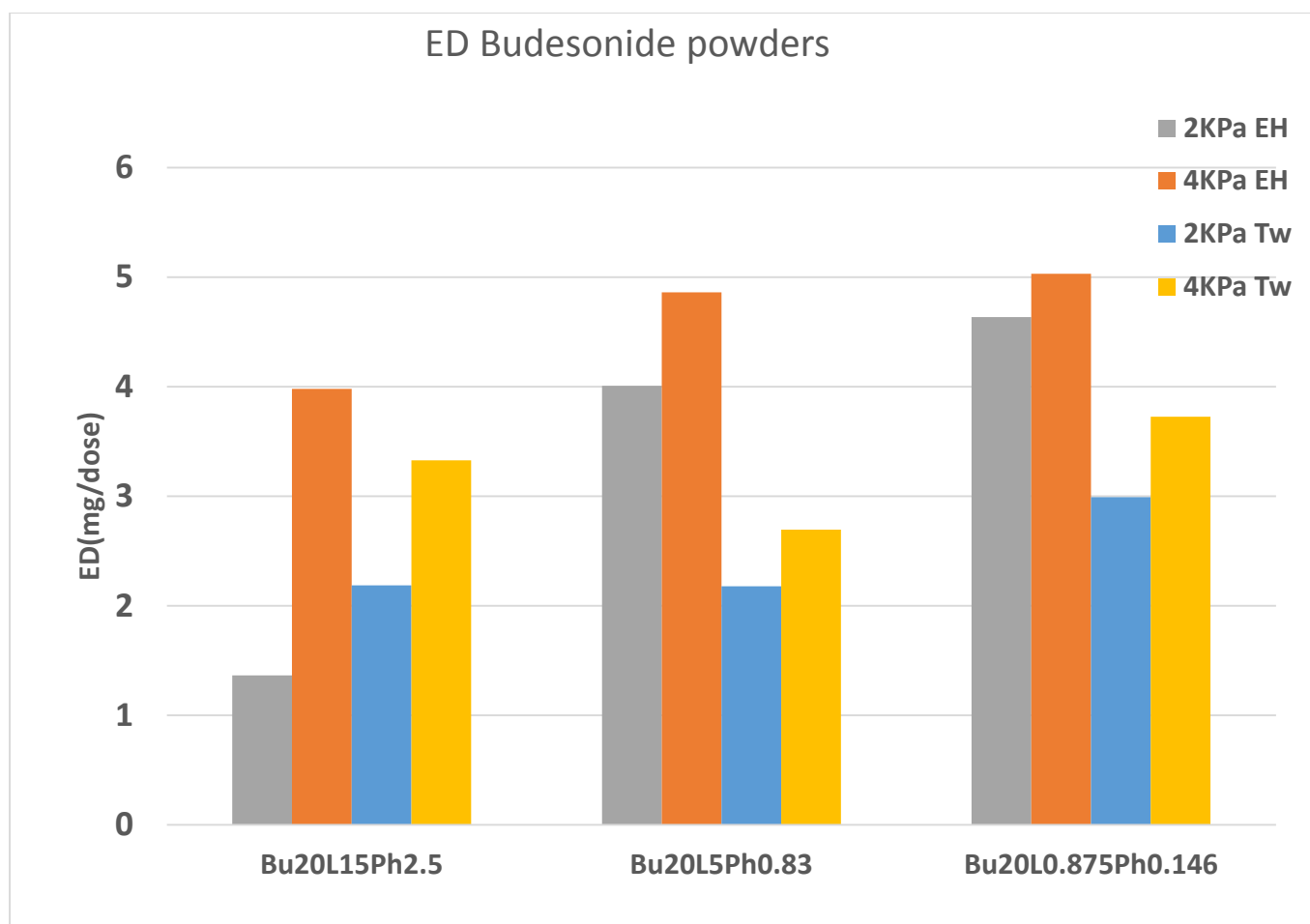


Figure 21. EDs of Budesonide powders at different pressure drops using different inhalers

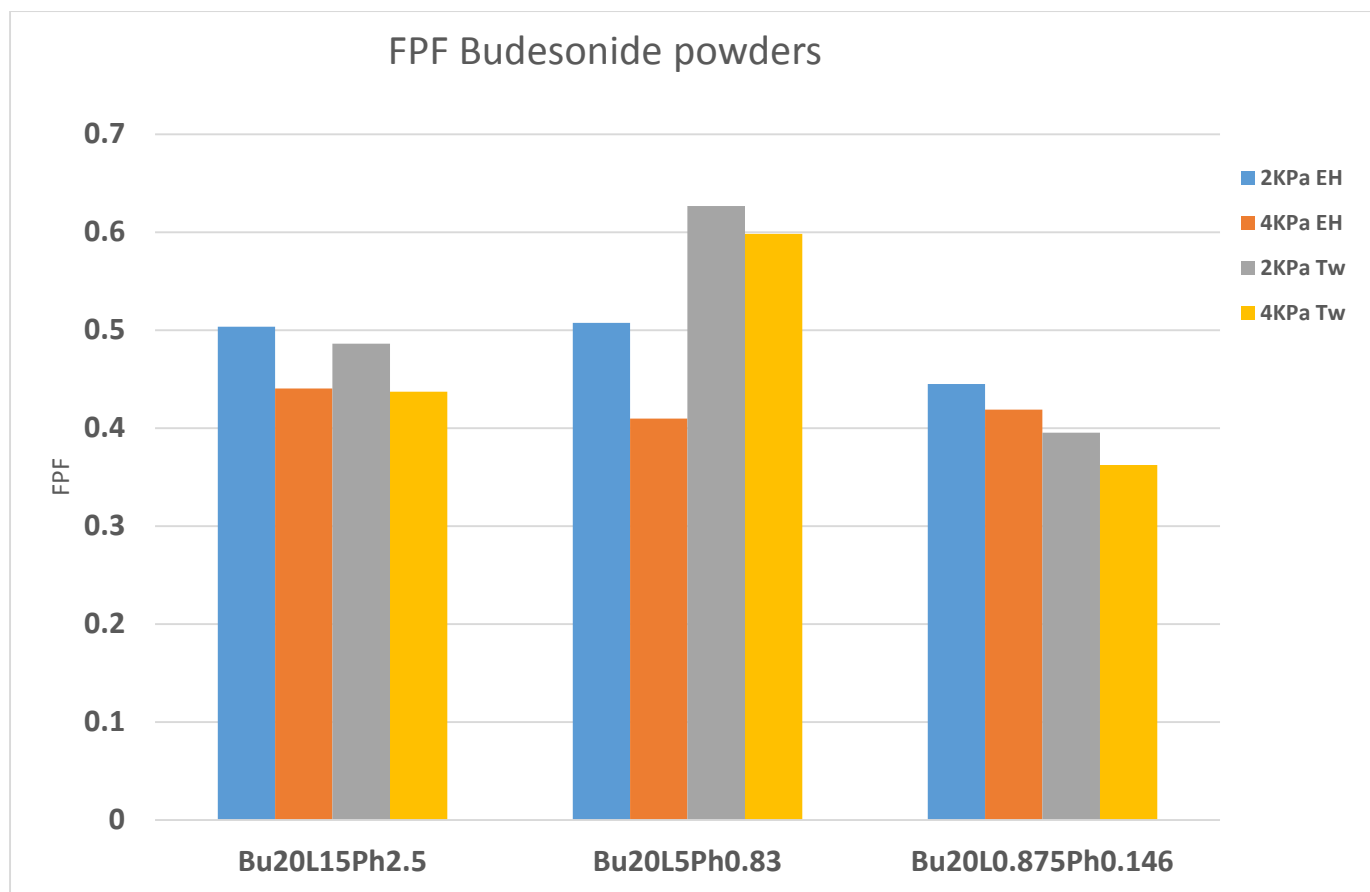


Figure 22. FPFs of Budesonide powders at different pressure drops using different inhalers

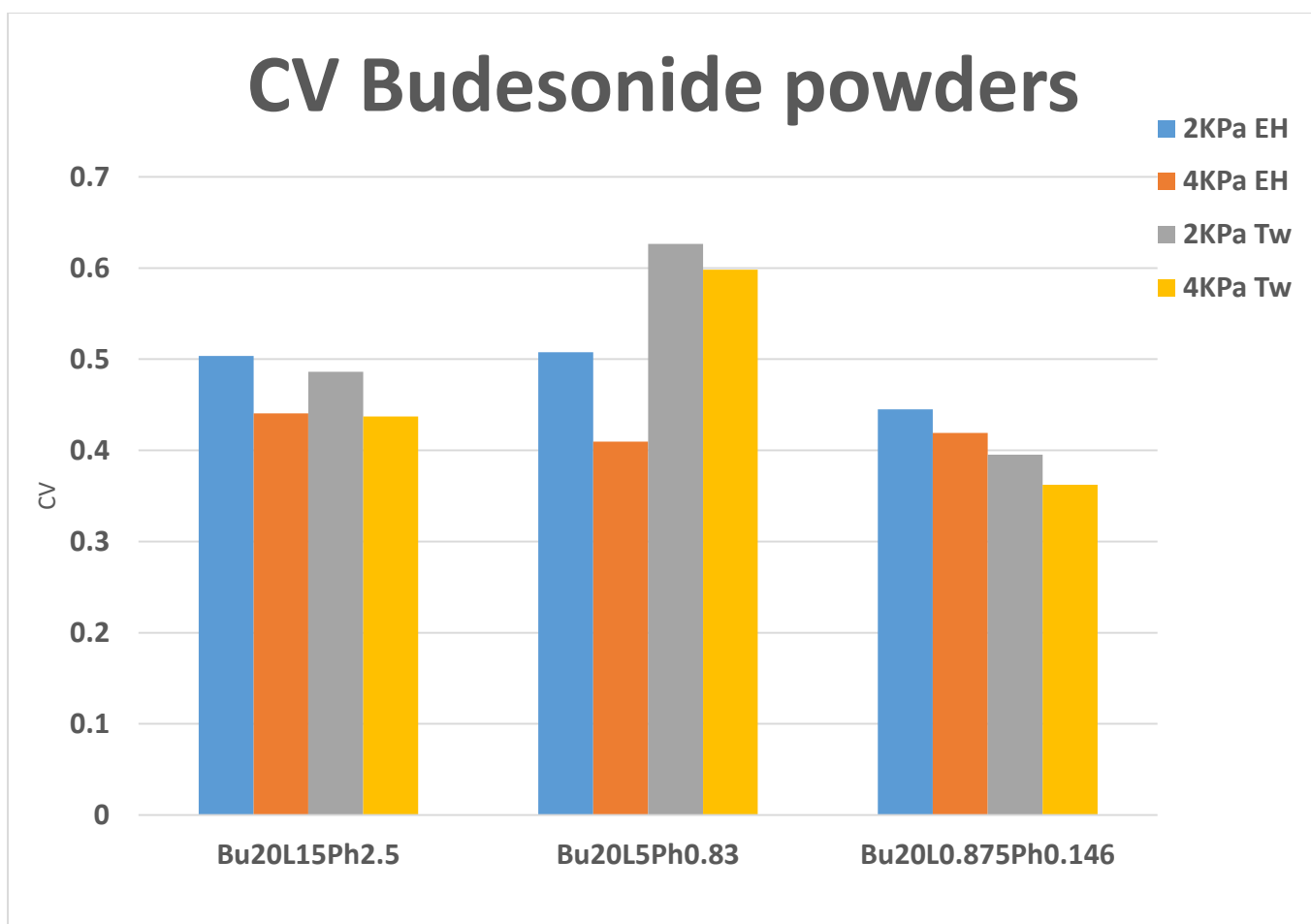


Figure 23. Variation coefficients of EDs (CVs) of Budesonide powders at different pressure drops using different inhalers

Assuming the density of the fine powder particles to be 1g/cm^3 , their MMAD and GSD values were obtained as shown in tables 8 to 11 below.

Table 8. Dispersion results using Easyhaler with pressure drop of 2 kPa across device

Sample	ED (mg)	CV _{ED}	FPF (%)	MMAD (μm)	GSD
Pi20L0.875Ph0.146	2.45	0.07	13.6	5.69	1.77
Pi20L5Ph0.83	2.34	0.10	30.7	5.48	1.47
Pi20L15Ph2.5	1.86	0.09	30.0	2.52	1.09
Bu20L0.875Ph0.146	4.63	0.04	44.5	2.05	1.66

Bu20L5Ph0.83	4.01	0.16	50.8	2.33	1.62
Bu20L15Ph2.5	1.36	0.49	50.4	1.93	1.60

Table 9. Dispersion results using Easyhaler with pressure drop of 4 kPa across device

Sample	ED (mg)	CV_{ED}	FPF (%)	MMAD (μm)	GSD
Pi20L0.875Ph0.146	2.54	0.08	10.8	6.29	1.73
Pi20L5Ph0.83	1.95	0.26	34.1	3.61	1.54
Pi20L15Ph2.5	2.22	0.08	29.5	3.96	1.44
Bu20L0.875Ph0.146	5.03	0.13	41.9	1.61	1.72
Bu20L5Ph0.83	4.86	0.09	41.0	2.44	1.68
Bu20L15Ph2.5	3.98	0.21	44.1	1.87	1.65

Table 10. Dispersion results using Twister with pressure drop of 2 kPa across device

Sample	ED (mg)	CV_{ED}	FPF (%)	MMAD (μm)	GSD
Pi20L0.875Ph0.146	3.95	0.61	26.3	5.10	1.39
Pi20L5Ph0.83	3.11	0.66	31.5	4.08	1.46
Pi20L15Ph2.5	3.46	0.47	43.4	4.09	1.55
Bu20L0.875Ph0.146	2.99	0.11	39.5	1.16	1.72
Bu20L5Ph0.83	2.18	0.58	62.7	1.53	1.69
Bu20L15Ph2.5	2.19	0.57	48.6	1.42	1.67

Table 11. Dispersion results using Twister with pressure drop of 4 kPa across device

Sample	ED (mg)	CV_{ED}	FPF (%)	MMAD (μm)	GSD
Pi20L0.875Ph0.146	5.10	0.38	24.9	5.66	1.53
Pi20L5Ph0.83	4.86	0.49	32.4	4.40	1.49
Pi20L15Ph2.5	3.51	0.60	47.6	4.10	1.77
Bu20L0.875Ph0.146	3.73	0.20	36.2	1.19	1.93
Bu20L5Ph0.83	2.69	0.26	59.8	1.41	1.66
Bu20L15Ph2.5	3.33	0.14	43.7	1.40	1.65

6. DISCUSSION

6.1. Particle Composition and Morphology

6.1.1. Particle composition

Fine powder particles were formed by the aerosol flow reactor method and the PVD of leucine onto the dried spherical drug particles. When using leucine as a coating material, two main features associated with the saturation of leucine are exploited as described above. Table 7 summarises the compositions of precursor solutions and their respective fine powders. Precursor solutions were prepared using a constant leucine/DPPC mass ratio of 6:1. However, this leucine/DPPC ratio was not maintained after the aerosol process, as seen in table 7. It is observed that there was a tremendous reduction in leucine content in all the powders produced. The leucine contents in Pi20L0.875Ph0.146, Pi20L5Ph0.83 and Pi20L15Ph2.5 decreased from 4.2%, 19.4% and 40.0% in the precursor solutions to 0.7%, 0.9% and 0.9% in the fine powders produced, respectively. Similar leucine reductions also occurred in the budesonide powders. The leucine concentrations in Bu20L0.875Ph0.146, Bu20L5Ph0.83 and Bu20L15Ph2.5 dropped from 4.2%, 19.4% and 40.0% in the precursor solutions to 0.4%, 0.5% and 0.5% in the fine powders respectively.

This study was performed at a reactor temperature of 180°C. At this temperature, all of the leucine present in the precursor solution may not be completely vaporized. The partial evaporation of leucine apart from heterogeneous nucleation and subsequent crystal growth on drug particle leads to homogenous nucleation (self-nucleation) of leucine vapour forming small nano-sized leucine particles resulting in bimodal size distribution composed of two size fractions. These self-nucleated leucine particles formed by are smaller in size than the cut off limit of the cyclone used, hence they were not collected by the cyclone.

Another possible cause of leucine loss in the fine powders could be due to some leucine vapour being lost to the internal walls of the reactor. However, this might only be a minor issue. The major part of the leucine losses is suspected to have resulted from the homogenous nucleation leading to cyclone losses as explained above. These losses affected the leucine/DPPC ratio in the produced fine powders and they did not have the 6:1 leucine/DPPC ratio as in their precursor solutions. Therefore, the content of leucine by back-calculation method should be taken with caution. The actual reason for the losses was not investigated in this work.

6.1.2. Particle morphology

Figures 16 and 17 show the SEM images of the leucine coated fine powders with pirfenidone and budesonide. The particles in figure 16 looked wrinkled and not perfectly spherical. The non-spherical appearance of the particles could be possibly linked to thermodynamics properties such melting and glass transition temperature of core drug, pirfenidone. Budesonide, being able to withstand high temperatures of over 200°C produced perfectly spherical powder particles as seen in figure 17. The budesonide powders were much less agglomerated than the pirfenidone powders. At even low leucine concentrations (Figure 16a), there was no agglomeration due to the spherical nature of the particles and hence very little surface contact of the particles. The little surface contact between some of the particles is not expected to negatively affect the powder flowability or dispersibility.

The pirfenidone powders from figure 16 indicate much more surface contact between the particles. However, the presence of the leucine coating on the surface is expected to counteract the effect the surface contact might have on the powder dispersibility. The pirfenidone particles being non-spherical were also rough on the surface. This means although the particles are in close contact with each other, they can be easily dispersed into individual particles with the aid of the proper inhalation device. As seen in figure 16, the agglomeration of particles tends to increase more with decreasing leucine content. The leucine coating provides the particles with some surface roughness to improve the powder flowability. With decreasing leucine concentration, there is less roughness and more agglomeration between the particles.

In figure 17, the leucine coated budesonide powders being perfect spheres also had some asperities on the surface. The roughness from the leucine coating is seen to decrease with decreasing leucine concentration.

6.2. Powder Dispersibility and Particle Size Distribution

6.2.1. Powder dispersibility

ED, CV_{ED} and FPF are essential parameters for inhalation therapy. This is because dose uniformity or repeatability and powder flowability are determined by the CV_{ED} and ED respectively. The lower the CV_{ED} , the better the dose uniformity or repeatability. Higher ED values means better powder flowability. The FPF gives an indication of the powders' dispersibility i.e. deagglomeration, and MMAD and related GSD give an indication of the size range of particles being emitted. In carrier-free drug formulations, the results of these parameters yield solely from the fine powders' properties such as shape, size and surface roughness. For fine particles within the respirable size range of 1-5 μ m, the strong inter-particulate cohesive forces cause the particles to agglomerate, leading to poor powder flow and dispersion. The leucine coating on the spherical fine particles formed from the aerosol reactor

reduce powder agglomeration and improve the flow. With an improved flow, there is better dose uniformity of the drug powder.

The results are from the experiments performed under two pressure drops (2kPa and 4kPa), using two different inhalers (Easyhaler and Twister). The fine powders behaved differently with different inhalers and at different pressure drops. All the experiments were performed under fast inhalation profiles, where the fine powder emission from the inhalation device was completed in 2 seconds. ED of the same powder varied under different pressure drops and also with the different inhalers. Using the Easyhaler at a pressure drop of 2kPa, EDs of the fine coated powders decreased with increasing leucine content. The powders with the least leucine concentration showed the highest ED values. The variation coefficients of these ED values (CV_{ED} in table 8) were very low; approximately 0.1 in all the fine powders except Bu20L15Ph2.5 (whose CV_{ED} was almost 0.5). This means the dose delivery were consistent in most powders. The lower the CV_{ED} , the better the dose uniformity.

Budesonide powders showed good FPF values which were higher than those of pirfenidone powders. The FPF values of the budesonide powders ranged from 44.5% to 50.8%. Pirfenidone fine powders, on the other hand showed low FPF values ranging from 13.6% to 30.7%. In both cases (pirfenidone and budesonide powders), the powders with least leucine content (Pi20L0.875Ph0.146 and Bu20L0.875Ph0.146) had the lowest FPF values, followed by powders with highest leucine concentration. Among the pirfenidone fine powders, Pi20L5Ph0.83 had the highest FPF value and Bu20L5Ph0.83 had the overall highest FPF value in all of the fine powders produced. The budesonide powder with highest leucine content which did not perform too well in terms of dose consistency also showed a good FPF of over 50%. Using the Easyhaler at a pressure drop of 2kPa, the budesonide powders, even with the least leucine concentration showed better dispersibility capabilities than the pirfenidone powders. This is due to the well-rounded particles with little inter-particulate surface contact.

At a higher pressure drop (4 kPa) across the same inhalation device, higher doses of all the fine powders were emitted, except for the Pi20L5Ph0.83 powder which had a lower ED when the pressure drop was increased. The CV_{ED} and FPF values showed similar results to those in table 8. There was good dose consistency in all powders, even in the Bu20L15Ph2.5 powder. Budesonide powders again showed higher FPF (over 40%) than the pirfenidone powders (ranging from 10% to 30%). The change in pressure drop across the inhalation device did not significantly affect the powders' dispersibilities.

In the case of Twister inhaler, the CV_{ED} values of the fine powders (ranging from 0.11 to 0.66) were higher than from the Easyhaler used at the same pressure drop (table 8). This means there was poor dose uniformity when the capsule inhaler was used. In terms of FPF values, pirfenidone powders showed better dispersibility with the Twister inhaler than when the Easyhaler was used. Bu20L5Ph0.83 powder achieved the highest and best FPF of 62.7% when the Twister inhaler was used. This was also the overall highest and best FPF of all the powders at both pressure drops and both inhalation devices. The EDs of all the powders was increased when the pressure drop was increased from 2kPa to 4kPa. At 2kPa, the EDs of the fine powders

ranged from 2.18 to 3.95mg/dose. These values increased when the pressure drop across the same device was increased. At 4kPa, the ED values ranged from 2.69 to 5.10mg/dose. The CV_{ED} values were similar to those at 2kPa with the same inhalation device, Twister (table 10). In both tables 10 and 11, CV_{ED} values were higher than when Easyhaler was used at the same pressure drop. This shows that there was lesser dose uniformity when the Twister inhaler was used. FPF values in tables 10 and 11 were quite similar. The change in pressure drop did not significantly affect the powder dispersibility. The Twister inhaler again improved the powders' dispersibilities.

This was especially beneficial to the pirfenidone powders, as they were strongly agglomerated and did not show good enough dispersibilities when Easyhaler was used. The particle detachment mechanism achieved with the capsule-based inhaler, Twister, also improved the flowability (higher EDs) of pirfenidone coated powders which were rather agglomerated.

6.2.2. Particle size distribution

Generally, particles with MMAD of over 5µm are considered to be too large for deep lung deposition. Finer particles with MMAD less than 5µm are often preferred for inhalation therapy. Achieving an MMAD of 2-3µm is a frequent goal in formulating inhalation drugs. Particles sizes within this diameter are most probable to be successfully inhaled and deposited in the deep lungs. A relatively low MMAD coupled with a low GSD indicates narrow particle distribution centred on a fine particle size, meaning the particles are better suited for deep lung deposition as desired.

Comparing the different inhalers at the same pressure drops (comparing tables 8 and 10, and tables 9 and 11), all the budesonide powders showed a decrease in MMADs with the Twister inhaler. However, even with the Easyhaler where the particles could not be detached properly upon emission, the particle sizes were still relatively low. MMADs of all budesonide powders irrespective of the type of inhaler or the pressure drop ranged from 2.44 to 1.16µm. These MMADs were coupled with relatively low GSDs (<2.0) which makes the budesonide powder particles most probable to be deposited in the deep lungs. However, the budesonide powders with higher leucine contents seemed to have higher MMADs than the powder with least leucine content (Bu20L0.875Ph0.146). In all the experiments with both inhalation devices and different pressure drops, the Bu20L0.875Ph0.146 powder particles had the lowest MMAD. In figure 17, the SEM images of budesonide powders at varying leucine concentrations revealed spherical particles with minor inter-particulate surface contact. The powder particles with the least leucine content showed much smoother spheres than the powder particles with higher leucine content. The leucine coating created surface asperities or roughness on the powder particles. In spherical particles with little surface contact, there could be a possibility that the asperities created by leucine could interlock with each other as the particles come in close contact. Hence more asperities will cause more interlocking of the particles and consequently result in slightly larger (higher MMADs) particles being emitted. In the powder with the least leucine concentration (Bu20L0.875Ph0.146), there is less leucine coating and hence less

asperities which could cause the particles to adhere to each other. This powder yielded particles with the lowest MMAD values in all the dispersion experiments performed. The increase in MMAD was only slight reaching a maximum of 2.44 μ m, which is still within the desired range (<5 μ m) for deeper lung deposition.

In the pirfenidone powders, the SEM images showed agglomeration of the powder particles which increased as the leucine concentration reduced. The particles were not as spherical as seen in the budesonide powder particles. As a result, there was greater surface contact between the pirfenidone powder particles. In this case, the leucine coating (asperities) seemed to help to separate the particle agglomerates and hence lower MMADs. The choice of inhalation device also affected the MMAD of the particles after emission. The particle detachment mechanism of the Twister helped to break particle agglomerates apart. This mechanism helped to bring the MMAD values of powders with more surface roughness (Pi20L15Ph2.5 and Pi20L5Ph0.83) lower to <5 μ m. The powder with the least leucine content (Pi20L0.875Ph0.146) had MMAD values greater than 5 μ m even when Twister inhaler was used. This powder had particles with much less surface asperities and hence more agglomerated. The particles were also not spherical so it was rather difficult for the agglomerates to be detached.

7. CONCLUSIONS

Carrier-free drug formulation with leucine coating have been produced for inhalation therapy for poorly soluble drugs. Anti-inflammatory corticosteroid, Budesonide and anti-fibrotic drug, Pirfenidone have been used as the APIs. Both of these drugs are soluble in ethanol and their precursor solutions were ethanol-based. A small amount (least concentration of the powder components) of surfactant, DPPC, was added to the formulation to enhance the powder properties. Precursor solutions were prepared at various leucine concentrations for both drugs.

The aerosol flow reactor method was used to produce spherical drug particles which were coated with leucine by PVD. The coated drug powders with varying concentrations of leucine were produced and their aerosolization behaviours were investigated in vitro. The aerosolization behaviour of the coated fine powders were studied with different inhalation devices and at varying pressure drops set across the devices.

With the same inhaler, pressure drop did not affect dispersibility or FPF, but affects the ED. Higher pressure drop emitted higher doses. The choice of inhalation device showed some variations in the CV_{ED} values. Doses were more uniform (lower CV_{ED}) when the Easyhaler was used. The use of Twister showed much higher CV_{ED} values, which means less repeatability in the doses.

The inhalation device affected the dose uniformity. Experiments performed with reservoir type inhaler Easyhaler produced more uniform emitted doses (lower CV_{ED}) than capsule single dose Twister. Using the Twister inhaler, the CV_{ED} values were higher in both pressure drops. This means the inhalation device did not provide highly consisted emitted doses. However, the use of Twister inhaler improved the powder dispersibility especially in the agglomerated pirfenidone powders. The FPFs were higher than when Easyhaler was used. The emission technology used by the Twister inhaler helps to break agglomerated particles apart as the powder leaves the inhaler mouthpiece.

Comparing fine powders with same leucine contents in their precursor solutions but with different APIs (Pirfenidone and Budesonide), their morphologies were different. The Pirfenidone powders being agglomerated affected their aerosolization properties when Easyhaler was used. The Budesonide powders, on the other hand, with very spherical particles showed good dispersibility as well as particle size distribution with both inhalers. The best powder being Bu20L5Ph0.83 with the overall highest FPF (fraction of emitted dose less than $5\mu\text{m}$) had good flowability and particle size distribution at both pressure drops and varying inhalers, making it suitable for deep lung deposition. The Pirfenidone powder Pi20L0.875Ph0.146 showed the worst aerosolization properties due to strong particle agglomeration and low leucine concentration. Although the Twister inhaler improved the aerosolization properties to an extent, this powder still had the lowest FPF and highest MMAD of over $5\mu\text{m}$. Among the Pirfenidone powders, Pi20L15Ph2.5 showed the best properties with

the use of Twister inhaler. FPFs at different pressure drops reached over 40% and MMAD values were below 5 μ m. This same powder also had MMAD values below 5 μ m with the Easyhaler, but FPF not as high as when Twister was used. This formulation may also be suited for deep lung deposition. The presence of leucine nanocrystals coated around fine powder particles have improved their aerosolization behaviours for pulmonary therapy. The amount of leucine required for the best properties varied between the APIs, due to differences in their fine particle morphologies. From this work, it has been shown that the aerosol flow reactor method is a feasible way to formulate carrier -poorly soluble drugs. Even when the particles were not perfectly spherical (as seen in Pirfenidone powders), the leucine coating and presence of DPPC improved the powder aerosolization properties.

REFERENCES

- [1] K. Wadher, R. Kalsait, and M. Umekar, "Pulmonary Insulin Delivery: Challenges and Current Status," vol. 3, no. 2, pp. 1052–1059, 2011.
- [2] N. R. Labiris and M. B. Dolovich, "Pulmonary drug delivery. Part II: The role of inhalant delivery devices and drug formulation in therapeutic effectiveness of aerosolized medications," *Br. J. Clin. Pharmacol.*, vol. 56, no. 6, pp. 588–599, 2003.
- [3] C. Schleh, B. Rothen-Rutishauser, and W. G. Kreyling, "The influence of pulmonary surfactant on nanoparticulate drug delivery systems," *Eur. J. Pharm. Biopharm.*, vol. 77, no. 3, pp. 350–352, Apr. 2011.
- [4] J. S. Patil and S. Sarasija, "Pulmonary drug delivery strategies: A concise, systematic review," *Lung India*, vol. 29, no. 1, pp. 44–49, 2012.
- [5] Z. Liang, R. Ni, J. Zhou, and S. Mao, "Recent advances in controlled pulmonary drug delivery.," *Drug Discov. Today*, vol. 20, no. 3, pp. 380–9, Mar. 2015.
- [6] J. S. Patton, J. G. Bukar, and M. A. Eldon, "Clinical pharmacokinetics and pharmacodynamics of inhaled insulin.," *Clin. Pharmacokinet.*, vol. 43, no. 12, pp. 781–801, Jan. 2004.
- [7] M. Haghi, H. X. Ong, D. Traini, and P. Young, "Across the pulmonary epithelial barrier: Integration of physicochemical properties and human cell models to study pulmonary drug formulations.," *Pharmacol. Ther.*, vol. 144, no. 3, pp. 235–52, Dec. 2014.
- [8] N. R. Labiris and M. B. Dolovich, "Pulmonary drug delivery. Part I: Physiological factors affecting therapeutic effectiveness of aerosolized medications," *Br. J. Clin. Pharmacol.*, vol. 56, no. 6, pp. 588–599, Aug. 2003.
- [9] J. A. Tolman and R. O. Williams, "Advances in the pulmonary delivery of poorly water-soluble drugs: influence of solubilization on pharmacokinetic properties," *Drug Development and Industrial Pharmacy*, vol. 36, no. 1, pp. 1–30, 2010.
- [10] A. S. PhD, "Pulmonary Drug Delivery—Particle Engineering for Inhaled Therapeutics."
- [11] A. A. of P. Scientists, *AAPS Advances in the Pharmaceutical Sciences Series*. .
- [12] H. W. Frijlink and a H. De Boer, "Dry powder inhalers for pulmonary drug delivery.," *Expert Opin. Drug Deliv.*, vol. 1, no. 1, pp. 67–86, 2004.
- [13] J. Raula, A. Lähde, and E. I. Kauppinen, "Aerosolization behaviour of carrier-free l-leucine coated salbutamol sulphate powders," *Int. J. Pharm.*, vol. 365, no. November, pp. 18–25, 2009.
- [14] N. El-Gendy, M. Bailey, and C. Berkland, "Particle Engineering Technologies for

- Pulmonary Drug Delivery,” *Control. Pulm. Drug Deliv.*, vol. 24, no. 3, pp. 283–312, 2011.
- [15] G. Chimote and R. Banerjee, “Evaluation of antitubercular drug-loaded surfactants as inhalable drug-delivery systems for pulmonary tuberculosis,” *J. Biomed. Mater. Res. A*, vol. 89, no. 2, pp. 281–92, May 2009.
 - [16] Y. Kawabata, K. Wada, M. Nakatani, S. Yamada, and S. Onoue, “Formulation design for poorly water-soluble drugs based on biopharmaceutics classification system: Basic approaches and practical applications,” *Int. J. Pharm.*, vol. 420, no. 1, pp. 1–10, 2011.
 - [17] J. A. Tolman and R. O. Williams, “Advances in the pulmonary delivery of poorly water-soluble drugs: influence of solubilization on pharmacokinetic properties,” *Drug Dev. Ind. Pharm.*, vol. 36, no. 1, pp. 1–30, 2010.
 - [18] E. Procedures, “New Technology for,” vol. 47, no. 3, pp. 195–198, 2008.
 - [19] R. Stevens, “Gray’s Anatomy for Students,” *Annals of the Royal College of Surgeons of England*, vol. 88, no. 5. pp. 513–514, 2006.
 - [20] D. A. Groneberg, C. Witt, U. Wagner, K. F. Chung, And A. Fischer, “Fundamentals of pulmonary drug delivery,” *Respir. Med.*, vol. 97, no. 4, pp. 382–387, 2003.
 - [21] Q. Hamid, Joanne Shannon, and James Martin, “Physiological basis of respiratory disease: Histology and gross anatomy of the respiratory tract,” 2005.
 - [22] C. G. Irvin, “Pulmonary physiology,” in *Asthma and COPD*, 2009, pp. 53–69.
 - [23] V. C. Scanlon and T. Sanders, *Essentials of anatomy and physiology*. 2007.
 - [24] A. Hidalgo, A. Cruz, and J. Pérez-Gil, “Barrier or carrier? Pulmonary surfactant and drug delivery,” *Eur. J. Pharm. Biopharm.*, no. November, 2015.
 - [25] N. Wauthoz and K. Amighi, “Phospholipids in pulmonary drug delivery,” *Eur. J. Lipid Sci. Technol.*, vol. 116, no. 9, pp. 1114–1128, 2014.
 - [26] W. Beachey, *Respiratory Care Anatomy and Physiology, Foundations for Clinical Practice, 3: Respiratory Care Anatomy and Physiology*. Elsevier Health Sciences, 2013.
 - [27] J. E. Tomashefski, P. T. Cagle, C. F. Farver, and A. E. Fraire, *Dail and Hammar’s Pulmonary Pathology*, vol. I. New York, NY: Springer New York, 2008.
 - [28] C. de Souza Carvalho, N. Daum, and C.-M. Lehr, “Carrier interactions with the biological barriers of the lung: Advanced in vitro models and challenges for pulmonary drug delivery,” *Adv. Drug Deliv. Rev.*, vol. 75, pp. 129–140, 2014.
 - [29] J. J. Haitisma, U. Lachmann, and B. Lachmann, “Exogenous surfactant as a drug delivery agent,” *Adv. Drug Deliv. Rev.*, vol. 47, no. 2–3, pp. 197–207, 2001.
 - [30] M. Hoppentocht, P. Hagedoorn, H. W. Frijlink, and A. H. de Boer, “Technological and practical challenges of dry powder inhalers and formulations,” *Adv. Drug Deliv. Rev.*,

- vol. 75, pp. 18–31, 2014.
- [31] B. K. Rubin and R. W. Williams, “Emerging aerosol drug delivery strategies: From bench to clinic,” *Adv. Drug Deliv. Rev.*, vol. 75, pp. 141–148, 2014.
 - [32] J. G. Weers, T. E. Tarara, and A. R. Clark, “Design of fine particles for pulmonary drug delivery,” *Expert Opin. Drug Deliv.*, vol. 4, no. 3, pp. 297–313, 2007.
 - [33] R. W. Dal Negro, “Dry powder inhalers and the right things to remember: a concept review,” *Multidiscip. Respir. Med.*, vol. 10, no. 1, p. 13, Jan. 2015.
 - [34] P. Khadka, J. Ro, H. Kim, I. Kim, J. T. Kim, H. Kim, J. M. Cho, G. Yun, and J. Lee, “Pharmaceutical particle technologies: An approach to improve drug solubility, dissolution and bioavailability,” *Asian J. Pharm. Sci.*, vol. 9, no. 6, pp. 304–316, 2014.
 - [35] A. Dahan and J. M. Miller, “The Solubility–Permeability Interplay and Its Implications in Formulation Design and Development for Poorly Soluble Drugs,” *AAPS J.*, vol. 14, no. 2, pp. 244–251, 2012.
 - [36] E. M. Merisko-Liversidge and G. G. Liversidge, “Drug Nanoparticles: Formulating Poorly Water-Soluble Compounds,” *Toxicol. Pathol.*, vol. 36, no. 1, pp. 43–48, 2008.
 - [37] A. Nokhodchi and G. P. Martin, *Pulmonary Drug Delivery: Advances and Challenges*. Wiley, 2015.
 - [38] B. Ganesh, R. Ankita, and K. Preeti, “A New Emerging Technique for Bioavailability Enhancement,” 2013.
 - [39] R. Yadollahi, K. Vasilev, and S. Simovic, “Nanosuspension Technologies for Delivery of Poorly Soluble Drugs,” vol. 2015, no. iii, 2015.
 - [40] V. R. Patel and Y. K. Agrawal, “Nanosuspension: An approach to enhance solubility of drugs,” *J. Adv. Pharm. Technol. Res.*, vol. 2, no. 2, pp. 81–7, Apr. 2011.
 - [41] G. Pilcer and K. Amighi, “Formulation strategy and use of excipients in pulmonary drug delivery,” *Int. J. Pharm.*, vol. 392, no. 1–2, pp. 1–19, 2010.
 - [42] P. Mack, K. Horvath, J. Tully, and B. Maynor, “Particle engineering for inhalation formulation and delivery of biotherapeutics,” *Inhalation*, vol. 6, pp. 16–20, 2012.
 - [43] A. M. Healy, M. I. Amaro, K. J. Paluch, and L. Tajber, “Dry powders for oral inhalation free of lactose carrier particles,” *Adv. Drug Deliv. Rev.*, vol. 75, pp. 32–52, 2014.
 - [44] Q. T. Zhou, S. S. Y. Leung, P. Tang, T. Parumasivam, Z. H. Loh, and H.-K. Chan, “Inhaled formulations and pulmonary drug delivery systems for respiratory infections,” *Adv. Drug Deliv. Rev.*, vol. 85, pp. 83–99, May 2015.
 - [45] J. Raula, A. Kuivanen, A. Lähde, and E. I. Kauppinen, “Gas-phase synthesis of l-leucine-coated micrometer-sized salbutamol sulphate and sodium chloride particles,” *Powder Technol.*, vol. 187, no. 3, pp. 289–297, 2008.

- [46] H. Eerikäinen, W. Watanabe, E. I. Kauppinen, and P. P. Ahonen, "Aerosol flow reactor method for synthesis of drug nanoparticles," *Eur. J. Pharm. Biopharm.*, vol. 55, no. 3, pp. 357–360, 2003.
- [47] E. I. Kauppinen, A. Lähde, and J. Raula, "Production of L-leucine nanoparticles under various conditions using an aerosol flow reactor method," *J. Nanomater.*, vol. 2008, no. 1, 2008.
- [48] J. Raula, A. Rahikkala, T. Halkola, J. Pessi, L. Peltonen, J. Hirvonen, K. Järvinen, T. Laaksonen, and E. I. Kauppinen, "Coated particle assemblies for the concomitant pulmonary administration of budesonide and salbutamol sulphate," *Int. J. Pharm.*, vol. 441, no. 1–2, pp. 248–54, Jan. 2013.
- [49] J. Raula, A. Kuivanen, A. Lähde, H. Jiang, M. Antopolsky, J. Kansikas, and E. I. Kauppinen, "Synthesis of L-leucine nanoparticles via physical vapor deposition at varying saturation conditions," *J. Aerosol Sci.*, vol. 38, no. 12, pp. 1172–1184, 2007.
- [50] D. Hira, T. Okuda, D. Kito, K. Ishizeki, T. Okada, and H. Okamoto, "Inhalation performance of physically mixed dry powders evaluated with a simple simulator for human inspiratory flow patterns," *Pharm. Res.*, vol. 27, no. 10, pp. 2131–40, 2010.
- [51] H. Hamishehkar, Y. Rahimpour, and Y. Javadzadeh, "The role of carrier in dry powder inhaler," *Recent Adv. Nov. Drug Carr. Syst. InTech Open Access Publ.*, pp. 39–66, 2012.
- [52] Q. T. Zhou, P. Tang, S. S. Y. Leung, J. G. Y. Chan, and H. K. Chan, "Emerging inhalation aerosol devices and strategies: Where are we headed?," *Adv. Drug Deliv. Rev.*, vol. 75, pp. 3–17, 2014.
- [53] T. Srichana, G. P. Martin, and C. Marriott, "Dry powder inhalers: The influence of device resistance and powder formulation on drug and lactose deposition in vitro," *Eur. J. Pharm. Sci.*, vol. 7, no. 1, pp. 73–80, 1998.
- [54] S. R. B. Behara, I. Larson, P. Kippax, P. Stewart, and D. A. V Morton, "Insight into pressure drop dependent efficiencies of dry powder inhalers," *Eur. J. Pharm. Sci.*, vol. 46, no. 3, pp. 142–148, 2012.
- [55] K. D. Vernon-Parry, "Scanning electron microscopy: an introduction," *III-Vs Rev.*, vol. 13, no. 4, pp. 40–44, 2000.
- [56] W. Zhou, R. P. Apkarian, and Z. L. Wang, "Fundamentals of Scanning Electron Microscopy," *Scanning Microsc. Nanotechnol.*, pp. 1–40, 2007.
- [57] T. B. Picture, "Scanning Electron Microscopy Primer," *Cities*, pp. 1–29, 2007.
- [58] M. Dunlap and J. E. Adaskaveg, "Introduction to the Scanning Electron Microscope," *Microsc. Microanal.*, p. 52, 1997.
- [59] D. Lewis and M. Copley, "Inhaled Product Characterization Calculating Particle-Size Distribution Metrics," *Pharm. Technol.*, pp. 33–37, 2011.
- [60] S. Jiménez and J. Ballester, "Use of a Berner Low-Pressure Impactor at Low Inlet

- Pressures. Application to the Study of Aerosols and Vapors at High Temperature,” *Aerosol Sci. Technol.*, vol. 45, no. 7, pp. 861–871, 2011.
- [61] R. E. Hillamo and E. I. Kauppinen, “On the Performance of the Berner Low Pressure Impactor ,” *Aerosol Sci. Technol.*, vol. 14, no. 1, pp. 33–47, 1991.
 - [62] W. H. Finlay, K. W. Stapleton, and P. Zuberbuhler, “Fine particle fraction as a measure of mass depositing in the lung during inhalation of nearly isotonic nebulized aerosols,” *J. Aerosol Sci.*, vol. 28, no. 7, pp. 1301–1309, 1997.
 - [63] F. Grasmeijer and A. H. de Boer, “The dispersion behaviour of dry powder inhalation formulations cannot be assessed at a single inhalation flow rate.,” *Int. J. Pharm.*, vol. 465, no. 1–2, pp. 165–8, 2014.
 - [64] J. Raula, “Developments in powder formulations of poorly water- soluble drugs,” 2015.
 - [65] E. Kauppinen, J. Kurkela, D. Brown, J. Jokiniemi, And T. Mattila, “Method and Apparatus for Studying Aerosol Sources.” 02-Aug-2002.

APPENDICES

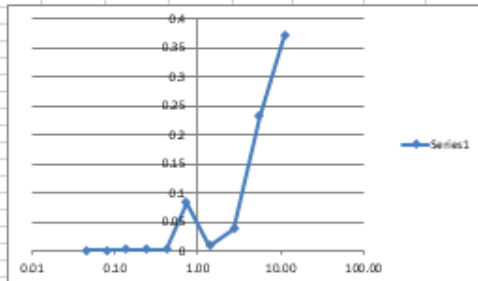
Main flow rate	60	lpm	total flow	175.00	lpm
Feeding rate	1.2	lpm	LPI flow	24.21	lpm
Purifier disc flow rate	38.2	lpm			
Purifier tube flow rate	54.3	lpm	Dilution factor	7.2	

Collection on the stage																
stage	Dq	carrier		fine particles												
		A	B	C	D	E	F	G	H							
start	end	start	end	start	end	start	end	start	end	start	end	start	end	start	end	start
1	0.04	107.931	107.931	87.1611	87.1616	106.174	106.174	106.705	106.705	106.913	106.913	106.751	106.751	107.711	107.712	108.507
2	0.08	106.367	106.367	87.2548	87.2561	107.333	107.333	107.174	107.174	106.96	106.96	107.847	107.847	106.694	106.701	106.821
3	0.13	106.806	106.806	87.3071	87.3092	107.532	107.532	107.066	107.066	107.405	107.405	108.165	108.191	106.404	106.427	107.216
4	0.24	107.032	107.032	87.2197	87.2219	107.007	107.008	107.08	107.096	106.751	106.761	106.577	106.659	107.043	107.129	107.007
5	0.42	107.431	107.431	87.5112	87.5132	107.672	107.673	107.181	107.215	106.345	106.369	107.661	107.802	106.906	107.04	107.377
6	0.72	106.941	106.941	87.7285	87.7311	107.241	107.251	106.326	106.377	106.486	106.521	106.971	107.167	107.143	107.33	107.057
7	1.38	107.825	107.826	87.0037	87.012	107.273	107.283	107.534	107.557	106.751	106.767	107.266	107.373	106.206	106.306	106.823
8	2.75	107.025	107.027	87.0635	87.1017	108.144	108.172	106.253	106.3	107.402	107.431	107.137	107.357	106.774	107.019	106.934
9	5.50	107.565	107.573	87.0401	87.2711	107.192	107.209	107.365	107.407	107.448	107.462	106.524	106.78	106.262	106.617	107.116
10	11.05			87.0812	87.451											107.254

Stage	Dq	A	B	C	D	E	F	G	H
1	0.04	0	0.0005	0	0	0	0	0.001	0
2	0.08	0	0.0013	0	0	0	0.015	0.007	0.005
3	0.13	0	0.0021	0	0.003	0	0.026	0.023	0.006
4	0.24	0	0.0021	0.001	0.016	0.01	0.082	0.086	0.047
5	0.42	0	0.002	0.001	0.034	0.023	0.141	0.134	0.073
6	0.72	0	0.0025	0.01	0.051	0.035	0.196	0.187	0.111
7	1.38	0.001	0.0082	0.01	0.023	0.016	0.107	0.1	0.057
8	2.75	0.002	0.0362	0.028	0.047	0.029	0.22	0.245	0.127
9	5.50	0.008	0.231	0.017	0.042	0.014	0.256	0.355	0.138
10	11.05	0.000	0.3698	0.000	0.000	0.000	0.000	0.000	0.000

Sum, dilution includ	A	B	C	D	E	F	G	H
Marr, total	0.0795	5.3322	0.48422	1.561066	0.91785	7.53793	8.22451	4.07612
Marr, Dq=5.501	0.0795	2.65959	0.48422	1.561066	0.91785	7.53793	8.22451	4.07612

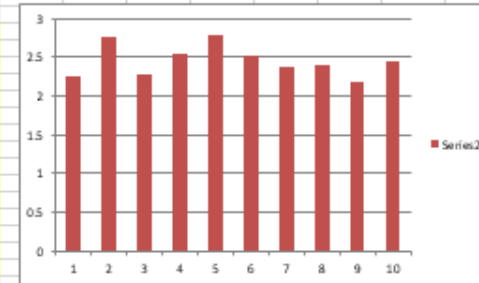
Sum, carrier exclud	A	B	C	D	E	F	G	H
Marr, total	5.253	0.405	1.4816	0.838	7.458	8.145	3.997	
Marr, Dq=5.501		2.58	0.405	1.4816	0.838	7.458	8.145	3.997



ED 2.45125
CV 0.0658

FPD 0.27191
FPF 0.13562

ED	
0	21219.3
1	21217
2	21214.3
3	21212
4	21209.4
5	21206.7
6	21204.1
7	21201.7
8	21199.3
9	21197.1
10	21194.7
TOT	19.61 mg
AVEG	2.45125 mg
STDEV	0.16128



APPENDIX 1: ED, CV_{ED} and FPF of Pi20L0.875Ph0.146 at 2kPa with Easyhaler®

Main flow rate	60	lpm	total flow	175.00	lpm
Feeding rate	1.2	lpm	HLPI flow	24.21	lpm
Purpur dir flow rate	38.2	lpm			
Purpur tube flow rate	54.3	lpm	Dilution factor	7.2	

Collection on the stage																	
		carrier				fine particles											
stage	Dq	A		B		C		D		E		F		G		H	
stage	Dq	start	end	start	end	start	end	start	end	start	end	start	end	start	end	start	end
1	0.04	107.931	107.931	88.1226	88.1294	106.174	106.174	106.705	106.705	106.913	106.913	106.751	106.751	107.711	107.712	108.507	108.507
2	0.08	106.367	106.367	88.1624	88.1635	107.333	107.333	107.174	107.174	106.96	106.96	107.847	107.847	106.694	106.701	106.816	106.821
3	0.13	106.806	106.806	88.122	88.1262	107.532	107.532	107.066	107.069	107.405	107.405	108.165	108.191	106.404	106.427	107.216	107.222
4	0.24	107.032	107.032	88.0928	88.1	107.007	107.008	107.08	107.096	106.751	106.761	106.577	106.659	107.043	107.129	107.007	107.054
5	0.42	107.431	107.431	88.4171	88.4478	107.672	107.673	107.181	107.215	106.345	106.368	107.661	107.802	106.906	107.04	107.377	107.45
6	0.72	106.941	106.941	88.2632	88.2832	107.241	107.251	106.326	106.377	106.486	106.521	106.971	107.167	107.143	107.33	107.057	107.168
7	1.38	107.825	107.826	88.0627	88.1812	107.273	107.283	107.534	107.557	106.751	106.767	107.266	107.373	106.206	106.306	106.823	106.88
8	2.75	107.025	107.027	88.1447	88.2286	108.144	108.172	106.253	106.3	107.402	107.431	107.137	107.357	106.774	107.019	106.934	107.061
9	5.50	107.565	107.573	88.0701	88.7481	107.192	107.209	107.365	107.407	107.448	107.462	106.524	106.78	106.262	106.617	107.116	107.254
10	11.05			88.2453	89.0203												

Stage	Dq	A	B	C	D	E	F	G	H
1	0.04	0	0.0068	0	0	0	0	0.001	0
2	0.08	0	0.0001	0	0	0	0.015	0.007	0.005
3	0.13	0	0.0042	0	0.003	0	0.026	0.023	0.006
4	0.24	0	0.0072	0.001	0.016	0.01	0.082	0.086	0.047
5	0.42	0	0.0307	0.001	0.034	0.023	0.141	0.134	0.073
6	0.72	0	0.12	0.01	0.051	0.035	0.196	0.187	0.111
7	1.38	0.001	0.1186	0.01	0.023	0.016	0.107	0.1	0.057
8	2.75	0.002	0.1839	0.028	0.047	0.029	0.22	0.245	0.127
9	5.50	0.008	0.678	0.017	0.042	0.014	0.256	0.255	0.138
10	11.05	0.000	0.775	0.000	0.000	0.000	0.000	0.000	0.000

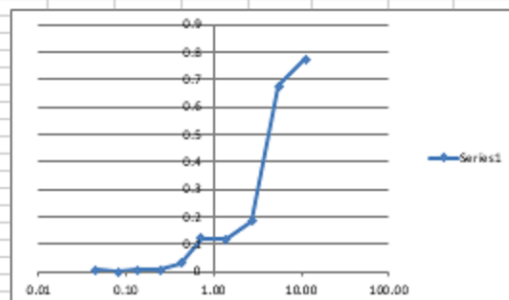
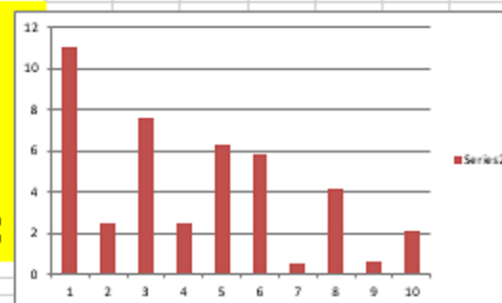
Sum, dilution include	A	B	C	D	E	F	G	H
Marr, total	0.079499	13.90867	0.48422	1.5610664	0.91785	7.537927	8.224507	4.076118
Marr, Dqs 5.501	0.079499	8.30762	0.48422	1.5610664	0.91785	7.537927	8.224507	4.076118

Sum, carrier exclude	A	B	C	D	E	F	G	H
Marr, total		13.83	0.405	1.4816	0.838	7.458	8.145	3.997
Marr, Dqs 5.501		8.228	0.405	1.4816	0.838	7.458	8.145	3.997

ED 3.95125
CV 0.608973

FPD 0.440008
FPF 0.262816

ED
0
1 15.4333 15.42229 11.01
2 15.4662 15.46371 2.49
3 15.51141 15.50384 7.57
4 15.55103 15.54855 2.48
5 15.59663 15.59033 6.3
6 15.63785 15.63206 5.79
7 15.68257 15.68207 0.5
8 15.73064 15.72645 4.19
9 15.77452 15.77387 0.65
10 15.823 15.82086 2.14
TOT 31.61 mq
AVEG 3.95125 mq
STDEV 2.496203



APPENDIX 2: ED, CV_{ED} and FPF of Pi20L0.875Ph0.146 at 2kPa with Twister™

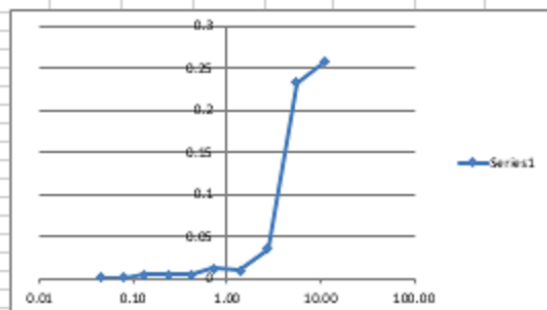
Main flow rate	60	lpm	total flow	175.00	lpm
Feeding rate	1.2	lpm	LPI flow	24.21	lpm
Pneum direct flow rate	38.2	lpm			
Pneum tube flow rate	54.3	lpm	Dilution factor	7.2	

Collection on the stage																	
		carrier				fine particles											
ramp		A		B		C		D		E		F		G		H	
stage	Dq	start	end	start	end	start	end	start	end	start	end	start	end	start	end	start	end
1	0.04	107.931	107.931	88.3312	88.3318	106.174	106.174	106.705	106.705	106.913	106.913	106.751	106.751	107.711	107.712	108.507	108.507
2	0.08	106.367	106.367	86.9863	86.9866	107.333	107.333	107.174	107.174	106.96	106.96	107.847	107.862	106.694	106.701	106.816	106.821
3	0.13	106.806	106.806	88.1676	88.1719	107.532	107.532	107.066	107.069	107.405	107.405	108.165	108.191	106.404	106.427	107.216	107.222
4	0.24	107.032	107.032	87.1832	87.1872	107.007	107.008	107.08	107.096	106.751	106.761	106.577	106.659	107.043	107.129	107.007	107.054
5	0.42	107.431	107.431	87.3375	87.3418	107.672	107.673	107.181	107.215	106.345	106.368	107.661	107.802	106.906	107.04	107.377	107.45
6	0.72	106.941	106.941	87.2225	87.2341	107.241	107.251	106.326	106.377	106.486	106.521	106.971	107.167	107.143	107.33	107.057	107.168
7	1.38	107.825	107.826	87.5525	87.5616	107.273	107.283	107.534	107.557	106.751	106.767	107.266	107.273	106.206	106.306	106.823	106.88
8	2.75	107.025	107.027	87.4688	87.5041	108.144	108.172	106.253	106.3	107.402	107.431	107.137	107.357	106.774	107.019	106.934	107.061
9	5.50	107.565	107.573	87.2909	87.5233	107.192	107.209	107.365	107.407	107.448	107.462	106.524	106.78	106.262	106.617	107.116	107.254
10	11.05			88.2686	88.5253												

Stage	Dq	A	B	C	D	E	F	G	H
1	0.04	0	0.0006	0	0	0	0	0.001	0
2	0.08	0	0.0003	0	0	0	0.015	0.007	0.005
3	0.13	0	0.0043	0	0.003	0	0.026	0.023	0.006
4	0.24	0	0.004	0.001	0.016	0.01	0.082	0.086	0.047
5	0.42	0	0.0043	0.001	0.034	0.023	0.141	0.134	0.073
6	0.72	0	0.0116	0.01	0.051	0.035	0.196	0.187	0.111
7	1.38	0.001	0.0091	0.01	0.023	0.016	0.107	0.1	0.057
8	2.75	0.002	0.0353	0.028	0.047	0.029	0.22	0.245	0.127
9	5.50	0.008	0.2324	0.017	0.042	0.014	0.256	0.355	0.138
10	11.05	0.000	0.2567	0.000	0.000	0.000	0.000	0.000	0.000

Sum, dilution include	A	B	C	D	E	F	G	H
Marr, total	0.079499	4.037091	0.48422	1.5610664	0.91785	7.537927	8.224507	4.076118
Marr, Dqs5.501	0.079499	2.181879	0.48422	1.5610664	0.91785	7.537927	8.224507	4.076118

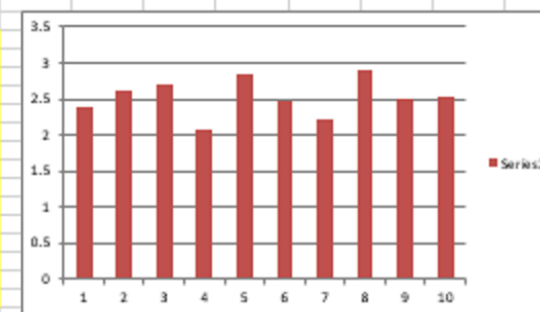
Sum, carrier exclude	A	B	C	D	E	F	G	H
Marr, total		3.958	0.405	1.4816	0.838	7.458	8.145	3.997
Marr, Dqs5.501		2.102	0.405	1.4816	0.838	7.458	8.145	3.997



ED 2.538
CV 0.075909

FPD 0.199048
FPF 0.107508

ED
0 4794.9
1 4792.5 2.4
2 4789.88 2.62
3 4787.19 2.69
4 4785.13 2.06
5 4782.28 2.85
6 4779.81 2.47
7 4777.6 2.21
8 4774.69 2.91
9 4772.18 2.51
10 4769.65 2.53
TOT 20.28 mg
AVEG 2.535 mg
STDEV 0.192428



APPENDIX 3: ED, CV_{ED} and FPF of Pi20L0.875Ph0.146 at 4kPa with Easyhaler® (link to file)

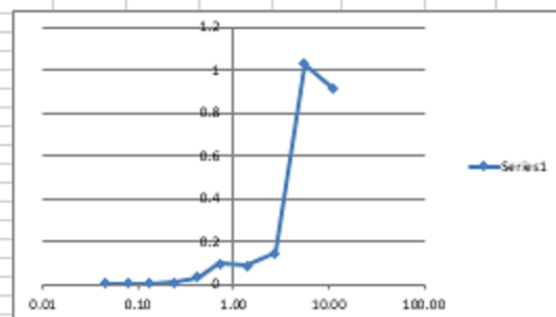
Main flow rate	49	lpm	total flow	175.00	lpm
Feeding rate	1.2	lpm	LPI flow	24.21	lpm
Purwar dir c flow rate	38.2	lpm			
Purwar tube flow rate	54.3	lpm	Dilution factor	7.2	

Collection on the stage																	
		carrier		fine particles													
sampler		A		B		C		D		E		F		G		H	
stage	Dq	start	end	start	end	start	end	start	end	start	end	start	end	start	end	start	end
1	0.04	107.931	107.931	88.2961	88.3001	106.174	106.174	106.705	106.705	106.913	106.913	106.751	106.751	107.711	107.712	108.507	108.507
2	0.08	106.367	106.367	88.4748	88.4774	107.333	107.333	107.174	107.174	106.96	106.96	107.847	107.862	106.694	106.701	106.816	106.821
3	0.13	106.806	106.806	88.4904	88.4953	107.532	107.532	107.066	107.069	107.405	107.405	108.165	108.191	106.404	106.427	107.216	107.222
4	0.24	107.032	107.032	88.1981	88.2064	107.007	107.008	107.08	107.096	106.751	106.761	106.577	106.659	107.043	107.129	107.007	107.054
5	0.42	107.431	107.431	88.281	88.3142	107.672	107.673	107.181	107.215	106.345	106.368	107.661	107.802	106.906	107.04	107.377	107.45
6	0.72	106.941	106.941	88.3278	88.4231	107.241	107.251	106.326	106.377	106.486	106.521	106.971	107.167	107.143	107.33	107.057	107.168
7	1.38	107.825	107.826	88.146	88.2201	107.273	107.283	107.534	107.557	106.751	106.767	107.266	107.373	106.206	106.306	106.823	106.88
8	2.75	107.025	107.027	88.1096	88.255	108.144	108.172	106.253	106.3	107.402	107.431	107.137	107.357	106.774	107.019	106.934	107.061
9	5.50	107.565	107.573	88.2614	88.2902	107.192	107.209	107.365	107.407	107.448	107.462	106.524	106.78	106.262	106.617	107.116	107.254
10	11.05			88.5695	89.4861												

Stage	Dq	A	B	C	D	E	F	G	H
1	0.04	0	0.004	0	0	0	0	0.001	0
2	0.08	0	0.0026	0	0	0	0.015	0.007	0.005
3	0.13	0	0.0049	0	0.003	0	0.026	0.023	0.006
4	0.24	0	0.0083	0.001	0.016	0.01	0.082	0.086	0.047
5	0.42	0	0.0332	0.001	0.034	0.023	0.141	0.134	0.073
6	0.72	0	0.0953	0.01	0.051	0.035	0.196	0.187	0.111
7	1.38	0.001	0.0841	0.01	0.023	0.016	0.107	0.1	0.057
8	2.75	0.002	0.1454	0.028	0.047	0.029	0.22	0.245	0.127
9	5.50	0.008	1.0288	0.017	0.042	0.014	0.256	0.355	0.138
10	11.05	0.000	0.9166	0.000	0.000	0.000	0.000	0.000	0.000

Sum, dilution include	A	B	C	D	E	F	G	H
Marr, total	0.079499	16.79014	0.48422	1.5610664	0.91785	7.537927	8.224507	4.076118
Marr, Dqs5.501	0.079499	16.16572	0.48422	1.5610664	0.91785	7.537927	8.224507	4.076118

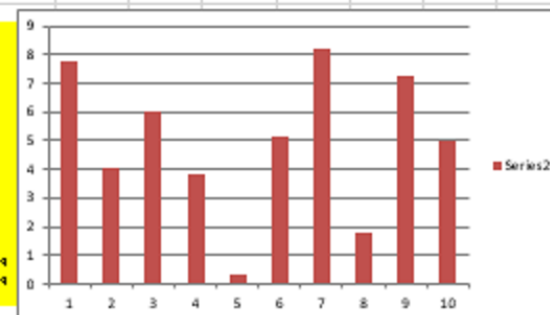
Sum, carrier exclude	A	B	C	D	E	F	G	H
Marr, total		16.71	0.485	1.4816	0.838	7.458	8.145	3.997
Marr, Dqs5.501		10.09	0.485	1.4816	0.838	7.458	8.145	3.997



ED 5.1025
CV 0.379931

FPD 0.411321
FPF 0.249038

ED			
0	15.42056	15.41282	7.74
1	15.46005	15.45603	4.02
2	15.50301	15.49699	6.02
3	15.54541	15.54161	3.8
4	15.58896	15.58861	0.35
5	15.63655	15.6314	5.15
6	15.68185	15.67368	8.17
7	15.72271	15.7209	1.81
8	15.77046	15.76317	7.29
9	15.81153	15.80654	4.99
TOT			40.82 mq
AVEG			5.1025 mq
STDEV			1.938599



APPENDIX 4: ED, CV_{ED} and FPF of Pi20L0.875Ph0.146 at 4kPa with Twister™

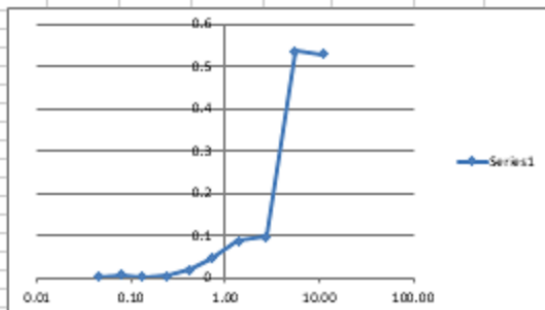
Main flow rate	60	lpm	total flow	175.00	lpm
Feeding rate	1.2	lpm	ELPI flow	24.21	lpm
Pneum. disc flow rate	38.2	lpm			
Pneum. tube flow rate	54.3	lpm	Dilution factor	7.2	

Collection on the stage																	
		carrier		fine particles													
sampler		A		B		C		D		E		F		G		H	
stage	D _g	start	end	start	end	start	end	start	end	start	end	start	end	start	end	start	end
1	0.04	107.931	107.931	119.723	119.7255	106.174	106.174	106.705	106.705	106.913	106.913	106.751	106.751	107.711	107.712	108.507	108.507
2	0.08	106.367	106.367	119.602	119.6079	107.333	107.333	107.174	107.174	106.96	106.96	107.847	107.862	106.694	106.701	106.816	106.821
3	0.13	106.806	106.806	119.83	119.8303	107.532	107.532	107.066	107.069	107.405	107.405	108.165	108.191	106.404	106.427	107.216	107.222
4	0.24	107.032	107.032	119.579	119.5832	107.007	107.008	107.08	107.096	106.751	106.761	106.577	106.659	107.043	107.129	107.007	107.054
5	0.42	107.431	107.431	88.5582	88.576	107.672	107.673	107.181	107.215	106.345	106.368	107.661	107.802	106.906	107.04	107.377	107.45
6	0.72	106.941	106.941	88.211	88.2565	107.241	107.251	106.326	106.377	106.486	106.521	106.971	107.167	107.143	107.33	107.057	107.168
7	1.38	107.825	107.826	88.4051	88.4911	107.273	107.283	107.534	107.557	106.751	106.767	107.266	107.373	106.206	106.306	106.823	106.88
8	2.75	107.025	107.027	88.2079	88.3053	108.144	108.172	106.253	106.3	107.402	107.431	107.137	107.357	106.774	107.019	106.934	107.061
9	5.50	107.565	107.573	119.942	120.4776	107.192	107.209	107.365	107.407	107.448	107.462	106.524	106.78	106.262	106.617	107.116	107.254
10	11.05			119.671	120.2005												

Stage	D _g	A	B	C	D	E	F	G	H
1	0.04	0	0.0024	0	0	0	0	0.001	0
2	0.08	0	0.0056	0	0	0	0.015	0.007	0.005
3	0.13	0	0.0002	0	0.003	0	0.026	0.023	0.006
4	0.24	0	0.0039	0.001	0.016	0.01	0.082	0.086	0.047
5	0.42	0	0.0178	0.001	0.034	0.023	0.141	0.134	0.073
6	0.72	0	0.0455	0.01	0.051	0.035	0.196	0.187	0.111
7	1.38	0.001	0.086	0.01	0.023	0.016	0.107	0.1	0.057
8	2.75	0.002	0.0974	0.028	0.047	0.029	0.22	0.245	0.127
9	5.50	0.008	0.5358	0.017	0.042	0.014	0.256	0.255	0.138
10	11.05	0.000	0.5294	0.000	0.000	0.000	0.000	0.000	0.000

Sum, dilution include	A	B	C	D	E	F	G	H
Marr, total	0.079499	9.569759	0.48422	1.5610664	0.91785	7.537927	8.224507	4.076118
Marr, D _g 5.501	0.079499	5.742701	0.48422	1.5610664	0.91785	7.537927	8.224507	4.076118

Sum, carrier exclude	A	B	C	D	E	F	G	H
Marr, total	9.489	0.405	1.4816	0.838	7.458	8.145	3.997	
Marr, D _g 5.501	5.663	0.405	1.4816	0.838	7.458	8.145	3.997	



ED 2.33875

CV 0.102043

FPD 0.511425

FPF 0.206932

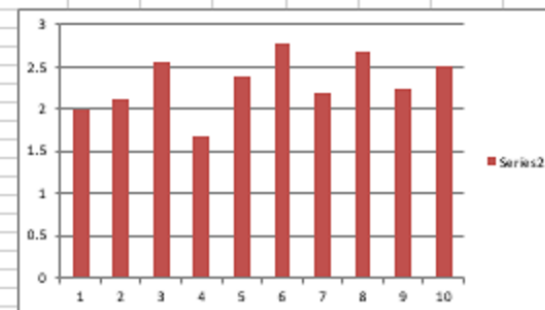
ED

0	20957.66	
1	20955.67	1.99
2	20953.55	2.12
3	20950.99	2.56
4	20949.3	1.69
5	20946.9	2.4
6	20944.12	2.78
7	20941.92	2.2
8	20939.23	2.69
9	20936.98	2.25
10	20934.48	2.5

TOT 19.71 mg

AVEG 2.33875 mg

STDEV 0.238653



APPENDIX 5: ED, CV_{ED} and FPF of Pi20L5Ph0.83 at 2kPa with Easyhaler®

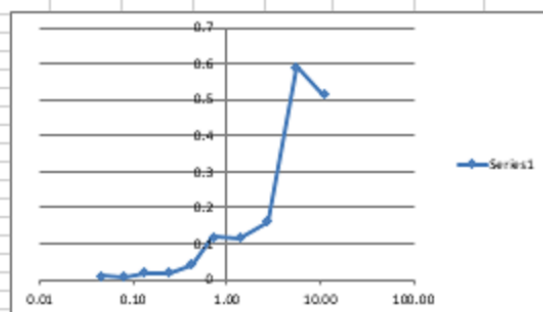
Main flow rate	60	lpm	total flow	175.00	lpm
Feeding rate	1.2	lpm	LPI flow	24.21	lpm
Purpur disc flow rate	38.2	lpm			
Purpur tube flow rate	54.3	lpm	Dilution factor	7.2	

Collection on the stage																	
		carrier		fine particles													
ramplow		A		B		C		D		E		F		G		H	
stage	Dq	start	end	start	end	start	end	start	end	start	end	start	end	start	end	start	end
1	0.04	107.931	107.931	114.724	114.7342	106.174	106.174	106.705	106.705	106.913	106.913	106.751	106.751	107.711	107.712	108.507	108.507
2	0.08	106.367	106.367	117.32	117.3282	107.333	107.333	107.174	107.174	106.96	106.96	107.847	107.862	106.694	106.701	106.816	106.821
3	0.13	106.806	106.806	117.132	117.1495	107.532	107.532	107.066	107.069	107.405	107.405	108.165	108.191	106.404	106.427	107.216	107.222
4	0.24	107.032	107.032	117.231	117.2502	107.007	107.008	107.08	107.096	106.751	106.761	106.577	106.659	107.043	107.129	107.007	107.054
5	0.42	107.431	107.431	115.941	115.9842	107.672	107.673	107.181	107.215	106.345	106.368	107.661	107.802	106.906	107.04	107.377	107.45
6	0.72	106.941	106.941	115.692	115.8096	107.241	107.251	106.326	106.377	106.486	106.521	106.971	107.167	107.143	107.33	107.057	107.168
7	1.38	107.825	107.826	115.439	115.556	107.273	107.283	107.534	107.557	106.751	106.767	107.266	107.373	106.206	106.306	106.823	106.88
8	2.75	107.025	107.027	117.37	117.5309	108.144	108.172	106.253	106.3	107.402	107.431	107.137	107.357	106.774	107.019	106.934	107.061
9	5.50	107.565	107.573	119.119	119.7112	107.192	107.209	107.365	107.407	107.448	107.462	106.524	106.78	106.262	106.617	107.116	107.254
10	11.05			118.96	119.4753												

Stage	Dq	A	B	C	D	E	F	G	H
1	0.04	0	0.0107	0	0	0	0	0.001	0
2	0.08	0	0.0087	0	0	0	0.015	0.007	0.005
3	0.13	0	0.0175	0	0.003	0	0.026	0.023	0.006
4	0.24	0	0.0192	0.001	0.016	0.01	0.082	0.086	0.047
5	0.42	0	0.0429	0.001	0.034	0.023	0.141	0.134	0.073
6	0.72	0	0.118	0.01	0.051	0.035	0.196	0.187	0.111
7	1.38	0.001	0.1166	0.01	0.023	0.016	0.107	0.1	0.057
8	2.75	0.002	0.1606	0.028	0.047	0.029	0.22	0.245	0.127
9	5.50	0.008	0.5927	0.017	0.042	0.014	0.256	0.355	0.138
10	11.05	0.000	0.5155	0.000	0.000	0.000	0.000	0.000	0.000

Sum, dilution include	A	B	C	D	E	F	G	H
Marr, total	0.079499	11.5808	0.48422	1.5610664	0.91785	7.537927	8.224507	4.076118
Marr, Dq5.501	0.079499	7.855199	0.48422	1.5610664	0.91785	7.537927	8.224507	4.076118

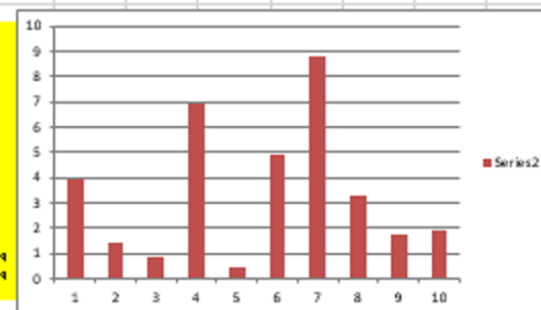
Sum, carrier exclude	A	B	C	D	E	F	G	H
Marr, total		11.5	0.405	1.4816	0.838	7.458	8.145	3.997
Marr, Dq5.501		7.776	0.405	1.4816	0.838	7.458	8.145	3.997



ED 3.11375
CV 0.664067

FPD 0.464906
FPF 0.315343

ED
0
1 15.42091 15.41697 3.94
2 15.46366 15.46228 1.38
3 15.50997 15.50916 0.81
4 15.55637 15.54946 6.91
5 15.59945 15.59897 0.48
6 15.64755 15.64263 4.92
7 15.69066 15.68186 8.8
8 15.72708 15.72382 3.26
9 15.77204 15.77029 1.75
10 15.81991 15.81797 1.94
TOT 24.91 m-q
AVEG 3.11375 m-q
STDEV 2.067738



APPENDIX 6: ED, CV_{ED} and FPF of Pi20L5Ph0.83 at 2kPa with Twister™

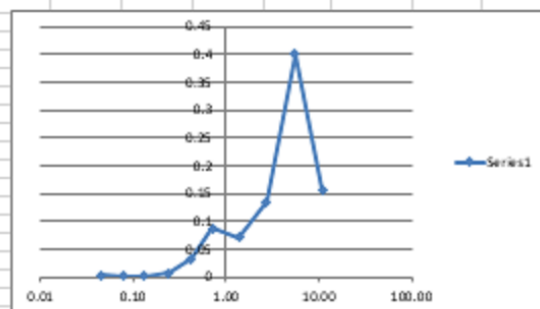
Main flow rate	60	lpm	total flow	175.00	lpm
Feeding rate	1.2	lpm	ELPI flow	24.21	lpm
Pneum. disp. flow rate	39.2	lpm			
Pneum. tube flow rate	54.3	lpm	Dilution factor	7.2	

Collection on the stage																	
		carrier		fine particles													
ramplor		A		B		C		D		E		F		G		H	
stage	Dg	start	end	start	end	start	end	start	end	start	end	start	end	start	end	start	end
1	0.04	107.931	107.931	119.797	119.7998	106.174	106.174	106.705	106.705	106.913	106.913	106.751	106.751	107.711	107.712	108.507	108.507
2	0.08	106.367	106.367	119.722	119.7225	107.333	107.333	107.174	107.174	106.96	106.96	107.847	107.862	106.694	106.701	106.816	106.821
3	0.13	106.806	106.806	120.321	120.3215	107.532	107.532	107.066	107.069	107.405	107.405	108.165	108.191	106.404	106.427	107.216	107.222
4	0.24	107.032	107.032	119.879	119.8845	107.007	107.008	107.08	107.096	106.751	106.761	106.577	106.659	107.043	107.129	107.007	107.054
5	0.42	107.431	107.431	119.048	119.0791	107.672	107.673	107.181	107.215	106.345	106.368	107.661	107.802	106.906	107.04	107.377	107.45
6	0.72	106.941	106.941	119.65	119.7371	107.241	107.251	106.326	106.377	106.406	106.521	106.971	107.167	107.143	107.33	107.057	107.168
7	1.38	107.825	107.826	120.044	120.1147	107.273	107.283	107.534	107.557	106.751	106.767	107.266	107.373	106.206	106.306	106.823	106.88
8	2.75	107.025	107.027	120.109	120.2439	108.144	108.172	106.253	106.3	107.402	107.431	107.137	107.357	106.774	107.019	106.934	107.061
9	5.50	107.565	107.573	119.726	120.1267	107.192	107.209	107.365	107.407	107.448	107.462	106.524	106.78	106.262	106.617	107.116	107.254
10	11.05			119.635	119.7924												

Stage	Dq	A	B	C	D	E	F	G	H
1	0.04	0	0.0026	0	0	0	0	0.001	0
2	0.08	0	0.0002	0	0	0	0.015	0.007	0.005
3	0.13	0	0.0008	0	0.003	0	0.026	0.023	0.006
4	0.24	0	0.0057	0.001	0.016	0.01	0.082	0.086	0.047
5	0.42	0	0.0315	0.001	0.034	0.023	0.141	0.124	0.073
6	0.72	0	0.0873	0.01	0.051	0.035	0.196	0.187	0.111
7	1.38	0.001	0.0703	0.01	0.023	0.016	0.107	0.1	0.057
8	2.75	0.002	0.1351	0.028	0.047	0.029	0.22	0.245	0.127
9	5.50	0.008	0.4007	0.017	0.042	0.014	0.256	0.355	0.138
10	11.05	0.000	0.1572	0.000	0.000	0.000	0.000	0.000	0.000

Sum, dilution include	A	B	C	D	E	F	G	H
Marr, total	0.079499	6.44229	0.48422	1.5610664	0.91785	7.537927	8.224507	4.076118
Marr, Dq5.501	0.079499	5.30618	0.48422	1.5610664	0.91785	7.537927	8.224507	4.076118

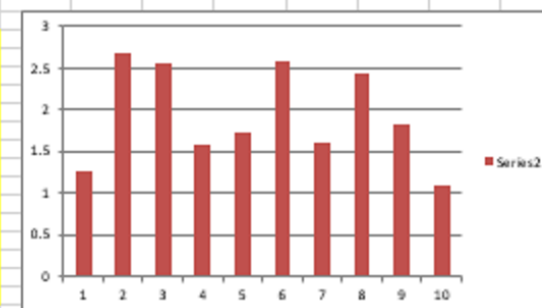
Sum, carrier exclude	A	B	C	D	E	F	G	H
Marr, total		6.363	0.405	1.4816	0.838	7.458	8.145	3.997
Marr, Dq5.501		5.227	0.405	1.4816	0.838	7.458	8.145	3.997



ED 1.94625
CV 0.261033

FPD 0.413763
FPF 0.340795

ED
0 4524.27
1 4523.01 1.26
2 4520.34 2.67
3 4517.78 2.56
4 4516.21 1.57
5 4514.48 1.73
6 4511.89 2.59
7 4510.29 1.6
8 4507.86 2.43
9 4506.03 1.83
10 4504.93 1.1
TOT 15.57 mg
AVEG 1.94625 mg
STDEV 0.509592



APPENDIX 7: ED, CV_{ED} and FPF of Pi20L5Ph0.83 at 4kPa with Easyhaler®

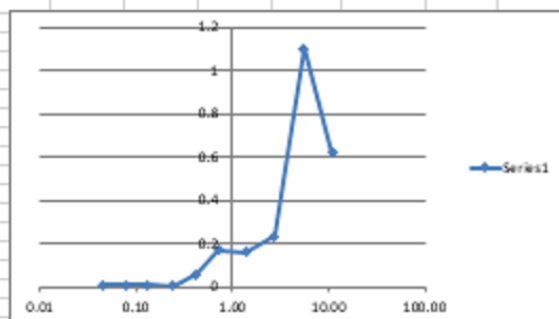
Main flow rate	60	lpm	total flow	175.00	lpm
Feeding rate	1.2	lpm	HLPI flow	24.21	lpm
Pneum disp flow rate	38.2	lpm			
Pneum tube flow rate	54.3	lpm	Dilution factor	7.2	

Collection on the stages																	
		carrier		fine particles													
sampler		A		B		C		D		E		F		G		H	
stage	Dq	start	end	start	end	start	end	start	end	start	end	start	end	start	end	start	end
1	0.04	107.931	107.931	120.174	120.1808	106.174	106.174	106.705	106.705	106.913	106.913	106.751	106.751	107.711	107.712	108.507	108.507
2	0.08	106.367	106.367	119.743	119.7482	107.333	107.333	107.174	107.174	106.96	106.96	107.847	107.862	106.694	106.701	106.816	106.821
3	0.13	106.806	106.806	119.429	119.439	107.532	107.532	107.066	107.069	107.405	107.405	108.165	108.191	106.404	106.427	107.216	107.222
4	0.24	107.032	107.032	119.637	119.638	107.007	107.008	107.08	107.096	106.751	106.761	106.577	106.659	107.043	107.129	107.007	107.054
5	0.42	107.431	107.431	120.07	120.1252	107.672	107.673	107.181	107.215	106.345	106.368	107.661	107.802	106.906	107.04	107.377	107.45
6	0.72	106.941	106.941	117.79	117.9579	107.241	107.251	106.326	106.377	106.486	106.521	106.971	107.167	107.143	107.33	107.057	107.168
7	1.38	107.825	107.826	118.308	118.4663	107.273	107.283	107.534	107.557	106.751	106.767	107.266	107.373	106.206	106.306	106.823	106.88
8	2.75	107.025	107.027	119.615	119.8484	108.144	108.172	106.253	106.3	107.402	107.431	107.137	107.357	106.774	107.019	106.934	107.061
9	5.50	107.565	107.573	119.307	120.4092	107.192	107.209	107.365	107.407	107.448	107.462	106.524	106.78	106.262	106.617	107.116	107.254
10	11.05			118.557	119.1768												

Stage	Dq	A	B	C	D	E	F	G	H
1	0.04	0	0.007	0	0	0	0	0.001	0
2	0.08	0	0.0053	0	0	0	0.015	0.007	0.005
3	0.13	0	0.0097	0	0.003	0	0.026	0.023	0.006
4	0.24	0	0.0007	0.001	0.016	0.01	0.082	0.086	0.047
5	0.42	0	0.0556	0.001	0.034	0.023	0.141	0.134	0.073
6	0.72	0	0.1678	0.01	0.051	0.035	0.196	0.187	0.111
7	1.38	0.001	0.1583	0.01	0.023	0.016	0.107	0.1	0.057
8	2.75	0.002	0.2336	0.028	0.047	0.029	0.22	0.245	0.127
9	5.50	0.008	1.1023	0.017	0.042	0.014	0.256	0.355	0.138
10	11.05	0.000	0.6198	0.000	0.000	0.000	0.000	0.000	0.000

Sum, dilution include	A	B	C	D	E	F	G	H
Marr, total	0.079499	17.05692	0.48422	1.5610664	0.91785	7.537927	8.224507	4.076118
Marr, Dqs5.501	0.079499	12.57743	0.48422	1.5610664	0.91785	7.537927	8.224507	4.076118

Sum, carrier exclude	A	B	C	D	E	F	G	H
Marr, total		16.98	0.405	1.4816	0.838	7.458	8.145	3.997
Marr, Dqs5.501		12.5	0.405	1.4816	0.838	7.458	8.145	3.997



ED 4.855

CV 0.492888

FPD 0.439156

FPF 0.323827

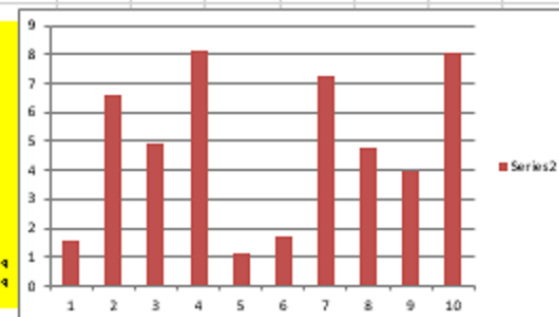
ED

0			
1	15.41753	15.41594	1.59
2	15.46515	15.45854	6.61
3	15.50373	15.49879	4.94
4	15.54731	15.5392	8.11
5	15.58758	15.50649	1.09
6	15.6327	15.63096	1.74
7	15.67749	15.67027	7.22
8	15.71793	15.71319	4.74
9	15.75951	15.75556	3.95
10	15.80432	15.79627	8.05

TOT 38.84 mq

AVEG 4.855 mq

STDEV 2.392972



APPENDIX 8: ED, CV_{ED} and FPF of Pi20L5Ph0.83 at 4kPa with Twister™

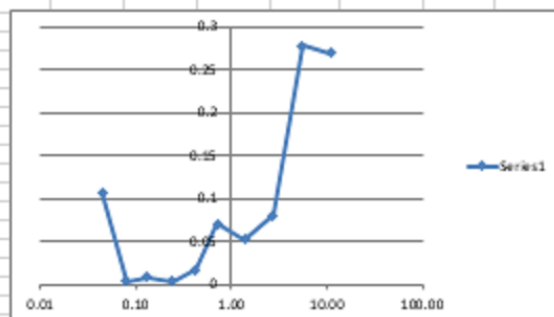
Main flow rate	60	lpm	total flow	175.00	lpm
Feeding rate	1.2	lpm	HLPI flow	24.21	lpm
Patient dir flow rate	38.2	lpm			
Patient tube flow rate	54.3	lpm	Dilution factor	7.2	

Collection on the stage																	
		carrier		fine particles													
stage	Dq	start	end	start	end	start	end	start	end	start	end	start	end	start	end	start	end
1	0.04	107.931	107.931	119.258	119.3652	106.174	106.174	106.705	106.705	106.913	106.913	106.751	106.751	107.711	107.712	108.507	108.507
2	0.08	106.367	106.367	119.041	119.0438	107.333	107.333	107.174	107.174	106.96	106.96	107.847	107.847	106.694	106.701	106.816	106.821
3	0.13	106.806	106.806	120.51	120.5174	107.532	107.532	107.066	107.069	107.405	107.405	108.165	108.191	106.404	106.427	107.216	107.222
4	0.24	107.032	107.032	118.044	118.0472	107.007	107.008	107.08	107.096	106.751	106.761	106.577	106.659	107.043	107.129	107.007	107.054
5	0.42	107.431	107.431	118.765	118.7816	107.672	107.673	107.181	107.215	106.345	106.368	107.661	107.802	106.906	107.04	107.377	107.45
6	0.72	106.941	106.941	120.432	120.5018	107.241	107.251	106.326	106.377	106.486	106.521	106.971	107.167	107.143	107.33	107.057	107.168
7	1.38	107.825	107.826	118.468	118.5202	107.273	107.283	107.534	107.557	106.751	106.767	107.266	107.373	106.206	106.306	106.823	106.88
8	2.75	107.025	107.027	119.697	119.7773	108.144	108.172	106.253	106.3	107.402	107.431	107.137	107.357	106.774	107.019	106.934	107.061
9	5.50	107.565	107.573	118.97	119.2482	107.192	107.209	107.365	107.407	107.448	107.462	106.524	106.78	106.262	106.617	107.116	107.254
10	11.05			119.408	119.677												

Stage	Dq	A	B	C	D	E	F	G	H
1	0.04	0	0.107	0	0	0	0	0.001	0
2	0.08	0	0.0029	0	0	0	0.015	0.007	0.005
3	0.13	0	0.0076	0	0.003	0	0.026	0.023	0.006
4	0.24	0	0.0034	0.001	0.016	0.01	0.082	0.086	0.047
5	0.42	0	0.0168	0.001	0.034	0.023	0.141	0.134	0.073
6	0.72	0	0.0699	0.01	0.051	0.035	0.196	0.187	0.111
7	1.38	0.001	0.0518	0.01	0.023	0.016	0.107	0.1	0.057
8	2.75	0.002	0.0806	0.028	0.047	0.029	0.22	0.245	0.127
9	5.50	0.008	0.2785	0.017	0.042	0.014	0.256	0.355	0.138
10	11.05	0.000	0.2694	0.000	0.000	0.000	0.000	0.000	0.000

Sum, dilution include	A	B	C	D	E	F	G	H
Marr, total	0.079499	6.416995	0.48422	1.5610664	0.91785	7.537927	8.224507	4.076118
Marr, Dq=5.501	0.079499	4.469998	0.48422	1.5610664	0.91785	7.537927	8.224507	4.076118

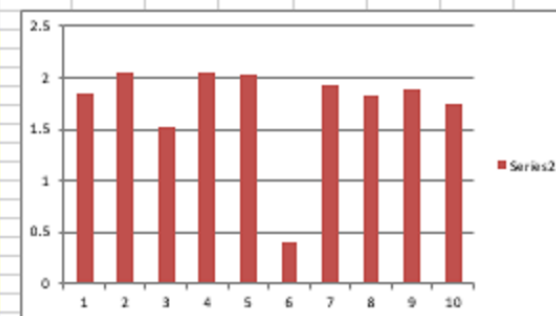
Sum, carrier exclude	A	B	C	D	E	F	G	H
Marr, total		6.337	0.405	1.4816	0.838	7.458	8.145	3.997
Marr, Dq=5.501		4.39	0.405	1.4816	0.838	7.458	8.145	3.997



ED 1.855
CV 0.090528

FPD 0.432412
FPF 0.301213

ED
0 20759.77
1 20757.93 1.84
2 20755.88 2.05
3 20754.35 1.53
4 20752.3 2.05
5 20750.26 2.04
6 20749.85 0.41
7 20747.93 1.92
8 20746.1 1.83
9 20744.21 1.89
10 20742.47 1.74
TOT 14.84 mg
AVEG 1.855 mg
STDEV 0.167929



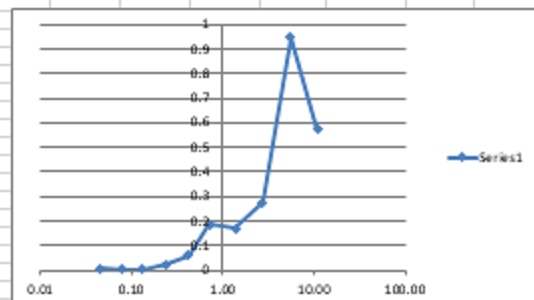
APPENDIX 9: ED, CV_{ED} and FPF of Pi20L15Ph2.5 at 2kPa with Easyhaler®

Main flow rate	60	lpm	total flow	175.00	lpm
Feeding rate	1.2	lpm	ELPI flow	24.21	lpm
Purifier direct flow rate	38.2	lpm			
Purifier tube flow rate	54.3	lpm	Dilution factor	7.2	

Collection on the stage																	
		carrier		fine particles													
stage	Dq	start	end	start	end	start	end	start	end	start	end	start	end	start	end	start	end
1	0.04	107.931	107.931	87.6609	87.6667	106.174	106.174	106.705	106.705	106.913	106.913	106.751	106.751	107.711	107.712	108.507	108.507
2	0.08	106.367	106.367	87.9292	87.9311	107.333	107.333	107.174	107.174	106.96	106.96	107.847	107.862	106.694	106.701	106.816	106.821
3	0.13	106.806	106.806	88.6953	88.696	107.532	107.532	107.066	107.069	107.405	107.405	108.165	108.191	106.404	106.427	107.216	107.222
4	0.24	107.032	107.032	87.9435	87.9654	107.007	107.008	107.08	107.096	106.751	106.761	106.577	106.659	107.043	107.129	107.007	107.054
5	0.42	107.431	107.431	87.3315	87.3916	107.672	107.673	107.181	107.215	106.345	106.368	107.661	107.802	106.906	107.04	107.377	107.45
6	0.72	106.941	106.941	87.9614	88.1467	107.241	107.251	106.326	106.377	106.486	106.521	106.971	107.167	107.143	107.33	107.057	107.168
7	1.38	107.825	107.826	87.4799	87.6484	107.273	107.283	107.534	107.557	106.751	106.767	107.266	107.373	106.206	106.306	106.823	106.88
8	2.75	107.025	107.027	88.3961	88.6692	108.144	108.172	106.253	106.3	107.402	107.431	107.137	107.357	106.774	107.019	106.934	107.061
9	5.50	107.573	107.573	88.2346	89.1825	107.192	107.209	107.365	107.407	107.448	107.462	106.524	106.78	106.262	106.617	107.116	107.254
10	11.05			87.8261	88.3987												

Stage	Dq	A	B	C	D	E	F	G	H
1	0.04	0	0.0058	0	0	0	0.001	0	0
2	0.08	0	0.0019	0	0	0	0.015	0.007	0.005
3	0.13	0	0.0007	0	0.003	0	0.026	0.023	0.006
4	0.24	0	0.0219	0.001	0.016	0.01	0.092	0.086	0.047
5	0.42	0	0.0601	0.001	0.034	0.023	0.141	0.134	0.073
6	0.72	0	0.1853	0.01	0.051	0.035	0.196	0.187	0.111
7	1.38	0.001	0.1685	0.01	0.023	0.016	0.107	0.1	0.057
8	2.75	0.002	0.2731	0.028	0.047	0.029	0.22	0.245	0.127
9	5.50	0.008	0.9479	0.017	0.042	0.014	0.256	0.355	0.138
10	11.05	0.000	0.5726	0.000	0.000	0.000	0.000	0.000	0.000

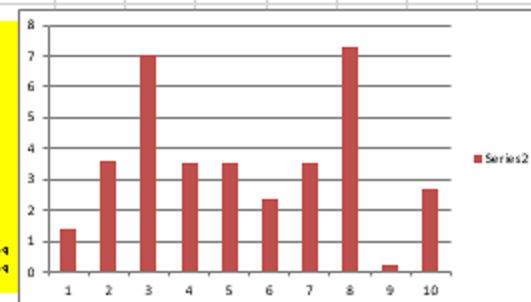
Sum, dilution include	A	B	C	D	E	F	G	H
Marr, total	0.079499	16.17294	0.48422	1.5610664	0.91785	7.537927	8.224507	4.076118
Marr, Dqs5.501	0.079499	12.03467	0.48422	1.5610664	0.91785	7.537927	8.224507	4.076118
Sum, carrier exclude	A	B	C	D	E	F	G	H
Marr, total		16.99	0.405	1.4816	0.838	7.458	8.145	3.997
Marr, Dqs5.501		11.96	0.405	1.4816	0.838	7.458	8.145	3.997



ED 3.4625
CV 0.471752

FPD 0.593861
FPF 0.434464

ED
0
1 15.42862 15.4272 1.42
2 15.47334 15.46974 3.6
3 15.51642 15.50939 7.03
4 15.55643 15.55292 3.51
5 15.59959 15.59604 3.55
6 15.64227 15.63988 2.39
7 15.68651 15.683 3.51
8 15.73131 15.72404 7.27
9 15.76817 15.76797 0.2
10 15.81374 15.81105 2.69
TOT 27.7 mq
AVEG 3.4625 mq
STDEV 1.633443



APPENDIX 10: ED, CV_{ED} and FPF of Pi20L15Ph2.5 at 2kPa with Twister™

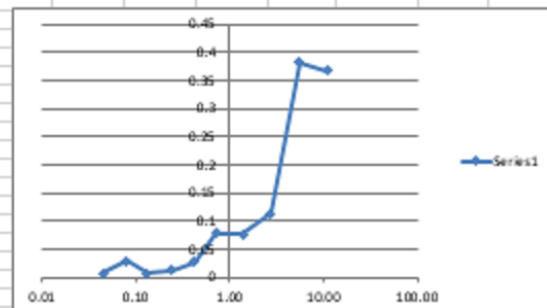
Main flow rate	60	lpm	total flow	175.00	lpm
Feeding rate	1.2	lpm	ELPI flow	24.21	lpm
Pneum. dir. flow rate	38.2	lpm			
Pneum. tube flow rate	54.3	lpm	Dilution factor	7.2	

Collection on the stage																	
		carrier		fine particles													
stage	Dq	A		B		C		D		E		F		G		H	
start	end	start	end	start	end	start	end	start	end	start	end	start	end	start	end	start	end
1	0.04	107.931	107.931	119.353	119.353	106.174	106.174	106.705	106.705	106.913	106.913	106.751	106.751	107.711	107.712	108.507	108.507
2	0.08	106.367	106.367	120.339	120.4181	107.333	107.333	107.174	107.174	106.96	106.96	107.847	107.847	106.694	106.701	106.816	106.821
3	0.13	106.806	106.806	120.387	120.3933	107.532	107.532	107.066	107.066	107.405	107.405	108.165	108.191	106.404	106.427	107.216	107.222
4	0.24	107.032	107.032	120.116	120.1273	107.007	107.008	107.08	107.096	106.751	106.761	106.577	106.659	107.043	107.129	107.007	107.054
5	0.42	107.431	107.431	119.852	119.8783	107.672	107.673	107.181	107.215	106.345	106.368	107.661	107.802	106.906	107.04	107.377	107.45
6	0.72	106.941	106.941	119.402	119.4804	107.241	107.251	106.326	106.377	106.486	106.521	106.971	107.167	107.143	107.33	107.057	107.168
7	1.38	107.825	107.826	119.912	119.9887	107.273	107.283	107.534	107.557	106.751	106.767	107.266	107.373	106.206	106.306	106.823	106.88
8	2.75	107.025	107.027	120.604	120.7167	108.144	108.172	106.253	106.3	107.402	107.431	107.137	107.357	106.774	107.019	106.934	107.061
9	5.50	107.565	107.573	119.471	119.8531	107.192	107.209	107.365	107.407	107.448	107.462	106.524	106.78	106.262	106.617	107.116	107.254
10	11.05			120.173	120.5397												

Stage	Dq	A	B	C	D	E	F	G	H
1	0.04	0	0.0059	0	0	0	0.001	0	0
2	0.08	0	0.0277	0	0	0	0.015	0.007	0.005
3	0.13	0	0.0062	0	0.003	0	0.026	0.023	0.006
4	0.24	0	0.0111	0.001	0.016	0.01	0.082	0.036	0.047
5	0.42	0	0.026	0.001	0.034	0.023	0.141	0.134	0.073
6	0.72	0	0.0788	0.01	0.051	0.035	0.196	0.187	0.111
7	1.38	0.001	0.0768	0.01	0.023	0.016	0.107	0.1	0.057
8	2.75	0.002	0.1129	0.028	0.047	0.029	0.22	0.245	0.127
9	5.50	0.008	0.3922	0.017	0.042	0.014	0.256	0.355	0.138
10	11.05	0.000	0.3666	0.000	0.000	0.000	0.000	0.000	0.000

Sum, dilution include	A	B	C	D	E	F	G	H
Marr, total	0.079499	7.907958	0.48422	1.5610664	0.91785	7.537927	8.224507	4.076118
Marr, Dq=5.501	0.079499	5.258481	0.48422	1.5610664	0.91785	7.537927	8.224507	4.076118

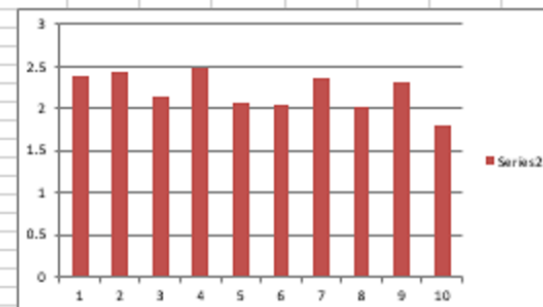
Sum, carrier exclude	A	B	C	D	E	F	G	H
Marr, total	7.828	0.405	1.4816	0.838	7.458	8.145	3.997	
Marr, Dq=5.501	5.179	0.405	1.4816	0.838	7.458	8.145	3.997	



ED 2.2225
CV 0.076451

FPD 0.444767
FPF 0.295783

ED
0 4326.11
1 4323.73 2.38
2 4321.3 2.43
3 4319.15 2.15
4 4316.66 2.49
5 4314.58 2.08
6 4312.54 2.04
7 4310.17 2.37
8 4308.16 2.01
9 4305.84 2.32
10 4304.05 1.79
TOT 17.78 mg
AVEG 2.2225 mg
STDEV 0.170357



APPENDIX 11: ED, CV_{ED} and FPF of Pi20L15Ph2.5 at 4kPa with Easyhaler®

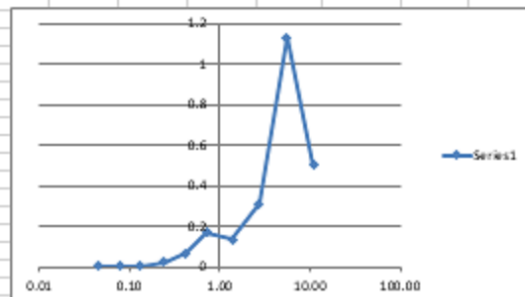
Main flow rate	60	lpm	total flow	175.00	lpm
Feeding rate	1.2	lpm	ELPI flow	24.21	lpm
Purifier disc flow rate	38.2	lpm			
Purifier tube flow rate	54.3	lpm	Dilution factor	7.2	

Collection on the stage															
		carrier		fine particles											
stage	Dq	A		B		C		D		E		F		G	
stage	Dq	start	end	start	end	start	end	start	end	start	end	start	end	start	end
1	0.04	107.931	107.931	88.0632	88.0661	106.174	106.174	106.705	106.705	106.913	106.913	106.751	106.751	107.711	107.712
2	0.08	106.367	106.367	88.0972	88.1017	107.333	107.333	107.174	107.174	106.96	106.96	107.847	107.862	106.694	106.701
3	0.13	106.806	106.806	87.7472	87.7523	107.532	107.532	107.066	107.066	107.405	107.405	108.165	108.191	106.404	106.427
4	0.24	107.032	107.032	87.8388	87.8616	107.007	107.007	107.008	107.008	107.096	107.096	106.751	106.761	106.577	106.599
5	0.42	107.431	107.431	87.4844	87.5511	107.672	107.673	107.181	107.215	106.345	106.368	107.661	107.802	106.906	107.04
6	0.72	106.941	106.941	87.8395	88.0096	107.241	107.251	106.326	106.377	106.486	106.521	106.971	107.167	107.143	107.33
7	1.38	107.825	107.826	87.6713	87.8038	107.273	107.283	107.534	107.557	106.751	106.767	107.266	107.373	106.206	106.206
8	2.75	107.025	107.027	87.7929	88.1062	108.144	108.172	106.253	106.3	107.402	107.431	107.137	107.357	106.774	107.019
9	5.50	107.565	107.573	87.6584	88.7893	107.192	107.209	107.365	107.407	107.448	107.462	106.524	106.78	106.262	106.617
10	11.05			87.5947	88.0946										

Stage	Dq	A	B	C	D	E	F	G	H
1	0.04	0	0.0029	0	0	0	0.001	0	0
2	0.08	0	0.0045	0	0	0	0.015	0.007	0.005
3	0.13	0	0.0051	0	0.003	0	0.026	0.023	0.006
4	0.24	0	0.0228	0.001	0.016	0.01	0.082	0.086	0.047
5	0.42	0	0.0667	0.001	0.034	0.023	0.141	0.134	0.073
6	0.72	0	0.1701	0.01	0.051	0.035	0.196	0.187	0.111
7	1.38	0.001	0.1325	0.01	0.023	0.016	0.107	0.1	0.057
8	2.75	0.002	0.3123	0.028	0.047	0.029	0.22	0.245	0.127
9	5.50	0.008	1.1309	0.017	0.042	0.014	0.256	0.355	0.138
10	11.05	0.000	0.4999	0.000	0.000	0.000	0.000	0.000	0.000

Sum, dilution include	A	B	C	D	E	F	G	H
Marr, total	0.079499	16.9672	0.48422	1.5610664	0.91785	7.537927	8.224507	4.076118
Marr, Dqs 5.501	0.079499	13.35424	0.48422	1.5610664	0.91785	7.537927	8.224507	4.076118

Sum, carrier exclude	A	B	C	D	E	F	G	H
Marr, total	16.89	0.405	1.4816	0.838	7.458	8.145	3.997	
Marr, Dqs 5.501	13.27	0.405	1.4816	0.838	7.458	8.145	3.997	



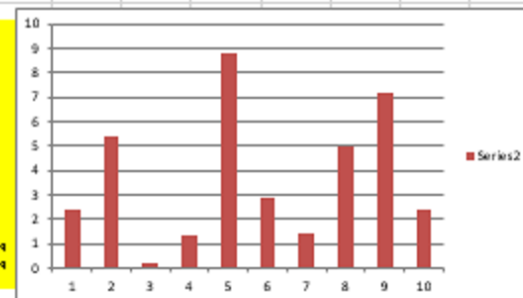
ED 3.505

CV 0.601523

FPD 0.605107

FPF 0.476261

ED			
0	15.41775	15.4154	2.35
1	15.4629	15.4575	5.4
2	15.5061	15.5093	0.17
3	15.55284	15.55148	1.36
4	15.60052	15.59171	8.81
5	15.64105	15.63815	2.9
6	15.68279	15.68136	1.43
7	15.72745	15.72245	5
8	15.7711	15.76392	7.18
9	15.81179	15.80937	2.42
TOT			28.04 mg
AVEG			3.505 mg
STDEV			2.109337



APPENDIX 12: ED, CV_{ED} and FPF of Pi20L15Ph2.5 at 4kPa with Twister™

Main flow rate	60	lpm	total flow	175.00	lpm
Feeding rate	1.2	lpm	ELPI flow	24.21	lpm
Pneum. dir. flow rate	39.2	lpm			
Pneum. tube flow rate	54.3	lpm	Dilution factor	7.2	

Collection on the stage																	
		carrier		fine particles													
sampler		A		B		C		D		E		F		G		H	
stage	D _g	start	end	start	end	start	end	start	end	start	end	start	end	start	end	start	end
1	0.04	107.931	107.931	87.5257	87.5517	106.174	106.174	106.705	106.705	106.913	106.913	106.751	106.751	107.711	107.712	108.507	108.507
2	0.08	106.367	106.367	87.1671	87.1987	107.333	107.333	107.174	107.174	106.96	106.96	107.847	107.862	106.694	106.701	106.816	106.821
3	0.13	106.806	106.806	87.388	87.4303	107.532	107.532	107.066	107.069	107.405	107.405	108.165	108.191	106.404	106.427	107.216	107.222
4	0.24	107.032	107.032	86.7996	86.9411	107.007	107.008	107.08	107.096	106.751	106.761	106.577	106.659	107.043	107.129	107.007	107.054
5	0.42	107.431	107.431	87.8233	88.0595	107.672	107.673	107.181	107.215	106.345	106.368	107.661	107.802	106.906	107.04	107.377	107.45
6	0.72	106.941	106.941	88.4675	88.8095	107.241	107.251	106.326	106.377	106.486	106.521	106.971	107.167	107.143	107.33	107.057	107.168
7	1.38	107.825	107.826	88.6244	88.8313	107.273	107.283	107.534	107.557	106.751	106.767	107.266	107.373	106.206	106.306	106.823	106.88
8	2.75	107.025	107.027	88.2969	88.8867	108.144	108.172	106.253	106.3	107.402	107.431	107.137	107.357	106.774	107.019	106.934	107.061
9	5.50	107.565	107.573	88.2327	89.0194	107.192	107.209	107.365	107.407	107.448	107.462	106.524	106.78	106.262	106.617	107.116	107.254
10	11.05			88.1851	88.4681												

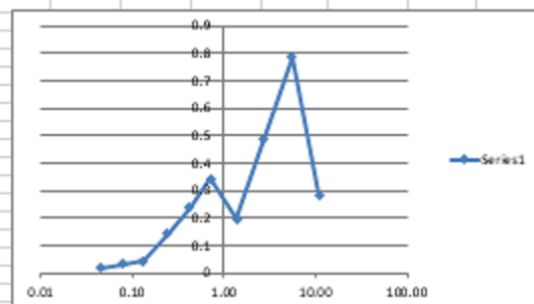
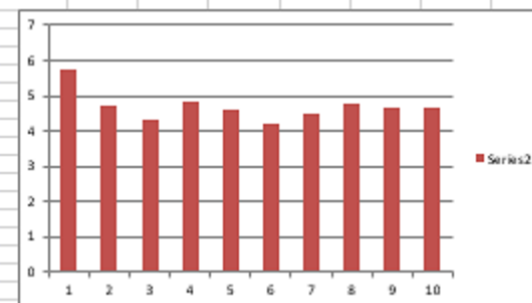
Stage	D _g	A	B	C	D	E	F	G	H
1	0.04	0	0.016	0	0	0	0.015	0.007	0.005
2	0.08	0	0.0316	0	0	0	0.026	0.023	0.006
3	0.13	0	0.0423	0	0.003	0	0.026	0.023	0.006
4	0.24	0	0.1415	0.001	0.016	0.01	0.082	0.086	0.047
5	0.42	0	0.2342	0.001	0.034	0.023	0.141	0.134	0.073
6	0.72	0	0.342	0.01	0.051	0.035	0.196	0.187	0.111
7	1.38	0.001	0.1969	0.01	0.023	0.016	0.107	0.1	0.057
8	2.75	0.002	0.4898	0.028	0.047	0.029	0.22	0.245	0.127
9	5.50	0.008	0.7867	0.017	0.042	0.014	0.256	0.355	0.138
10	11.05	0.000	0.283	0.000	0.000	0.000	0.000	0.000	0.000

Sum, dilution include	A	B	C	D	E	F	G	H
Marr, total	0.079499	18.54489	0.48422	1.5610664	0.91785	7.537927	8.224507	4.076118
Marr, D _{gs} 5.501	0.079499	16.4996	0.48422	1.5610664	0.91785	7.537927	8.224507	4.076118
Sum, carrier exclude	A	B	C	D	E	F	G	H
Marr, total		18.47	0.405	1.4816	0.838	7.458	8.145	3.997
Marr, D _{gs} 5.501		16.42	0.405	1.4816	0.838	7.458	8.145	3.997

ED 4.635
CV 0.03724

FPD 0.500102
FPF 0.444973

ED
0 4770.57
1 4764.82 5.75
2 4760.09 4.73
3 4755.79 4.3
4 4750.98 4.81
5 4746.35 4.63
6 4742.16 4.19
7 4737.69 4.47
8 4732.89 4.8
9 4728.23 4.66
10 4723.55 4.68
TOT 37.08 mg
AVEG 4.635 mg
STDEV 0.172792



APPENDIX 13: ED, CV_{ED} and FPF of Bu20L0.875Ph0.146 at 2kPa with Easyhaler®

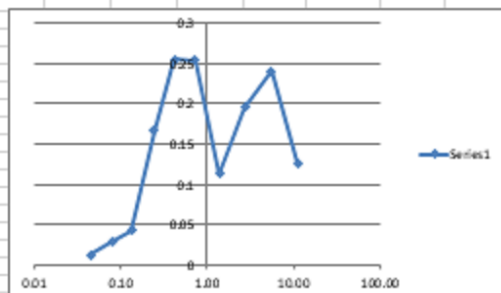
Main flow rate	60	lpm	total flow	175.00	lpm
Feeding rate	1.2	lpm	LPI flow	24.21	lpm
Purwar dirc flow rate	38.2	lpm			
Purwar tube flow rate	54.3	lpm	Dilution factor	7.2	

Collection on the stage													
stage	Dq	carrier		fine particles									
		A		B		C		D		E		F	
stage	Dq	start	end	start	end	start	end	start	end	start	end	start	end
1	0.04	107.931	107.931	87.9473	87.9599	106.174	106.174	106.705	106.705	106.913	106.913	106.751	106.751
2	0.08	106.367	106.367	87.9406	87.9702	107.333	107.333	107.174	107.174	106.96	106.96	107.847	107.862
3	0.13	106.806	106.806	88.6715	88.7142	107.532	107.532	107.066	107.066	107.405	107.405	108.165	108.191
4	0.24	107.032	107.032	88.1542	88.3206	107.007	107.008	107.08	107.096	106.751	106.761	106.577	106.659
5	0.42	107.431	107.431	87.9223	88.177	107.672	107.673	107.181	107.215	106.345	106.348	107.661	107.802
6	0.72	106.941	106.941	88.3864	88.6406	107.241	107.251	106.326	106.377	106.486	106.521	106.971	107.167
7	1.38	107.825	107.826	87.881	87.9948	107.273	107.283	107.534	107.557	106.751	106.767	107.266	107.373
8	2.75	107.025	107.027	88.176	88.3713	108.144	108.172	106.253	106.3	107.402	107.431	107.137	107.357
9	5.50	107.565	107.573	88.0343	88.2743	107.192	107.209	107.365	107.407	107.448	107.462	106.524	106.78
10	11.05			88.1382	88.2652								

Stage	Dq	A	B	C	D	E	F	G	H
1	0.04	0	0.0126	0	0	0	0	0.001	0
2	0.08	0	0.0296	0	0	0	0.015	0.007	0.005
3	0.13	0	0.0427	0	0.003	0	0.026	0.023	0.006
4	0.24	0	0.1664	0.001	0.016	0.01	0.082	0.086	0.047
5	0.42	0	0.2547	0.001	0.034	0.023	0.141	0.124	0.073
6	0.72	0	0.2542	0.01	0.051	0.035	0.196	0.187	0.111
7	1.38	0.001	0.1138	0.01	0.023	0.016	0.107	0.1	0.057
8	2.75	0.002	0.1953	0.028	0.047	0.029	0.22	0.245	0.127
9	5.50	0.008	0.24	0.017	0.042	0.014	0.256	0.355	0.138
10	11.05	0.000	0.127	0.000	0.000	0.000	0.000	0.000	0.000

Sum, dilution includ	A	B	C	D	E	F	G	H
Marr, total	0.0795	10.3804	0.48422	1.561066	0.91785	7.53793	8.22451	4.07612
Marr, Dqs5.501	0.0795	9.46252	0.48422	1.561066	0.91785	7.53793	8.22451	4.07612

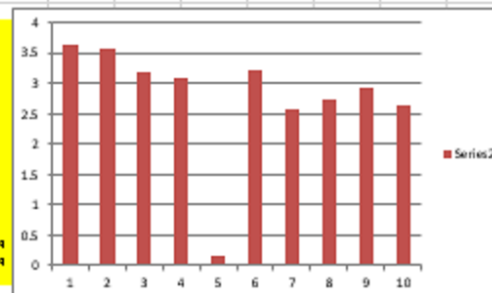
Sum, carrier exclud	A	B	C	D	E	F	G	H
Marr, total		10.3	0.405	1.4816	0.838	7.458	8.145	3.997
Marr, Dqs5.501		9.383	0.405	1.4816	0.838	7.458	8.145	3.997



ED 2.99125
CV 0.11374

FPD 0.43378
FPF 0.39542

ED	0
1	15.2098 15.2062 3.44
2	15.2087 15.2051 3.58
3	15.2107 15.2075 3.19
4	15.2131 15.21 3.08
5	15.2091 15.2089 0.15
6	15.2146 15.2114 3.2
7	15.2144 15.2119 2.58
8	15.2142 15.2115 2.74
9	15.2148 15.2118 2.94
10	15.2153 15.2127 2.42
TOT	23.93 mq
AVEG	2.99125 mq
STDEV	0.34023



APPENDIX 14: ED, CV_{ED} and FPF of Bu20L0.875Ph0.146 at 2kPa with Twister™ (link to file)

Main flow rate	60	lpm	total flow	175.00	lpm
Feeding rate	1.2	lpm	ELPI flow	24.21	lpm
Parasol disc flow rate	39.2	lpm			
Parasol tube flow rate	54.3	lpm	Dilution factor	7.2	

Collection on the stage																	
		carrier		fine particles													
ramplor		A		B		C		D		E		F		G		H	
stage	D _g	start	end	start	end	start	end	start	end	start	end	start	end	start	end	start	end
1	0.04	107.931	107.931	88.0773	88.0928	106.174	106.174	106.705	106.705	106.913	106.913	106.751	106.751	107.711	107.712	108.507	108.507
2	0.08	106.367	106.367	87.8333	87.8717	107.333	107.333	107.174	107.174	106.96	106.96	107.847	107.862	106.694	106.701	106.816	106.821
3	0.13	106.806	106.806	88.3961	88.446	107.532	107.532	107.066	107.069	107.405	107.405	108.165	108.191	106.404	106.427	107.216	107.222
4	0.24	107.032	107.032	88.0396	88.2317	107.007	107.008	107.08	107.096	106.751	106.761	106.577	106.659	107.043	107.129	107.007	107.054
5	0.42	107.431	107.431	87.9785	88.2992	107.672	107.673	107.181	107.215	106.345	106.368	107.661	107.802	106.906	107.04	107.377	107.45
6	0.72	106.941	106.941	88.0253	88.4288	107.241	107.251	106.326	106.377	106.486	106.521	106.971	107.167	107.143	107.33	107.057	107.168
7	1.38	107.825	107.826	87.9077	88.106	107.273	107.283	107.534	107.557	106.751	106.767	107.266	107.373	106.206	106.306	106.823	106.88
8	2.75	107.025	107.027	87.7842	88.2718	108.144	108.172	106.253	106.3	107.402	107.431	107.137	107.357	106.774	107.019	106.934	107.061
9	5.50	107.565	107.573														
10	11.05																

Stage	D _g	A	B	C	D	E	F	G	H
1	0.04	0	0.0155	0	0	0	0	0.001	0
2	0.08	0	0.0384	0	0	0	0.015	0.007	0.005
3	0.13	0	0.0499	0	0.002	0	0.026	0.023	0.006
4	0.24	0	0.1921	0.001	0.016	0.01	0.082	0.086	0.047
5	0.42	0	0.3207	0.001	0.034	0.023	0.141	0.134	0.073
6	0.72	0	0.4035	0.01	0.051	0.035	0.196	0.187	0.111
7	1.38	0.001	0.1983	0.01	0.023	0.016	0.107	0.1	0.057
8	2.75	0.002	0.4876	0.028	0.047	0.029	0.22	0.245	0.127
9	5.50	0.008	0.6274	0.017	0.042	0.014	0.256	0.355	0.138
10	11.05	0.000	0.2165	0.000	0.000	0.000	0.000	0.000	0.000

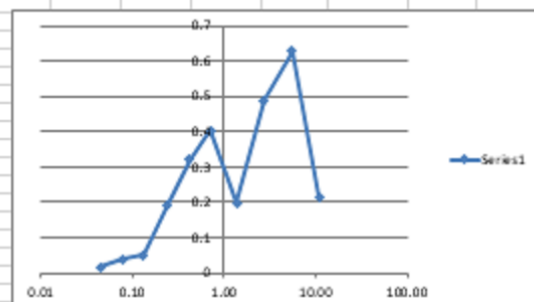
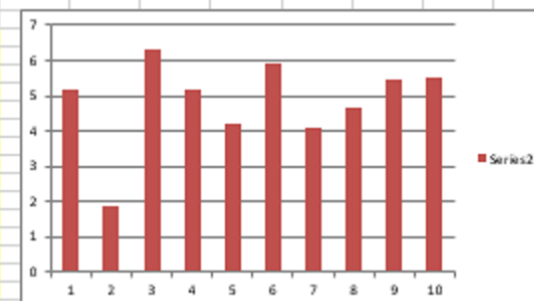
Sum, dilution include	A	B	C	D	E	F	G	H
Marr, total	0.079499	18.42853	0.48422	1.5610664	0.91785	7.537927	8.224507	4.076118
Marr, Dqs5.501	0.079499	16.86385	0.48422	1.5610664	0.91785	7.537927	8.224507	4.076118

Sum, carrier exclude	A	B	C	D	E	F	G	H
Marr, total		18.35	0.405	1.4816	0.838	7.458	8.145	3.997
Marr, Dqs5.501		16.78	0.405	1.4816	0.838	7.458	8.145	3.997

ED 5.03125
CV 0.126374

FPD 0.457852
FPF 0.418978

ED
0 4839.63
1 4834.43 5.2
2 4832.55 1.88
3 4826.26 6.29
4 4821.06 5.2
5 4816.84 4.22
6 4810.93 5.91
7 4806.82 4.11
8 4802.15 4.67
9 4796.7 5.45
10 4791.21 5.49
TOT 40.25 mg
AVEG 5.03125 mg
STDEV 0.638333



APPENDIX 15: ED, CV_{ED} and FPF of Bu20L0.875Ph0.146 at 4kPa with Easyhaler®

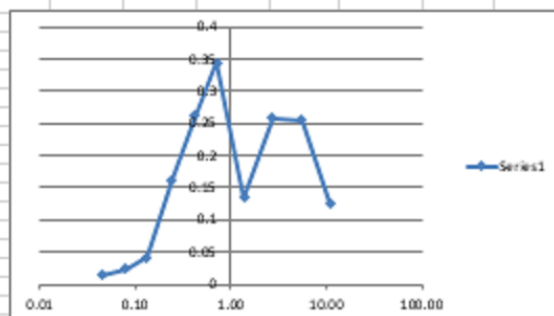
Main flow rate	60	lpm	total flow	175.00	lpm
Feeding rate	1.2	lpm	ELPI flow	24.21	lpm
Pursur disc flow rate	39.2	lpm			
Pursur tube flow rate	54.3	lpm	Dilution factor	7.2	

Collection on the stage																	
		carrier		fine particles													
ramp		A		B		C		D		E		F		G		H	
stage	Dq	start	end	start	end	start	end	start	end	start	end	start	end	start	end	start	end
1	0.04	107.931	107.931	88.1803	88.1945	106.174	106.174	106.705	106.705	106.913	106.913	106.751	106.751	107.711	107.712	108.507	108.507
2	0.08	106.367	106.367	88.7448	88.7683	107.333	107.333	107.174	107.174	106.96	106.96	107.847	107.862	106.694	106.701	106.816	106.821
3	0.13	106.806	106.806	87.8245	87.8667	107.532	107.532	107.066	107.069	107.405	107.405	108.165	108.191	106.404	106.427	107.216	107.222
4	0.24	107.032	107.032	88.0439	88.2067	107.007	107.008	107.08	107.096	106.751	106.761	106.577	106.659	107.043	107.129	107.007	107.054
5	0.42	107.431	107.431	88.5045	88.7654	107.672	107.673	107.181	107.215	106.345	106.368	107.661	107.802	106.906	107.04	107.377	107.45
6	0.72	106.941	106.941	88.2698	88.6141	107.241	107.251	106.326	106.377	106.486	106.521	106.971	107.167	107.143	107.33	107.057	107.168
7	1.38	107.825	107.826	87.6697	87.8029	107.273	107.283	107.534	107.557	106.751	106.767	107.266	107.373	106.206	106.306	106.823	106.88
8	2.75	107.025	107.027	87.6875	87.9453	108.144	108.172	106.253	106.3	107.402	107.431	107.137	107.357	106.774	107.019	106.934	107.061
9	5.50	107.565	107.573	88.0164	88.2711	107.192	107.209	107.365	107.407	107.448	107.462	106.524	106.78	106.262	106.617	107.116	107.254
10	11.05			88.1499	88.2769												

Stage	Dq	A	B	C	D	E	F	G	H
1	0.04	0	0.0142	0	0	0	0	0.001	0
2	0.08	0	0.0235	0	0	0	0.015	0.007	0.005
3	0.13	0	0.0422	0	0.003	0	0.026	0.023	0.006
4	0.24	0	0.1628	0.001	0.016	0.01	0.082	0.086	0.047
5	0.42	0	0.2609	0.001	0.034	0.023	0.141	0.134	0.073
6	0.72	0	0.3443	0.01	0.051	0.035	0.196	0.187	0.111
7	1.38	0.001	0.1342	0.01	0.023	0.016	0.107	0.1	0.057
8	2.75	0.002	0.2578	0.028	0.047	0.029	0.22	0.245	0.127
9	5.50	0.008	0.2547	0.017	0.042	0.014	0.256	0.355	0.138
10	11.05	0.000	0.127	0.000	0.000	0.000	0.000	0.000	0.000

Sum, dilution include	A	B	C	D	E	F	G	H
Marr, total	0.079499	11.71956	0.48422	1.5610664	0.91785	7.537927	8.224507	4.076118
Marr, Dq5.501	0.079499	10.80171	0.48422	1.5610664	0.91785	7.537927	8.224507	4.076118

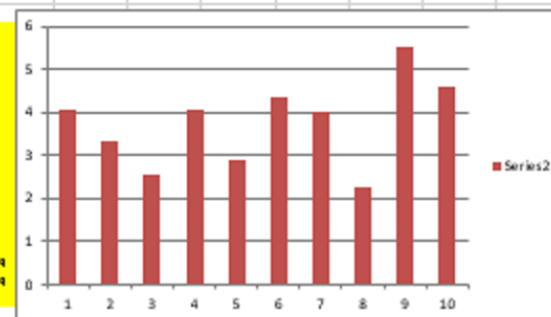
Sum, carrier exclude	A	B	C	D	E	F	G	H
Marr, total	11.64	0.405	1.4816	0.838	7.458	8.145	3.997	
Marr, Dq5.501	10.72	0.405	1.4816	0.838	7.458	8.145	3.997	



ED 3.72625
CV 0.196251

FPD 0.393142
FPF 0.362352

ED
0
1 15.42284 15.41877 4.07
2 15.46628 15.46297 3.31
3 15.50849 15.50595 2.54
4 15.55078 15.54673 4.05
5 15.59302 15.59094 2.88
6 15.63727 15.6329 4.37
7 15.68094 15.67693 4.01
8 15.72528 15.72301 2.27
9 15.7733 15.76777 5.53
10 15.81709 15.81251 4.58
TOT 29.81 mg
AVEG 3.72625 mg
STDEV 0.731279



APPENDIX 16: ED, CV_{ED} and FPF of Bu20L0.875Ph0.146 at 4kPa with Twister™

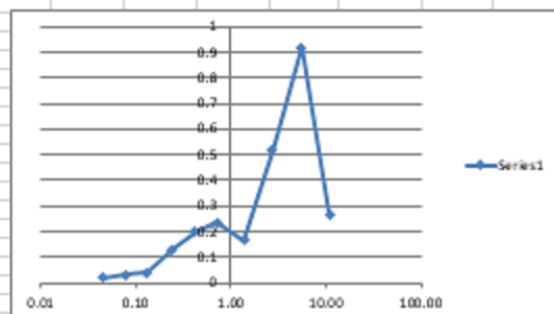
Main flow rate	60	lpm	total flow	175.00 lpm
Feeding rate	1.2	lpm	ELPI flow	24.21 lpm
Passive direct flow rate	38.2	lpm		
Passive tube flow rate	54.3	lpm	Dilution factor	7.2

Collection on the stage																	
		carrier		fine particles													
sampler		A		B		C		D		E		F		G		H	
stage	Dq	start	end	start	end	start	end	start	end	start	end	start	end	start	end	start	end
1	0.04	107.931	107.931	88.5883	88.6053	106.174	106.174	106.705	106.705	106.913	106.913	106.751	106.751	107.711	107.712	108.507	108.507
2	0.08	106.367	106.367	88.2785	88.3098	107.333	107.333	107.174	107.174	106.96	106.96	107.847	107.862	106.694	106.701	106.816	106.821
3	0.13	106.806	106.806	88.007	88.0476	107.532	107.532	107.066	107.069	107.405	107.405	108.165	108.191	106.404	106.427	107.216	107.222
4	0.24	107.032	107.032	88.4876	88.6179	107.007	107.008	107.08	107.096	106.751	106.761	106.577	106.659	107.043	107.129	107.007	107.054
5	0.42	107.431	107.431	88.5348	88.7332	107.672	107.673	107.181	107.215	106.345	106.368	107.661	107.802	106.906	107.04	107.377	107.45
6	0.72	106.941	106.941	88.3658	88.6001	107.241	107.251	106.326	106.377	106.486	106.521	106.971	107.167	107.143	107.33	107.057	107.168
7	1.38	107.825	107.826	88.2174	88.3835	107.273	107.283	107.534	107.557	106.751	106.767	107.266	107.373	106.206	106.306	106.823	106.88
8	2.75	107.025	107.027	88.7147	89.2285	108.144	108.172	106.253	106.3	107.402	107.431	107.137	107.357	106.774	107.019	106.934	107.061
9	5.50	107.565	107.573	88.2444	89.164	107.192	107.209	107.365	107.407	107.448	107.462	106.524	106.78	106.262	106.617	107.116	107.254
10	11.05			88.1743	88.4423												

Stage	Dq	A	B	C	D	E	F	G	H
1	0.04	0	0.017	0	0	0	0.015	0.007	0.005
2	0.08	0	0.0313	0	0	0	0.026	0.023	0.006
3	0.13	0	0.0406	0	0.003	0	0.082	0.086	0.047
4	0.24	0	0.1303	0.001	0.016	0.01	0.134	0.134	0.073
5	0.42	0	0.1984	0.001	0.034	0.023	0.196	0.187	0.111
6	0.72	0	0.2343	0.01	0.051	0.035	0.107	0.1	0.057
7	1.38	0.001	0.1661	0.01	0.023	0.016	0.22	0.245	0.127
8	2.75	0.002	0.5138	0.028	0.047	0.029	0.256	0.355	0.138
9	5.50	0.008	0.9196	0.017	0.042	0.014	0.000	0.000	0.000
10	11.05	0.000	0.268	0.000	0.000	0.000	0.000	0.000	0.000

Sum, dilution include	A	B	C	D	E	F	G	H
Marr, total	0.079499	18.2081	0.48422	1.5610664	0.91785	7.537927	8.224507	4.076118
Marr, Dqs 5.501	0.079499	16.27123	0.48422	1.5610664	0.91785	7.537927	8.224507	4.076118

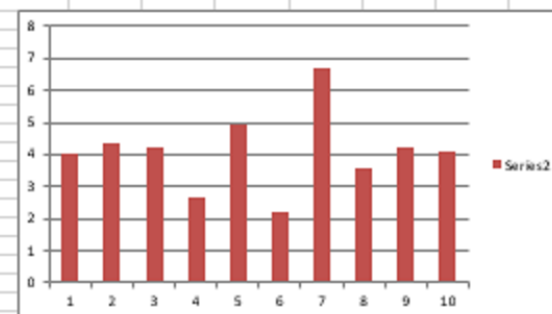
Sum, carrier exclude	A	B	C	D	E	F	G	H
Marr, total		18.13	0.405	1.4816	0.838	7.458	8.145	3.997
Marr, Dqs 5.501		16.19	0.405	1.4816	0.838	7.458	8.145	3.997



ED 4.0075
CV 0.164452

FPD 0.567938
FPF 0.507524

ED
0 20847.84
1 20843.8 4.04
2 20839.46 4.34
3 20835.24 4.22
4 20832.57 2.67
5 20827.64 4.93
6 20825.41 2.23
7 20818.74 6.67
8 20815.17 3.57
9 20810.94 4.23
10 20806.88 4.06
TOT 32.06 mg
AVEG 4.0075 mg
STDEV 0.659042



APPENDIX 17: ED, CV_{ED} and FPF of Bu20L5Ph0.83 at 2kPa with Easyhaler®

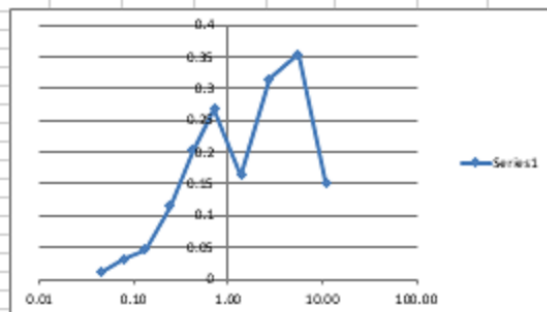
Main flow rate	60	lpm	total flow	175.00	lpm
Feeding rate	1.2	lpm	ELPI flow	24.21	lpm
Purifier direct flow rate	38.2	lpm			
Purifier tube flow rate	54.3	lpm	Dilution factor	7.2	

Collection on the stages																	
		carrier		fine particles													
stage	Dq	start	end	start	end	start	end	start	end	start	end	start	end	start	end	start	end
1	0.04	107.931	107.931	87.9093	87.9193	106.174	106.174	106.705	106.705	106.913	106.913	106.751	106.751	107.711	107.712	108.507	108.507
2	0.08	106.367	106.367	88.1569	88.1894	107.333	107.333	107.174	107.174	106.96	106.96	107.847	107.862	106.694	106.701	106.816	106.821
3	0.13	106.806	106.806	88.3074	88.3545	107.532	107.532	107.066	107.069	107.405	107.405	108.165	108.191	106.404	106.427	107.216	107.222
4	0.24	107.032	107.032	88.2975	88.4127	107.007	107.008	107.08	107.096	106.751	106.761	106.577	106.659	107.043	107.129	107.007	107.054
5	0.42	107.431	107.431	87.6839	87.8872	107.672	107.673	107.181	107.215	106.345	106.368	107.641	107.802	106.906	107.04	107.377	107.45
6	0.72	106.941	106.941	87.8337	88.1013	107.241	107.251	106.326	106.377	106.486	106.521	106.971	107.167	107.143	107.33	107.057	107.168
7	1.38	107.925	107.926	88.3981	88.5626	107.273	107.283	107.534	107.557	106.751	106.767	107.266	107.373	106.206	106.306	106.823	106.88
8	2.75	107.025	107.027	87.8056	88.1208	108.144	108.172	106.253	106.3	107.402	107.431	107.137	107.357	106.774	107.019	106.934	107.061
9	5.50	107.573	107.573	88.0983	88.4531	107.192	107.209	107.365	107.407	107.448	107.462	106.524	106.78	106.262	106.617	107.116	107.254
10	11.05			88.0001	88.152												

Stage	Dq	A	B	C	D	E	F	G	H
1	0.04	0	0.01	0	0	0	0	0.001	0
2	0.08	0	0.0325	0	0	0	0.015	0.007	0.005
3	0.13	0	0.0471	0	0.003	0	0.026	0.023	0.006
4	0.24	0	0.1152	0.001	0.016	0.01	0.082	0.086	0.047
5	0.42	0	0.2033	0.001	0.034	0.023	0.141	0.134	0.073
6	0.72	0	0.2676	0.01	0.051	0.035	0.196	0.187	0.111
7	1.38	0.001	0.1645	0.01	0.023	0.016	0.107	0.1	0.057
8	2.75	0.002	0.3152	0.028	0.047	0.029	0.22	0.245	0.127
9	5.50	0.008	0.3548	0.017	0.042	0.014	0.256	0.355	0.138
10	11.05	0.000	0.1519	0.000	0.000	0.000	0.000	0.000	0.000

Sum, dilution include	A	B	C	D	E	F	G	H
Mazz, total	0.079499	12.01226	0.48422	1.5610664	0.91785	7.537927	8.224507	4.076118
Mazz, Dqs5.501	0.079499	10.91446	0.48422	1.5610664	0.91785	7.537927	8.224507	4.076118

Sum, carrier exclude	A	B	C	D	E	F	G	H
Mazz, total		11.93	0.405	1.4816	0.838	7.458	8.145	3.997
Mazz, Dqs5.501		10.83	0.405	1.4816	0.838	7.458	8.145	3.997

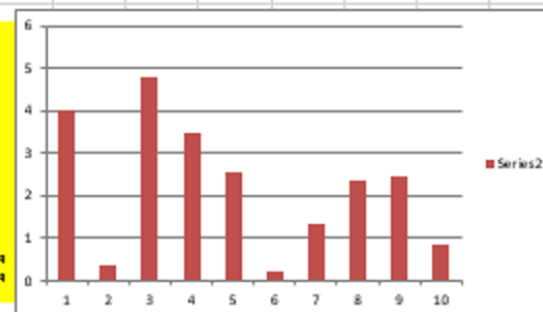


ED 2.1775
CV 0.575867

FPD 0.689567
FPF 0.626547

ED

0		
1	15.21167	15.20765
2	15.20923	15.20885
3	15.2138	15.209
4	15.20973	15.20625
5	15.21223	15.20968
6	15.21163	15.2114
7	15.20936	15.20801
8	15.2126	15.21025
9	15.21364	15.2112
10	15.21485	15.214
TOT		17.42 mq
AVEG		2.1775 mq
STDEV		1.253951



APPENDIX 18: ED, CV_{ED} and FPF of Bu20L5Ph0.83 at 2kPa with Twister™

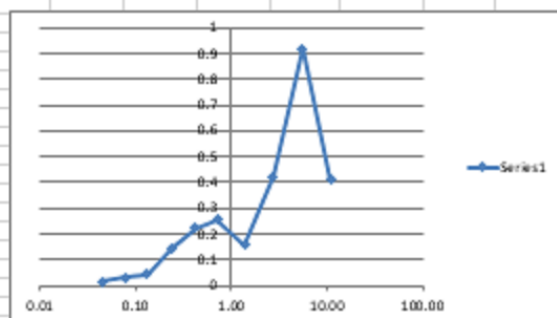
Main flow rate	60	lpm	total flow	175.00	lpm
Feeding rate	1.2	lpm	HLPI flow	24.21	lpm
Pneum. disc. flow rate	39.2	lpm			
Pneum. tube flow rate	54.3	lpm	Dilution factor	7.2	

Collection on the stage																	
		carrier		fine particles													
sampler		A		B		C		D		E		F		G		H	
stage	Dq	start	end	start	end	start	end	start	end	start	end	start	end	start	end	start	end
1	0.04	107.931	107.931	88.685	88.698	106.174	106.174	106.705	106.705	106.913	106.913	106.751	106.751	107.711	107.712	108.507	108.507
2	0.08	106.367	106.367	88.3933	88.4134	107.333	107.333	107.174	107.174	106.96	106.96	107.847	107.862	106.694	106.701	106.816	106.821
3	0.13	106.806	106.806	88.7775	88.8196	107.532	107.532	107.066	107.066	107.405	107.405	108.165	108.191	106.404	106.427	107.216	107.222
4	0.24	107.032	107.032	88.3798	88.5265	107.007	107.008	107.08	107.096	106.751	106.761	106.577	106.659	107.043	107.129	107.007	107.054
5	0.42	107.431	107.431	88.4638	88.6874	107.672	107.673	107.181	107.215	106.345	106.368	107.661	107.802	106.906	107.04	107.377	107.45
6	0.72	106.941	106.941	88.2321	88.4864	107.241	107.251	106.326	106.377	106.486	106.521	106.971	107.167	107.143	107.33	107.057	107.168
7	1.38	107.925	107.926	88.6995	88.8547	107.273	107.283	107.534	107.557	106.751	106.767	107.266	107.373	106.206	106.306	106.823	106.88
8	2.75	107.025	107.027	88.3444	88.7654	108.144	108.172	106.253	106.3	107.402	107.431	107.137	107.357	106.774	107.019	106.934	107.061
9	5.50	107.565	107.573	88.5155	89.4322	107.192	107.209	107.365	107.407	107.448	107.462	106.524	106.78	106.262	106.617	107.116	107.254
10	11.05			88.6942	89.0947												

Stage	Dq	A	B	C	D	E	F	G	H
1	0.04	0	0.0138	0	0	0	0	0.001	0
2	0.08	0	0.0301	0	0	0	0.015	0.007	0.005
3	0.13	0	0.0421	0	0.003	0	0.026	0.023	0.006
4	0.24	0	0.1467	0.001	0.016	0.01	0.082	0.086	0.047
5	0.42	0	0.2236	0.001	0.034	0.023	0.141	0.134	0.073
6	0.72	0	0.2543	0.01	0.051	0.035	0.196	0.187	0.111
7	1.38	0.001	0.1552	0.01	0.023	0.016	0.107	0.1	0.057
8	2.75	0.002	0.421	0.028	0.047	0.029	0.22	0.245	0.127
9	5.50	0.008	0.9168	0.017	0.042	0.014	0.256	0.355	0.138
10	11.05	0.000	0.4105	0.000	0.000	0.000	0.000	0.000	0.000

Sum, dilution include	A	B	C	D	E	F	G	H
Marr, total	0.079499	18.89252	0.48422	1.5610664	0.91785	7.537927	8.224507	4.076118
Marr, Dqs5.501	0.079499	15.92577	0.48422	1.5610664	0.91785	7.537927	8.224507	4.076118

Sum, carrier exclude	A	B	C	D	E	F	G	H
Marr, total		18.81	0.405	1.4816	0.838	7.458	8.145	3.997
Marr, Dqs5.501		15.85	0.405	1.4816	0.838	7.458	8.145	3.997



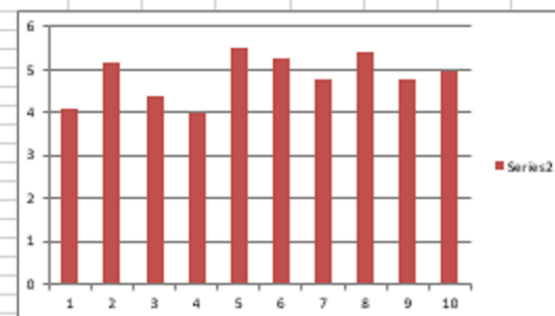
ED 4.36
CV 0.09014

FPD 0.405919
FPF 0.409612

ED

0	4455.35	
1	4451.24	4.11
2	4446.05	5.19
3	4441.65	4.4
4	4437.68	3.97
5	4432.18	5.5
6	4426.93	5.25
7	4422.16	4.77
8	4416.77	5.39
9	4411.98	4.79
10	4407	4.98

TOT 38.88 mg
AVEG 4.86 mg
STDEV 0.43898



APPENDIX 19: ED, CV_{ED} and FPF of Bu20L5Ph0.83 at 4kPa with Easyhaler®

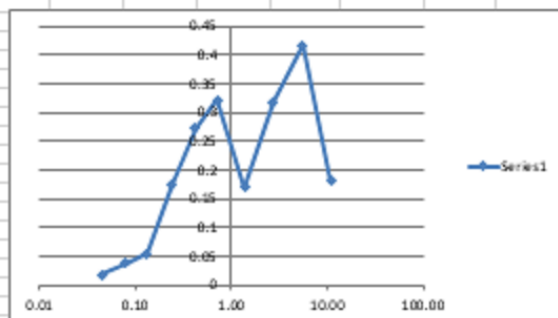
Main flow rate	60	lpm	total flow	175.00	lpm
Feeding rate	1.2	lpm	PLI flow	24.21	lpm
Purpur dirc flow rate	38.2	lpm			
Purpur tube flow rate	54.3	lpm	Dilution factor	7.2	

Collection on the stage																	
		carrier		fine particles													
sampler		A		B		C		D		E		F		G		H	
stage	Dq	start	end	start	end	start	end	start	end	start	end	start	end	start	end	start	end
1	0.04	107.931	107.931	88.1923	88.2117	106.174	106.174	106.705	106.705	106.913	106.913	106.751	106.751	107.711	107.712	108.507	108.507
2	0.08	106.367	106.367	88.0055	88.0432	107.333	107.333	107.174	107.174	106.96	106.96	107.847	107.862	106.694	106.701	106.816	106.821
3	0.13	106.806	106.806	88.2369	88.2907	107.532	107.532	107.066	107.069	107.405	107.405	108.165	108.191	106.404	106.427	107.216	107.222
4	0.24	107.032	107.032	88.0811	88.2554	107.007	107.008	107.08	107.096	106.751	106.761	106.577	106.659	107.043	107.129	107.007	107.054
5	0.42	107.431	107.431	87.923	88.2059	107.672	107.673	107.181	107.215	106.345	106.368	107.661	107.802	106.906	107.04	107.377	107.45
6	0.72	106.941	106.941	88.1948	88.5171	107.241	107.251	106.326	106.377	106.486	106.521	106.971	107.167	107.143	107.33	107.057	107.168
7	1.38	107.825	107.826	87.6748	87.8447	107.273	107.283	107.534	107.557	106.751	106.767	107.266	107.373	106.206	106.306	106.823	106.88
8	2.75	107.025	107.027	88.2274	88.5447	108.144	108.172	106.253	106.3	107.402	107.431	107.137	107.357	106.774	107.019	106.934	107.061
9	5.50	107.565	107.573	88.3425	88.7604	107.192	107.209	107.365	107.407	107.448	107.462	106.524	106.78	106.262	106.617	107.116	107.254
10	11.05			88.2461	88.5264												

Stage	Dq	A	B	C	D	E	F	G	H
1	0.04	0	0.0184	0	0	0	0	0.001	0
2	0.08	0	0.0377	0	0	0	0.015	0.007	0.005
3	0.13	0	0.0538	0	0.003	0	0.026	0.023	0.006
4	0.24	0	0.1743	0.001	0.016	0.01	0.082	0.086	0.047
5	0.42	0	0.2729	0.001	0.034	0.023	0.141	0.134	0.073
6	0.72	0	0.3223	0.01	0.051	0.035	0.196	0.187	0.111
7	1.38	0.001	0.1699	0.01	0.023	0.016	0.107	0.1	0.057
8	2.75	0.002	0.3173	0.028	0.047	0.029	0.22	0.245	0.127
9	5.50	0.008	0.4169	0.017	0.042	0.014	0.256	0.355	0.138
10	11.05	0.000	0.1803	0.000	0.000	0.000	0.000	0.000	0.000

Sum, dilution include	A	B	C	D	E	F	G	H
Marr, total	0.079499	14.1927	0.48422	1.5610664	0.91785	7.537927	8.224507	4.076118
Marr, Dqs5.501	0.079499	12.88964	0.48422	1.5610664	0.91785	7.537927	8.224507	4.076118

Sum, carrier exclude	A	B	C	D	E	F	G	H
Marr, total		14.11	0.405	1.4816	0.838	7.458	8.145	3.997
Marr, Dqs5.501		12.81	0.405	1.4816	0.838	7.458	8.145	3.997



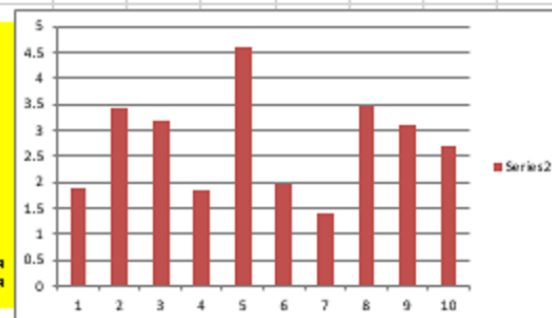
ED 2.69375
CV 0.26073

FPD 0.658594
FPF 0.598127

ED

Stage	Dq	ED	CV
1	0.04	15.20144	15.19956
2	0.08	15.2043	15.20089
3	0.13	15.20486	15.20167
4	0.24	15.20234	15.20051
5	0.42	15.20633	15.20175
6	0.72	15.20609	15.20411
7	1.38	15.20452	15.20313
8	2.75	15.20679	15.20332
9	5.50	15.20881	15.2057
10	11.05	15.20853	15.20585

TOT 21.55 mq
AVEG 2.69375 mq
STDEV 0.702342



APPENDIX 20: ED, CV_{ED} and FPF of Bu20L5Ph0.83 at 4kPa with Twister™

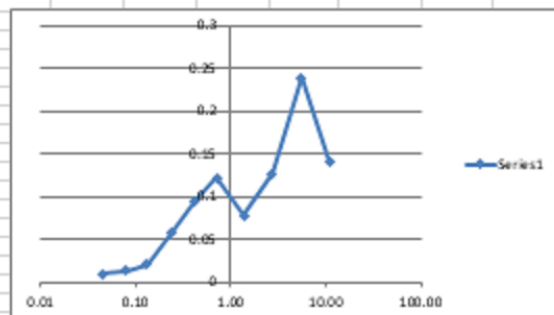
Main flow rate	50	lpm	total flow	175.00	lpm
Feeding rate	1.2	lpm	LPI flow	24.21	lpm
Purwar disc flow rate	38.2	lpm			
Purwar tube flow rate	56.3	lpm	Dilution factor	7.2	

Collection on the stage															
ramp		carrier		fine particles											
stage	Dq	start	end	start	end	start	end	start	end	start	end	start	end	start	end
1	0.04	107.931	107.931	88.1383	88.1475	106.174	106.174	106.705	106.705	106.913	106.913	106.751	106.751	107.711	108.507
2	0.08	106.367	106.367	87.7823	87.7947	107.333	107.333	107.174	107.174	106.96	106.96	107.847	107.862	106.694	106.816
3	0.13	106.806	106.806	87.6086	87.6291	107.532	107.532	107.066	107.066	107.405	107.405	108.165	108.191	106.404	107.216
4	0.24	107.032	107.032	88.124	88.192	107.007	107.008	107.08	107.096	106.751	106.761	106.577	106.659	107.043	107.129
5	0.42	107.431	107.431	87.8528	87.9488	107.672	107.673	107.181	107.215	106.345	106.368	107.661	107.802	106.906	107.04
6	0.72	106.941	106.941	87.9708	88.0926	107.241	107.251	106.326	106.377	106.486	106.521	106.971	107.167	107.143	107.33
7	1.38	107.825	107.826	88.0266	88.1042	107.273	107.283	107.534	107.557	106.751	106.767	107.266	107.373	106.206	106.306
8	2.75	107.025	107.027	88.086	88.2125	108.144	108.172	106.253	106.3	107.402	107.431	107.137	107.357	106.774	107.019
9	5.50	107.565	107.573	88.2576	88.4967	107.192	107.209	107.365	107.407	107.448	107.462	106.524	106.78	106.262	106.617
10	11.05			87.911	88.0527										

Stage	Dq	A	B	C	D	E	F	G	H
1	0.04	0	0.0092	0	0	0	0	0.001	0
2	0.08	0	0.0124	0	0	0.015	0.007	0.005	0.005
3	0.13	0	0.0205	0	0.003	0	0.026	0.023	0.006
4	0.24	0	0.058	0.001	0.016	0.01	0.082	0.086	0.047
5	0.42	0	0.095	0.001	0.034	0.023	0.141	0.134	0.073
6	0.72	0	0.1218	0.01	0.051	0.035	0.196	0.187	0.111
7	1.38	0.001	0.0776	0.01	0.023	0.016	0.107	0.1	0.057
8	2.75	0.002	0.1265	0.028	0.047	0.029	0.22	0.245	0.127
9	5.50	0.008	0.2391	0.017	0.042	0.014	0.256	0.355	0.138
10	11.05	0.000	0.1417	0.000	0.000	0.000	0.000	0.000	0.000

Sum, dilution include	A	B	C	D	E	F	G	H
Maz, total	0.079499	6.517452	0.48422	1.5610664	0.91785	7.537927	8.224507	4.076118
Maz, Dq5.501	0.079499	5.493364	0.48422	1.5610664	0.91785	7.537927	8.224507	4.076118

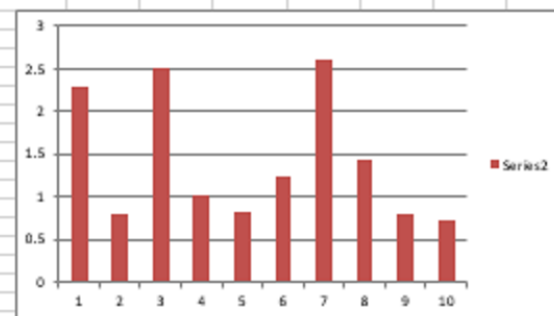
Sum, carrier exclude	A	B	C	D	E	F	G	H
Maz, total		6.438	0.405	1.4816	0.838	7.458	8.145	3.997
Maz, Dq5.501		5.414	0.405	1.4816	0.838	7.458	8.145	3.997



ED 1.36375
CV 0.497684

FPD 0.597383
FPF 0.503516

ED
0 20717.5
1 20715.22 2.28
2 20714.43 0.79
3 20711.92 2.51
4 20710.9 1.02
5 20710.07 0.83
6 20708.83 1.24
7 20706.23 2.6
8 20704.79 1.44
9 20703.99 0.8
10 20703.26 0.73
TOT 10.91 mg
AVEG 1.36375 mg
STDEV 0.678716



APPENDIX 21: ED, CV_{ED} and FPF of Bu20L15Ph2.5 at 2kPa with Easyhaler®

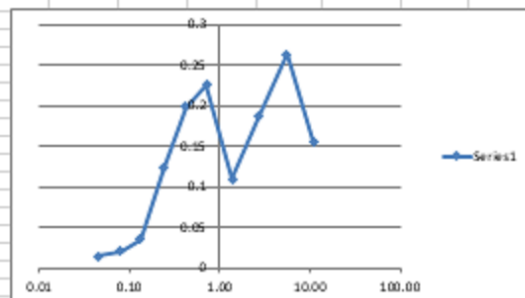
Main flow rate	60	lpm	total flow	175.00	lpm
Feeding rate	1.2	lpm	LPI flow	24.21	lpm
Purwar disc flow rate	38.2	lpm			
Purwar tube flow rate	54.3	lpm	Dilution factor	7.2	

Collection on the stage																
			carrier		fine particles											
stage	Dq		A	B	C	D	E	F	G	H						
stage	Dq	start	end	start	end	start	end	start	end	start	end	start	end	start	end	end
1	0.04	107.931	107.931	88.0581	88.0718	106.174	106.174	106.705	106.705	106.913	106.913	106.751	106.751	107.711	107.712	108.507
2	0.08	106.267	106.267	88.0129	88.0287	107.333	107.333	107.174	107.174	106.96	106.96	107.847	107.862	106.694	106.701	106.816
3	0.13	106.806	106.806	88.1225	88.1574	107.532	107.532	107.066	107.069	107.405	107.405	108.165	108.191	106.404	106.427	107.216
4	0.24	107.032	107.032	87.9899	88.1138	107.007	107.008	107.08	107.096	106.751	106.761	106.577	106.659	107.043	107.129	107.007
5	0.42	107.431	107.431	88.2577	88.5558	107.672	107.673	107.181	107.215	106.345	106.368	107.661	107.802	106.906	107.04	107.377
6	0.72	106.941	106.941	88.2108	88.4363	107.241	107.251	106.326	106.377	106.486	106.521	106.971	107.167	107.143	107.33	107.057
7	1.38	107.825	107.826	88.0377	88.1473	107.273	107.283	107.534	107.557	106.751	106.767	107.266	107.373	106.206	106.306	106.823
8	2.75	107.025	107.027	88.0453	88.2233	108.144	108.172	106.253	106.3	107.402	107.431	107.137	107.357	106.774	107.019	106.934
9	5.50	107.565	107.573	87.8629	88.1261	107.192	107.209	107.365	107.407	107.448	107.462	106.524	106.78	106.262	106.617	107.116
10	11.05			88.2806	88.4362											107.254

Stage	Dq	A	B	C	D	E	F	G	H
1	0.04	0	0.0137	0	0	0	0	0.001	0
2	0.08	0	0.0198	0	0	0	0.015	0.007	0.005
3	0.13	0	0.0349	0	0.003	0	0.026	0.023	0.006
4	0.24	0	0.1239	0.001	0.016	0.01	0.082	0.086	0.047
5	0.42	0	0.1981	0.001	0.034	0.023	0.141	0.134	0.073
6	0.72	0	0.2255	0.01	0.051	0.035	0.196	0.187	0.111
7	1.38	0.001	0.1096	0.01	0.023	0.016	0.107	0.1	0.057
8	2.75	0.002	0.1977	0.028	0.047	0.029	0.22	0.245	0.127
9	5.50	0.008	0.2632	0.017	0.042	0.014	0.256	0.355	0.138
10	11.05	0.000	0.1556	0.000	0.000	0.000	0.000	0.000	0.000

Sum, dilution include	A	B	C	D	E	F	G	H
Max, total	0.079499	9.626576	0.48422	1.5610664	0.91785	7.537927	8.224507	4.076118
Max, Dq5.501	0.079499	8.50203	0.48422	1.5610664	0.91785	7.537927	8.224507	4.076118

Sum, carrier exclude	A	B	C	D	E	F	G	H
Max, total		9.547	0.405	1.4816	0.838	7.458	8.145	3.997
Max, Dq5.501		8.423	0.405	1.4816	0.838	7.458	8.145	3.997



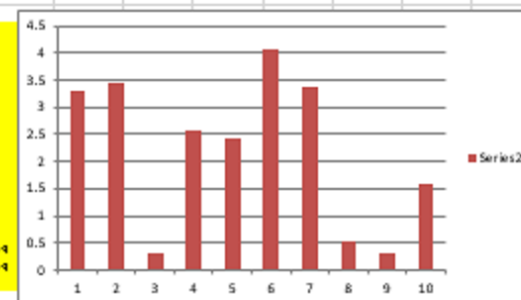
ED 2.18625

CV 0.573063

FPD 0.550405

FPF 0.486108

ED			
0			
1	15.2131	15.20981	3.29
2	15.21518	15.21175	3.43
3	15.21663	15.21634	0.29
4	15.2125	15.20994	2.56
5	15.2139	15.21148	2.42
6	15.21746	15.21341	4.05
7	15.2155	15.21213	3.37
8	15.21504	15.21452	0.52
9	15.21422	15.2139	0.32
10	15.21412	15.21254	1.58
TOT			17.49 m.g
AVEG			2.18625 m.g
STDEV			1.252859



APPENDIX 22: ED, CV_{ED} and FPF of Bu20L15Ph2.5 at 2kPa with Twister™

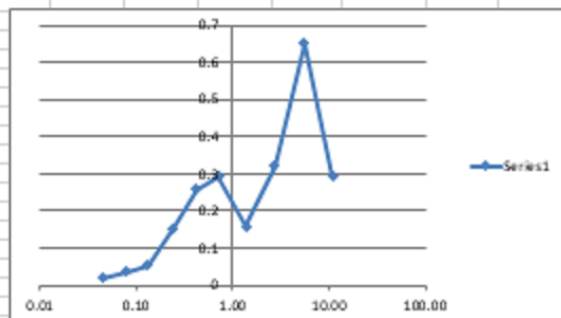
Main flow rate	60	lpm	total flow	175.00	lpm
Feeding rate	1.2	lpm	LP1 flow	24.21	lpm
Passive dir flow rate	38.2	lpm			
Passive tube flow rate	54.3	lpm	Dilution factor	7.2	

Collection on the stage																	
		carrier		fine particles													
sampler		A		B		C		D		E		F		G		H	
stage	Dq	start	end	start	end	start	end	start	end	start	end	start	end	start	end	start	end
1	0.04	107.931	107.931	88.0735	88.0916	106.174	106.174	106.705	106.705	106.913	106.913	106.751	106.751	107.711	107.711	108.507	108.507
2	0.08	106.367	106.367	88.2967	88.3324	107.333	107.333	107.174	107.174	106.96	106.96	107.847	107.847	106.694	106.701	106.816	106.821
3	0.13	106.806	106.806	88.2337	88.2875	107.532	107.532	107.066	107.066	107.405	107.405	108.165	108.191	106.404	106.427	107.216	107.222
4	0.24	107.032	107.032	88.1805	88.3336	107.007	107.008	107.08	107.096	106.751	106.761	106.577	106.659	107.043	107.129	107.007	107.054
5	0.42	107.431	107.431	88.0884	88.3462	107.672	107.673	107.181	107.215	106.345	106.368	107.661	107.802	106.906	107.04	107.377	107.45
6	0.72	106.941	106.941	88.0149	88.3059	107.241	107.251	106.326	106.377	106.486	106.521	106.971	107.167	107.143	107.33	107.057	107.168
7	1.38	107.825	107.826	88.266	88.4248	107.273	107.283	107.534	107.557	106.751	106.767	107.266	107.373	106.206	106.306	106.823	106.88
8	2.75	107.025	107.027	88.2151	88.5364	108.144	108.172	106.253	106.3	107.402	107.431	107.137	107.357	106.774	107.019	106.934	107.061
9	5.50	107.573	107.573	87.9616	88.6137	107.192	107.209	107.365	107.407	107.448	107.462	106.524	106.78	106.262	106.617	107.116	107.254
10	11.05			88.3113	88.6023												

Stage	Dq	A	B	C	D	E	F	G	H
1	0.04	0	0.0181	0	0	0	0	0.001	0
2	0.08	0	0.0357	0	0	0	0.015	0.007	0.005
3	0.13	0	0.0538	0	0.003	0	0.026	0.023	0.006
4	0.24	0	0.1531	0.001	0.016	0.01	0.082	0.086	0.047
5	0.42	0	0.2576	0.001	0.034	0.023	0.141	0.134	0.073
6	0.72	0	0.291	0.01	0.051	0.035	0.196	0.187	0.111
7	1.38	0.001	0.1588	0.01	0.023	0.016	0.107	0.1	0.057
8	2.75	0.002	0.3213	0.028	0.047	0.029	0.22	0.245	0.127
9	5.50	0.008	0.6521	0.017	0.042	0.014	0.256	0.355	0.138
10	11.05	0.000	0.291	0.000	0.000	0.000	0.000	0.000	0.000

Sum, dilution include	A	B	C	D	E	F	G	H
Marr, total	0.079499	16.13463	0.48422	1.5610664	0.91785	7.537927	8.224507	4.076118
Marr, Dqs5.501	0.079499	14.03153	0.48422	1.5610664	0.91785	7.537927	8.224507	4.076118

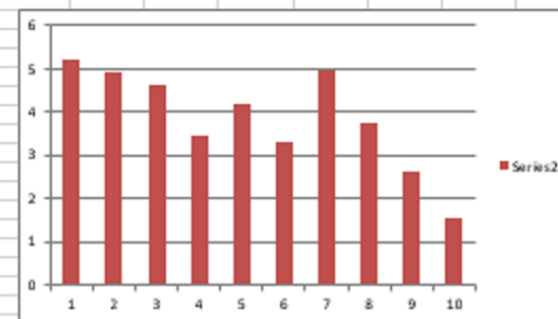
Sum, carrier exclude	A	B	C	D	E	F	G	H
Marr, total		16.06	0.405	1.4816	0.838	7.458	8.145	3.997
Marr, Dqs5.501		13.95	0.405	1.4816	0.838	7.458	8.145	3.997



ED 3.98125
CV 0.212629

FPD 0.506582
FPF 0.44055

ED
0 4292.02
1 4286.79 5.23
2 4281.85 4.94
3 4277.23 4.62
4 4273.77 3.46
5 4269.56 4.21
6 4266.27 3.29
7 4261.31 4.96
8 4257.55 3.76
9 4254.94 2.61
10 4253.39 1.55
TOT 31.85 mg
AVEG 3.98125 mg
STDEV 0.84653



APPENDIX 23: ED, CV_{ED} and FPF of Bu20L15Ph2.5 at 4kPa with Easyhaler®

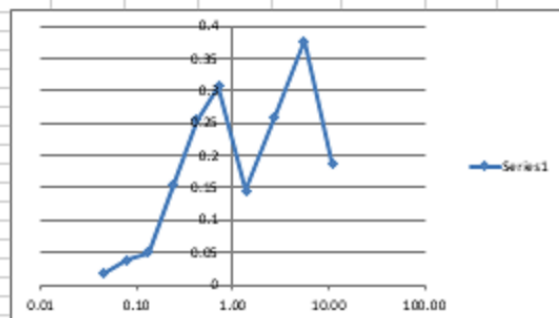
Main flow rate	60	lpm	total flow	175.00	lpm
Feeding rate	1.2	lpm	ILPI flow	24.21	lpm
Purser disc flow rate	38.2	lpm			
Purser tube flow rate	54.3	lpm	Dilution factor	7.2	

Collection on the stage																	
		carrier		fine particles													
sampler		A		B		C		D		E		F		G		H	
stage	Dq	start	end	start	end	start	end	start	end	start	end	start	end	start	end	start	end
1	0.04	107.931	107.931	88.1504	88.1678	106.174	106.174	106.705	106.705	106.913	106.913	106.751	106.751	107.711	107.712	108.507	108.507
2	0.08	106.367	106.367	88.1933	88.2321	107.333	107.333	107.174	107.174	106.96	106.96	107.847	107.862	106.694	106.701	106.816	106.821
3	0.13	106.806	106.806	87.6687	87.719	107.532	107.532	107.066	107.066	107.405	107.405	108.165	108.191	106.404	106.427	107.216	107.222
4	0.24	107.032	107.032	88.3343	88.4907	107.007	107.008	107.08	107.096	106.751	106.761	106.577	106.659	107.043	107.129	107.007	107.054
5	0.42	107.431	107.431	88.3007	88.5564	107.672	107.673	107.181	107.215	106.345	106.368	107.661	107.802	106.906	107.04	107.377	107.45
6	0.72	106.941	106.941	88.3056	88.6134	107.241	107.251	106.326	106.377	106.486	106.521	106.971	107.167	107.143	107.33	107.057	107.168
7	1.38	107.825	107.826	88.2113	88.3567	107.273	107.283	107.534	107.557	106.751	106.767	107.266	107.373	106.206	106.306	106.823	106.88
8	2.75	107.025	107.027	87.9491	88.209	108.144	108.172	106.253	106.3	107.402	107.431	107.137	107.357	106.774	107.019	106.934	107.061
9	5.50	107.565	107.573	88.0547	88.4322	107.192	107.209	107.365	107.407	107.448	107.462	106.524	106.78	106.262	106.617	107.116	107.254
10	11.05			87.962	88.1504												

Stage	Dq	A	B	C	D	E	F	G	H
1	0.04	0	0.0174	0	0	0	0	0.001	0
2	0.08	0	0.0388	0	0	0.015	0.007	0.005	0.005
3	0.13	0	0.0503	0	0.003	0	0.026	0.023	0.006
4	0.24	0	0.1564	0.001	0.016	0.01	0.082	0.086	0.047
5	0.42	0	0.2557	0.001	0.034	0.023	0.141	0.134	0.073
6	0.72	0	0.3078	0.01	0.051	0.035	0.196	0.187	0.111
7	1.38	0.001	0.1454	0.01	0.023	0.016	0.107	0.1	0.057
8	2.75	0.002	0.2599	0.028	0.047	0.029	0.22	0.245	0.127
9	5.50	0.008	0.3775	0.017	0.042	0.014	0.256	0.355	0.138
10	11.05	0.000	0.1884	0.000	0.000	0.000	0.000	0.000	0.000

Sum, dilution include	A	B	C	D	E	F	G	H
Marr, total	0.079499	12.99154	0.48422	1.5610664	0.91785	7.537927	8.224507	4.076118
Marr, Dqs 5.501	0.079499	11.62994	0.48422	1.5610664	0.91785	7.537927	8.224507	4.076118

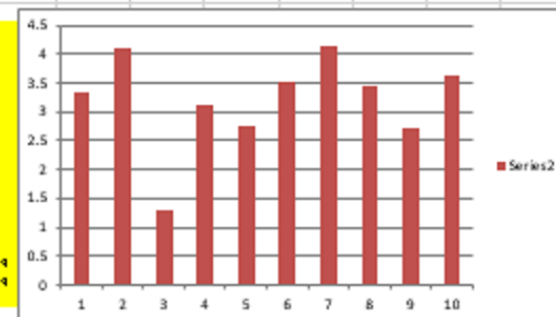
Sum, carrier exclude	A	B	C	D	E	F	G	H
Marr, total		12.91	0.485	1.4816	0.838	7.458	8.145	3.997
Marr, Dqs 5.501		11.55	0.485	1.4816	0.838	7.458	8.145	3.997



ED 3.32625
CV 0.139242

FPD 0.48822
FPF 0.437052

ED
0
1 15.20185 15.19851 3.34
2 15.20539 15.20129 4.1
3 15.20734 15.20603 1.31
4 15.21012 15.20699 3.13
5 15.20706 15.20432 2.74
6 15.20706 15.20353 3.53
7 15.20615 15.20201 4.14
8 15.20657 15.20313 3.44
9 15.20669 15.20398 2.71
10 15.2113 15.20768 3.62
TOT 26.61 mg
AVEG 3.32625 mg
STDEV 0.463155



APPENDIX 24: ED, CV_{ED} and FPF of Bu20L15Ph2.5 at 4kPa with Twister™